

**TURKISH REPUBLIC  
ERCIYES UNIVERSITY  
GRADUATE SCHOOL OF  
NATURAL AND APPLIED SCIENCES  
DEPARTMENT OF MECHANICAL ENGINEERING**

**NUMERICAL INVESTIGATION OF HEAT TRANSFER  
ENHANCEMENT ON THE EFFECT OF ADDING (AL<sub>2</sub>O<sub>3</sub>)  
NANOPARTICLES TO WATER FLOW IN A  
HORIZONTAL TUBE INSERTED PENTAGON RINGS**

**Prepared by  
Muqdad Khamees Hameed AL-JANABI**

**SUPERVISOR  
Prof.Dr. Veysel ÖZCEYHAN**

**MSc / Thesis**

**December, 2017  
KAYSERİ**

**TURKISH REPUBLIC  
ERCIYES UNIVERSITY  
GRADUATE SCHOOL OF  
NATURAL AND APPLIED SCIENCES  
DEPARTMENT OF MECHANICAL ENGINEERING**

**NUMERICAL INVESTIGATION OF HEAT TRANSFER  
ENHANCEMENT ON THE EFFECT OF ADDING (AL<sub>2</sub>O<sub>3</sub>)  
NANOPARTICLES TO WATER FLOW IN A  
HORIZONTAL TUBE INSERTED PENTAGON RINGS**

**Prepared by  
Muqdad Khamees Hameed AL-JANABI**

**SUPERVISOR  
Prof.Dr. Veysel ÖZCEYHAN**

**MSc / Thesis**

**This study was supported by Erciyes University Scientific Research Projects  
Unit under the code of FYL-2017-7284**

**December, 2017  
KAYSERİ**

## SCIENTIFIC ETHICS SUITABILITY

I declare that all information's in this work were obtained in accordance with academic and ethical rules. All results and material that not been at the essence of this work are also transferred and expressed by giving reference as required by these rules and behavior,



Owner of the Thesis

Muqdad Khamees Hameed AL-JANABI

## SUITABILITY FOR GUIDE

The MSc / thesis entitled “**Numerical Investigation of Heat Transfer Enhancement on the Effect of Adding (AL<sub>2</sub>O<sub>3</sub>) nanoparticles To Water Flow in a Horizontal Tube Inserted Pentagon Rings** ” has been prepared in accordance with Erciyes University Graduate Education and Teaching Institute Thesis Preparation and Writing Guide.



Owner of the Thesis

Muqdad Khamees Hameed AL-JANABI



Supervisor

Prof. Dr. Veysel ÖZCEYHAN



Chairman of the Department of Mechanical Engineering

Prof. Dr. Necdet ALTUNTOP




## ACCEPTANCE AND APPROVAL PAGE

This study entitled “**Numerical Investigation Of Heat Transfer Enhancement On The Effect Of Adding (  $AL_2O_3$  ) nanoparticles To Water Flow In a Horizontal Tube Inserted Pentagon Rings**” prepared by **Muqdad Khamees Hameed AL-JANABI** under the supervision of **Prof.Dr. Veysel ÖZCEYHAN** was accepted by the jury as MSc. Thesis at Erciyes University, Graduate School of Natural and Applied Sciences, Mechanical Engineering Department.

25 /12 / 2017

(Thesis defense exam date)

### JURY:

Supervisor	:	Prof.Dr. Veysel ÖZCEYHAN.....	
Juror	:	Prof. Dr. Necdet ALTUNTOP.....	
Juror	:	Prof. Dr.Hüseyin AKILLI .....	

### APPROVAL

That the acceptance of this thesis has been approved by the decision of the Institute's Board of Directors with the 26/12/2017 , date and 2017/55-17 numbered decision.

  
  
26 / 12 / 2017

**Director of the Institute  
Prof. Dr. Mehmet AKKURT**

## ACKNOWLEDGEMENTS

I would like to express my special appreciation and thanks to my advisor Prof. Dr. Veysel ÖZCEYHAN, you have been a tremendous mentor for me. I would like to thank you for encouraging my research and for allowing me to grow as a research scientist. Your advice on both research as well as on my career have been priceless. I would also like to thank my committee members, Prof. Dr. Necdet ALTUNTOP, Prof. Dr. Hüseyin AKILLI. I also want to thank you for letting my defense be an enjoyable moment, and for your brilliant comments and suggestions, thanks to you.

I would especially like to thank Res. Assist. Orhan KEKLIKÇİOĞLU and Res. Assist. Toygun DAĞDEVİR. All of you have been there to support me when I collected data for my MSc thesis. A special thanks to my colleagues in the work Sana Abdullah Ghulam, Akil Ashour Abdel, and Karim Abdel - Zahra Salman who supported me strongly.

A very special thanks to my family. Words cannot express how grateful I am to my mother, and father for all of the sacrifices that you've made on my behalf. Your prayer for me was what sustained me thus far. I would also like to thank all of my friends who supported me in writing and incited me to strive towards my goal. At the end, I would like express appreciation to my beloved wife and son who spent sleepless nights with and was always my support in the moments when there was no one to answer my queries.

Muqdad Khamees Hameed AL-JANABI

Kayseri, December 2017

**NUMERICAL INVESTIGATION OF HEAT TRANSFER ENHANCEMENT ON  
THE EFFECT OF ADDING (AL<sub>2</sub>O<sub>3</sub>) NANOPARTICLES TO WATER FLOW IN  
A HORIZONTAL TUBE INSERTED PENTAGON RINGS**

**Muqdad Khamees Hameed AL-JANABI**  
**Erciyes University, Graduate School of Natural and Applied Sciences**  
**M.sc. Thesis, December 2017**  
**Thesis Supervisors: Prof.Dr. Veysel ÖZCEYHAN**

**ABSTRACT**

In this work, a numerical study has been presented to investigate heat transfer characteristics of (Al<sub>2</sub>O<sub>3</sub>-Water) nanofluids flow in a circular horizontal tube that fitted pentagon rings by three different pitch lengths ( $d$ ,  $2d$ , and  $3d$ ). To provide fully developed flow inside the test section, specified distances are performed on the entrance and the exit of the tube. The analyses are carried out with three different nanofluids volume fractions 1.5, 3, and 4.5 % in the range of Reynolds number from 5,000 to 15,000. The numerical solution procedure includes the investigation of heat transfer coefficient, Nusselt number, friction factor, surface temperature and the pressure drop characteristics with using finite volume method by applying (k- $\omega$ ) Standard turbulence model to solve the equations of continuity, momentum, and energy in a three-dimensional domain. A single-phase approach is employed to model nanofluids and properties of the fluid are applied constant with temperature. The use of (Al<sub>2</sub>O<sub>3</sub>-Water) nanofluids with pentagon ring leads to increase in heat transfer and pressure drop over the smooth tube. The heat transfer coefficient increases with the increment of the nanofluid concentrations and Reynolds number, and it shows descending trend with the increment of pitch length or in another meaning increases with the increment of the number of pentagon rings into a tube. Finally, the results showed that the configuration of Al<sub>2</sub>O<sub>3</sub>-Water nanofluid with pentagon ring could be used effectively in heat transfer processes.

**Keywords:** Al<sub>2</sub>O<sub>3</sub>-Water nanofluids, Heat transfer, Pressure drop, Pentagon ring.

**BORU İÇİ AKIŞTA SUYA (AL<sub>2</sub>O<sub>3</sub>) NANO PARTİKÜL TAKVİYESİ VE  
BEŞGEN KESİTLİ HALKA ELEMANLAR YERLEŞTİRİLMESİ İLE ISI  
TRANSFERİNİ İYİLEŞTİRİLMESİNİN SAYISAL OLARAK İNCELENMESİ**

**Muqdad Khamees Hameed AL-JANABI**  
**Erciyes Üniversitesi, Fen Bilimleri Enstitüsü**  
**Yüksek Lisans Tez, Aralık 2017**  
**Tez Danışmanı: Prof.Dr. Veysel ÖZCEYHAN**

## **Özet**

Bu çalışmada silindirik bir boru içerisinde Al<sub>2</sub>O<sub>3</sub>—su nanoakışkanı ile birlikte üç farklı mesafe oranına sahip beşgen kestili iç elemanlar yerleştirilerek ısı transfer ve basınç düşümüne etkileri sayısal olarak incelenmiştir. Test bölgesinde hidrodinamik olarak gelişmiş akış sağlamak amacıyla, giriş ve çıkış boru bölgeleri kullanılmıştır. Analizler üç farklı hacimsel nanoakışkan fraksiyonu ve 5000-15,000 Reynolds sayısı aralığında gerçekleştirilmiştir. Isı transferi ve basınç düşümü çözümünü içeren sayısal çalışmada k-w Standart sonlu elemanlar çözümü ve süreklilik, momentum ve enerji denklemlerinin kullanıldığı üç boyutlu analizler gerçekleştirilmiştir. Çalışmada tek-model kullanılmış ve akışkan özellikleri sabit olarak kabul edilmiştir. Al<sub>2</sub>O<sub>3</sub>-su nanoakışkanı ve beşgen iç elemanların kullanımı, boş boruya oranla ısı transferi ve basınç düşümünde artışa sebep olmuştur. ısı transfer katsayısı nanoakışkan hacim fraksiyonunun artışı ve Reynolds sayısının artışı ile artmıştır ve mesafe oranının artmasıyla azalan bir eğim göstermiştir. Sonuç olarak Al<sub>2</sub>O<sub>3</sub>-su nanoakışkanı ve beşgen iç eleman kullanımının ısı transferi proseslerinde etkin bir biçimde kullanılabileceği görülmüştür.

**Anahtar Kelimeler:** Al<sub>2</sub>O<sub>3</sub>-su nanoakışkanı, Isı transferi, Basınç düşümü, Beşgen iç eleman.



## TABLE OF CONTENTS

### NUMERICAL INVESTIGATION OF HEAT TRANSFER ENHANCEMENT ON THE EFFECT OF ADDING (AL<sub>2</sub>O<sub>3</sub>) NANOPARTICLES TO WATER FLOW IN A HORIZONTAL TUBE INSERTED PENTAGON RINGS

	<u>Sayfa</u>
SCIENTIFIC ETHICS CONFORMITY PAGE .....	ii
SUITABILITY FOR INSTRUCTION GUIDE PAGE .....	iii
ACCEPTANCE AND APPROVAL PAGE .....	iv
ACKNOWLEDGEMENTS .....	v
ABSTRACT.....	vi
ÖZET.....	vii
TABLE OF CONTENTS .....	viii
LIST OF SYMBOLS AND/OR ABBREVIATIONS.....	xii
LIST OF TABLES AND CHARTS.....	xiv
LIST OF FIGURES .....	xvi
<b>INTRODUCTION.....</b>	<b>1</b>

## CHAPTER 1

### GENERAL INFORMATION

<b>1.1. Research background .....</b>	<b>2</b>
<b>1.2. Heat transfer enhancement techniques .....</b>	<b>3</b>
<b>1.2.1. Active technique .....</b>	<b>4</b>
<b>1.2.2. Passive technique .....</b>	<b>6</b>
<b>1.2.3. Compound technique .....</b>	<b>10</b>
<b>1.3. Introduction to nanofluids .....</b>	<b>10</b>
<b>1.3.1. Host liquid types .....</b>	<b>11</b>
<b>1.3.2. Nanoparticles material types .....</b>	<b>11</b>
<b>1.3.3. Application of nanofluids .....</b>	<b>12</b>
<b>1.4. Works established previously .....</b>	<b>12</b>
<b>1.4.1. Airflow fitted with inserts .....</b>	<b>13</b>

1.4.2. Water flow fitted with inserts .....	17
1.4.3. Nanofluids flow fitted with inserts .....	19
1.5. Thesis objectives .....	23
1.6. Thesis scope .....	24

## CHAPTER 2

### MATERIALS AND METHODS

2.1. Flow in circular tubes. ....	25
2.1.1. Velocity profiles.....	26
2.1.2. Temperature profiles. ....	27
2.1.3. Laminar and turbulent flow.....	28
2.1.4. Velocity boundary layer. ....	30
2.1.5. Thermal boundary layer. ....	31
2.1.6. Entry length in turbulent flow. ....	32
2.1.7. Turbulent flow correlations for smooth tube. ....	32
2.1.7.1. Pure fluids correlations. ....	32
2.1.7.2. (AL <sub>2</sub> O <sub>3</sub> -Water) nanofluid correlations.....	35
2.2. Useful parameters .....	36
2.2.1. Prandtl number. ....	36
2.2.2. Turbulent intensity. ....	36
2.2.3. Heat transfer coefficient. ....	36
2.2.4. Pressure drop.....	37
2.2.5. Nusselt number.....	37
2.2.6. Friction factor.....	37
2.2.7. Performance evaluation analysis. ....	37
2.3. Computational fluid dynamic (CFD) .....	38
2.3.1. Finite volume method (FVM).....	40
2.3.1.1. Center node based (FVM) .....	41
2.3.1.2. Vertex based (FVM).....	41
2.4. Configuration and assemblification of shapes .....	42
2.5. Boundary conditions .....	48
2.5.1. Governing equations .....	49

2.5.2. Numerical method .....	50
2.5.3. Grid independence study .....	51
2.6. Thermophysical properties of (water, nanoparticles, and nanofluids).....	53
2.6.1. Properties of water.....	53
2.6.2. Properties of nanoparticles. ....	54
2.6.3. Thermophysical properties of nanofluid.....	55
2.6.3.1. Density .....	55
2.6.3.2. Specific heat .....	55
2.6.3.3. Thermal conductivity .....	55
2.6.3.4. Dynamic viscosity .....	56

## CHABTER 3

### RESULTS AND DISCUSSION

3.1. Validation of the current numerical results. ....	57
3.1.1. Water flow in a smooth tube. ....	57
3.1.2. (AL <sub>2</sub> O <sub>3</sub> -Water) nanofluid flow in a smooth tube. ....	59
3.2. The effect of addition (9) of pentagon rings on the heat transfer characteristics For water flow and (AL <sub>2</sub> O <sub>3</sub> -water) nanofluidflow.....	63
3.2.1. On the (h). ....	63
3.2.2. On the (Nu). ....	64
3.2.3. On the (f). ....	65
3.2.4. On the (Ts). ....	66
3.2.5. On the (ΔP). ....	68
3.3. The effect of addition (14) of pentagon rings on the heat transfer..... Characteristics for water flow and (AL <sub>2</sub> O <sub>3</sub> -water) nanofluid flow. ....	69
3.3.1. On the (h). ....	69
3.3.2. On the (Nu). ....	70
3.3.3. On the (f). ....	71
3.3.4. On the (Ts). ....	72
3.3.5. On the (ΔP). ....	74
3.4. The effect of addition (29) of pentagon rings on the heat transfer..... Characteristics for water flow and (AL <sub>2</sub> O <sub>3</sub> -water) nanofluid flow. ....	75

3.4.1. On the (h). .....	75
3.4.2. On the (Nu). .....	76
3.4.3. On the (f). .....	77
3.4.4. On the (Ts). .....	78
3.4.5. On the ( $\Delta P$ ). .....	80
<b>3.5. The effects comparison of addition (9, 14, and 29) of pentagon rings on the Heat transfer characteristics for water flow only. ....</b>	<b>81</b>
3.5.1. On the (h). .....	81
3.5.2. On the (Nu). .....	82
3.5.3. On the (f). .....	83
3.5.4. On the (Ts). .....	84
3.5.5. On the ( $\Delta P$ ). .....	85
<b>3.6. The effect comparison of addition (9, 14, and 29) of pentagon rings on the heat Transfer characteristics for (<math>Al_2O_3</math>-water) nanofluid flow only. ....</b>	<b>89</b>
3.6.1. On the (h). .....	89
3.6.2. On the (Nu). .....	90
3.6.3. On the (f). .....	91
3.6.4. On the (Ts). .....	92
3.6.5. On the ( $\Delta P$ ). .....	94
<b>3.7. Summary Table of results comparison... ..</b>	<b>98</b>
<b>3.8. The performance evaluation analysis (<math>\eta</math>).....</b>	<b>98</b>

## CHAPTER 4

### CONCLUSION AND RECOMMENDATIONS

<b>4.1. Conclusion .....</b>	<b>101</b>
<b>4.2. Recommendations .....</b>	<b>102</b>
<b>REFERENCES.....</b>	<b>103</b>
<b>CURRICULUM VITAE.....</b>	<b>107</b>

## LIST OF SYMBOLS

$Al_2O_3$	Aluminum Oxide.
$C_p$	Specific heat (J/kg K).
$D$	Diameter of a tube (m).
$f$	Darcy friction factor.
$h$	heat transfer coefficient ( $W/m^2.K$ ).
$h_E$	Heat transfer coefficient with inserting pentagon rings(Enhanced).
$h_{NE}$	Heat transfer coefficient without inserts (Non-Enhanced).
$I$	Turbulent intensity (%).
$K$	Thermal conductivity (W/m. K).
$L$	Length (m).
$L_1$	Entrance Section length (m).
$L_2$	Test Section length (m).
$L_3$	Exit Section length (m).
$Nu$	Nusselt number.
$Pr$	Prandtl number.
$\Delta p$	Pressure drop (Pa).
$\dot{q}$	Heat flux of the tube ( $W/m^2$ ).
$Re$	Reynolds number.
$T_b$	Bulk temperature of a fluid (k).
$T_{in}$	Inlet thermal temperature (K).
$T_s$	Surface temperature (K).
$T_w$	Temperature at the wall (K).
$V$	Fluid velocity (m/s).

W Width of pentagonal ring (m).

### Greek symbols

$\Phi$  nanofluids volume fractions.

$\rho$  Density (kg/m<sup>3</sup>).

$\mu$  Dynamic viscosity (kg/m s).

$\eta$  The performance evaluation analysis.

### Subscripts

bf base fluid.

DR Distributing range.

in Velocity inlet.

LFE Length from entrance to first pentagon ring.

NOPR Number of pentagon rings.

nf nanofluid.

np nanoparticle.

out Pressure outlet.

PR Pentagonal ring.

PL Pitch length.

w water.

## LIST OF TABLES AND CHARTS

Table (1) Thermal conductivity of various solid and liquids.....	<b>03</b>
Table (2) Classification of various heat transfer enhancement techniques.....	<b>04</b>
Table (3) Properties of saturated water at 20 °C (SI Units) .....	<b>54</b>
Table (4) Properties of nanoparticles (AL <sub>2</sub> O <sub>3</sub> ) .....	<b>55</b>
Table (5) Thermophysical properties of (AL <sub>2</sub> O <sub>3</sub> /Water) nanofluids.....	<b>56</b>
Chart (1) Nu correlations vs. numerical result for (smooth tube) .....	<b>58</b>
Chart (2) Blasius correlation vs. numerical result for (smooth tube) .....	<b>58</b>
Chart (3) Nanofluid correlations vs. numerical result for (smooth tube) .....	<b>59</b>
Chart (4) Pak & Cho correlation vs. numerical result for (smooth tube) .....	<b>60</b>
Chart (5) h vs. Re for (AL <sub>2</sub> O <sub>3</sub> /Water) nanofluids flow (smooth tube) .....	<b>60</b>
Chart (6) f vs. Re number for (AL <sub>2</sub> O <sub>3</sub> /Water) nanofluids flow (smooth tube) .....	<b>61</b>
Chart (7) ΔP vs. Re number for (AL <sub>2</sub> O <sub>3</sub> /Water) nanofluids flow (smooth tube). .....	<b>62</b>
Chart (8) Ts vs. Re number for (AL <sub>2</sub> O <sub>3</sub> /Water) nanofluids flow (smooth tube). ..	<b>62</b>
Chart (9) Heat transfer coefficient vs. Reynolds number for 9 pentagon rings. ....	<b>64</b>
Chart (10) Nusselt number vs. Reynolds number for 9 pentagon rings .....	<b>65</b>
Chart (11) Friction factor vs. Reynolds number for 9 pentagon rings .....	<b>66</b>
Chart (12) Surface temperature vs. Reynolds number for 9 pentagon rings .....	<b>67</b>
Chart (13) Pressure drop vs. Reynolds number for 9 pentagon rings .....	<b>68</b>
Chart (14) Heat transfer coefficient vs. Reynolds number for 14 pentagon rings .....	<b>70</b>
Chart (15) Nusselt number vs. Reynolds number for 14 pentagon rings .....	<b>71</b>
Chart (16) Friction factor vs. Reynolds number for 14 pentagon rings .....	<b>72</b>
Chart (17) Surface temperature vs. Reynolds number for 14 pentagon rings .....	<b>73</b>
Chart (18) Pressure drop vs. Reynolds number for 14 pentagon rings .....	<b>74</b>
Chart (19) Heat transfer coefficient vs. Reynolds number for 29 pentagon rings ...	<b>76</b>
Chart (20) Nusselt number vs. Reynolds number for 29 pentagon rings .....	<b>77</b>
Chart (21) Friction factor vs. Reynolds number for 29 pentagon rings .....	<b>78</b>
Chart (22) Surface temperature vs. Reynolds number for 29 pentagon rings .....	<b>79</b>
Chart (23) Pressure drop vs. Reynolds number for 29 pentagon rings .....	<b>80</b>
Chart (24) h vs. Re number for water flow with (9, 14, 29) PR ...	<b>81</b>
Chart (25) Nu number vs. Reynolds number for water flow with (9, 14, 29) PR .....	<b>82</b>
Chart (26) Friction factor vs. Re number for water flow with (9, 14, and 29) PR .....	<b>83</b>

Chart (27) $T_s$ vs. Re number for water flow with (9, 14, and 29) PR.....	<b>84</b>
Chart (28) Pressure drop vs. Re numberfor water flow with (9, 14, and 29) PR .....	<b>85</b>
Chart (29) $h$ vs. Re number for nanofluids flow with (9, 14, and 29) PR.....	<b>90</b>
Chart (30) Nu number vs. Re number for nanofluids flow with (9, 14, and 29) PR.....	<b>91</b>
Chart (31) F. factor vs. Re number for nanofluids flow with (9, 14, and 29) PR.....	<b>92</b>
Chart (32) $T_s$ vs. Re number for nanofluids flow with (9, 14, and 29) PR.....	<b>93</b>
Chart (33) Pressure drop vs. Re numberfor nanofluids flow with (9, 14, and 29) PR.....	<b>94</b>
Table (6) Results comparison.....	<b>98</b>
Chart (34) $\eta$ vs. Reynolds number.....	<b>99</b>
Chart (35) $\eta$ vs. Re=15000.....	<b>100</b>



## LIST OF FIGURES

Figure (1) Most popular twisted tape formats.....	07
Figure (2) Actual velocity profiles for flow in a tube.....	27
Figure (3) Actual temperature profiles for flow in a tube.....	28
Figure (4) Transitional flow region.....	29
Figure (5) Velocity boundary layer.....	30
Figure (6) Thermal boundary layer.....	31
Figure (7) Overview of CFD.....	40
Figure (8) Schematic diagrams of the problem statement.....	42
Figure (9) Schematic diagrams shows the dimensions of tube sections.....	43
Figure (10) 3D view shows the dimensions of pentagon ring.....	43
Figure (11) 3D view shows distribution of the pentagon rings.....	44
Figure (12) Distribution of (29) of pentagon rings inside test section.....	45
Figure (13) Distribution of (14) of pentagon rings inside test section.....	46
Figure (14) Distribution of (9) of pentagon rings inside test section.....	47
Figure (15) 3D view mesh models for the pentagon ring .....	52
Figure (16) 3D view mesh models for the tube fitted with pentagon rings .....	52
Figure (17) Study of independence check .....	53
Figure (18) Comparison of (K) of common liquids, polymers and solids .....	54
Figure (19) Comparison of total pressure counters of (9, 14, and 29) Pentagon rings for water flow at Reynolds number 15,000.....	86
Figure (20) Comparison of total temperature counters of (9, 14, and 29) Pentagon rings for water flow at Reynolds number 15,000.....	87
Figure (21) Comparison of velocity magnitude counters of (9, 14, and 29) Pentagon rings for water flow at Reynolds number 15,000.....	88
Figure (22) Comparison of total pressure counters of (9, 14, and 29) Pentagon rings for 3% (AL <sub>2</sub> O <sub>3</sub> -Water) nanofluid flow at Reynolds number 15,000.....	95
Figure (23) Comparison of total temperature counters of (9, 14, and 29) Pentagon rings for 3% (AL <sub>2</sub> O <sub>3</sub> -Water) nanofluid flow at Reynolds number 15,000.....	96
Figure (24) Comparison of velocity magnitude counters of (9, 14, and 29) Pentagon rings for 3% (AL <sub>2</sub> O <sub>3</sub> -Water) nanofluid flow at Reynolds number 15,000.....	97

## INTRODUCTION

Several researchers have carried out numerical studies to study the impact of thermophysical properties on heat transfer promotion. Some researchers have studied both the single and dual phase models, which are either fixed or based on temperature characteristics with experimental data reference. The purpose of this research is to continue through numerical investigations in order to save cost and time compared to experimental devices by using (Al<sub>2</sub>O<sub>3</sub>-Water) Nanofluids in the tubes under turbulent flow conditions, by adding the Pentagon rings in an attempt to understand heat transfer characteristics after this change like thermophysical properties, thermal performance, the effect of nanofluid concentration, Nusselt number, etc. on heat transfer promotion. The method of the study was carried out by a numerical investigation by using computational fluid dynamics (CFD) program. The 3D model was created by the SolidWork2017 program. The length of entrance section (L1) was assumed to be equal to  $10 \times$  the diameter of the tube to provide a fully developed flow, and the length of the test section was assumed (L2) =1.5 m, and the length of exit section (L3) was assumed to be equal to  $5 \times$  the diameter of the tube to prevent reverse flow. To ensure the accuracy of using numerical methods and procedure, firstly, a previous experimental study was followed to guarantee the solution methodology. Water-liquid was created as a material of fluid to the validation process, by applying single-phase approach for (Al<sub>2</sub>O<sub>3</sub>-water) nanofluids in a turbulent flow inside a tube and under uniform heat flux was applied to the tube wall as a boundary condition. The CFD program solved and analyzed the problems statement which involve fluid flows, heat and momentum transfer, by using equations and algorithms of fluid mechanics and by using conservation equations of (mass, momentum, and energy). The results were examined in terms of (heat transfer coefficient, Nusselt number, friction factor, surface temperature, and pressure drop) versus six Reynolds numbers ranging from 5,000 to 15,000.

# CHAPTER 1

## GENERAL INFORMATIONS

### 1.1. Research background

The low conductivity characteristic of normal liquids such as water and ethylene glycol makes it unable to meet the growing demand for energy applications as shown in the Table (1) Wang & Mujumdar [1]. As a result, some years ago, the interest in promoting heat transfer by means of new techniques, namely, the use of nanofluids with the inclusion of a solid geometric shape to expand the surface of heat transfer, has begun to be of great interest to researchers. There are two methods, one is active and the other is passive, to improve heat transference rate in heat exchangers. Different methods were used to increase the rate of heat transferred including the passive method involving the inclusion of the steel body of nanofluids because of its low-cost effectiveness and have been widely used and many previous studies indicated the improvement in heat transferred without affecting significantly on overall performance.

Table 1: Thermal conductivity of various solid and liquids.

Material	Thermal conductivity K (w/m. k)	
Metallic solids	Copper	401
	Aluminum	237
Nonmetallic solids	Silicon	148
	Alumina( $Al_2O_3$ )	40
Metallic liquids	Sodium(644 K)	72.3
Nonmetallic liquids	Water	0.613
	Ethylene glycol(EG)	0.253
	Engine oil(EO)	0.145

## 1.2. Heat transfer enhancement techniques

The techniques were employed for developing the heat transferred without affecting the overall realization of the system significantly. Heat transfer techniques exist on three general classifications which are passive technique, active technique, and compound technique. These techniques are used in many fields including HVAC, power plants, refrigerators, heating, evaporators, cooling, and cars, etc. Urkude & Farkade [2] described passive & active techniques with examples in the following sub-sections. When both techniques were used together, this technique was named composite techniques. The composite method involves a complex design and therefore has limited applications. General techniques classifications are provided in Table (2) Manglik [3].

Table 2: Classification of various heat transfer enhancement techniques.

Passive Techniques	Active Techniques
Treated surface	Mechanical aids
Rough surface	Surface vibration
Extended surface	Fluid vibration
Displaced enhancement device	Electrostatic fields
Swirl flow devices	Injection
Coiled tubes	Section
Surface tension devices	Jet impingement
Additives for liquids	
Additives for gases	
Compound Enhancement	
Two or more passive and /or active techniques that are employed together	

### 1.2.1. Active technique

These mechanizations are more complex in the expression of design and use because of their necessity to use external energy to adjust the flow of fluid so as to obtain an improvement in thermal efficiency and for this reason, the use of these techniques in scientific fields is limited. Providing external energy in most applications is not easy. Examples of this mechanization are: using electrostatic fields, Mechanical Aids, pulse-induced by cams, surface or fluid vibrations, suction, magnetic field, injection, jet impingement, plungers, etc.

**A brief narrative of active techniques.Manglik [3]:**

### **1. Mechanical aids**

These include moving the fluid through stirring, Surface Scraping and rotating surfaces, as presented below:-

#### **❖ Stirring**

The fluid is moved by means of a mechanical device or by rotating the surface.

#### **❖ Surface Scraping**

This method has been used for viscous liquids on a large range and especially in the manufacture of chemical processes that can be carried out on the flow of gases in the duct.

#### **❖ Rotating Surfaces**

The use of equipment containing rotary tubular heat exchangers is observed in the commercial works.

### **2. Surface vibration**

For a better coefficient of heat transfer, this way is primarily used within a single-phase flow either with the high or low frequency.

### **3. Fluid vibration**

This method is mainly used within single-phase flow with vibrations varying from 1 Hz to 1 MHz which is an ultrasonic wave frequency. This technique may be one of the usual effective types of vibration enhancement technology.

#### **4. Electrostatic fields**

Applying magnetic fields or electric fields or mixtures produced from both, AC or DC sources can be employed in heat exchange systems but when used insulating liquids.

#### **5. Injection**

This method is used only in single-phase flow and is performed by injecting the main liquid with the same type of liquid or injecting it with different types of fluids. The injection process is done either with the same heat transfer direction or in the opposed direction for heat transfer.

#### **6. Suction**

This method is used within single-phase flow and summed up using heated porous surface able to extract the steam or withdraw the fluid.

#### **7. Jet impingement**

It includes direction of refrigeration or boiling liquid vertically or indirectly on the surface of heat transfer. Single or multiple jets (in groups or centrally organized along the flow channel) can be utilized in both single-phase and boiling applications.

### **1.2.2. Passive technique**

The passive techniques, as they have been defined in many of the previous researches do not require any direct input from external energy to improve heat transfer. The available power is used in the same system and eventually leading to an increase in pressure drop for fluid. Widespread passive techniques employed to promote heat transfer are: raising the active surface area and increasing the fluid retention time. They typically use surface or geometric adjustments on the flow via combining additional inserts or devices. In most liquids, using passive techniques results in a change in the

layer structure due to flow vortices with the increased surface region and fluid retention time and thus developed thermal performance. Some of the common twisted tape formats are presented in the figure (1) below.

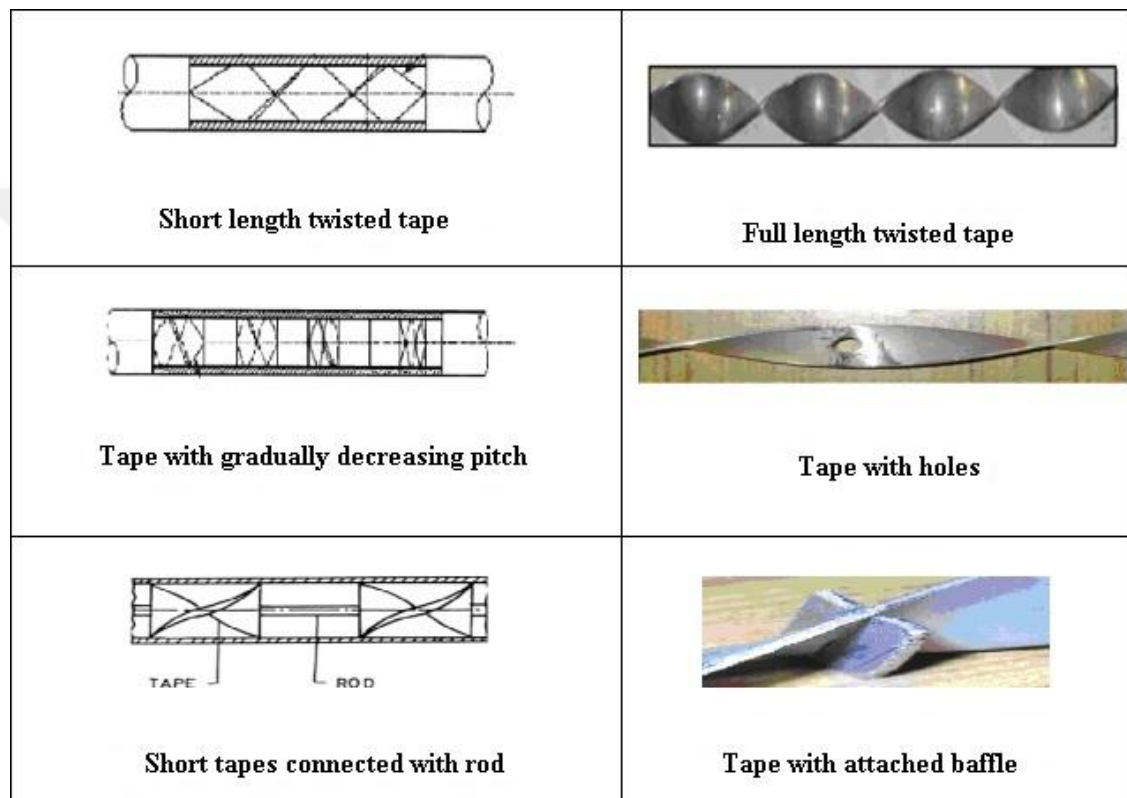


Figure 1. Most popular twisted tape formats. Joshis & Kriplani [4].

**Common methods used for these techniques are:**

- ❖ Inserts (insert geometrical shape like barbed wire, wire coiled ... etc.).
- ❖ Expanding or modifying the surface area (making protrusions or holes in the same surface ... etc.).
- ❖ Adding or mixing materials with essential fluids such as (nanofluid ... etc.).



The passive technique is more useful than the active ones because it is simple and inexpensive and we can also implement it by inserting a simple geometrical shape to create a vortex in fluid flow to achieve good thermal efficiency and it can be easily applied in heat exchangers.

**A brief narrative of passive techniques. Manglik [3]:**

**1. Treated surfaces**

The surface may be treated to improve thermal performance by thermal coating or resizing. In this kind of treatment, the surface is being treated completely or only parts of it are treated, thus reducing roughness and helping to transfer the heat of a single-phase. This treatment is usually used for condensation or boiling functions.

**2. Extend surfaces**

Initially, traditional fins were utilized in heat exchangers with the goal of expanding surfaces and providing improved thermal efficiency and were common. Thereafter, there were improvements in the modification of fin surfaces, which have driven to fluid flow disturbance in a way that increases the effective surface area. This change has driven to increment the heat transfer.

**3. Roughened surfaces**

These methods are well known and performed either randomly by stripping surfaces like using sand grains or using regular geometry to making the roughness. Also, with this method, there is a flow resistance accompanied with the advantage of heat transfer.

**4. Surface tension devices**

They consist of either making grooves on surfaces or wick them, which helps to boost the movement of liquid towards the heated or condensing surface.

## **5. Displaced enhancement devices**

The insertion method is typically used for the purpose of improving the heat transfer in an indirect way and through forced convection between the surfaces. The configuration of the shapes like disks, balls, rings and metallic mesh...etc. working like a fixed mixer, geometrical shapes force the fluid flow to rotate his direction from the center of flow to heated walls.

## **6. Swirl flow devices**

In general, we can generate the vortices with a diversity of insertion methods, including a geometrical flow arrangement or airflow adjustment, which produces secondary flows. Models of these procedures are twisted tape, helical twisted tube, and periodic tangent fluid injection. Among these examples, the twisted tape has been of vast interest in earlier studies.

## **7. Coiled tubes**

As the name proposes, they make heat exchangers stronger. The curvature of the tube due to the coiling produces a secondary flow, thereby promoting heat transfers, especially to single-phase flows in most of the condensation and boiling zones. The secondary fluid movement is generated mainly through a constant change in the direction of the tangent vector to the bounding curved surface of the duct and this leads to making deflection of the flow of velocity vectors.

## **8. Additives for liquids**

They improve thermal performance by adding solid particles that are soluble and improve performance depending on the type and concentration of the particulate matter and also on chemistry (ionic nature, chemical composition, molecular). Much of the work focuses on this technique for fluid flow, especially single-phase liquids flow because it usually reduces the surface stress.

## **9. Additives for gases**

The addition of solid particles or liquid droplets to the flow of gas, a dilute single-phase such as a suspension of solid gas or a dense phase like fluidized beds.

### **1.2.3. Compound technique**

It is a hybrid technique in which two or more active or passive techniques are used together to promote heat transfer, and the output of heat transfer is greater than that is produced by any technique when used individually. This technique is called a composite method.

### **1.3. Introduction to nanofluids**

After numerous times of concentrating the advancement of nanofluids, their thermophysical properties are not yet known precisely and judging their actual potential is troublesome. Choi & Eastman [5] defined the term of nanofluids for this new class. Nanofluids are other groups of heat transfers fluids known as nanofluids and have been proposed to add nanometer sizes to fluid base particles. The normal molecule estimates utilized as a part of nanofluids is under 100 nm.

Uddin et al. [6] called nanofluids equal to a liquid-nanometer-sized fluid mix nanoparticles. In particular, nanofluids are a new noble class that has been engineered by a constant suspension of a little amount, 1% volume or less of particles with the lengths arranged on regular heat transfer liquids. These colloidal suspension fluids are designed from nanoparticles in the fluid base. The idea of particles that can be converted from millimeters to micrometers in the late 19th century has become part of a modern adventure in a new world. Working together on two things to produce an effect is greater than the total effect obtained from their individual use which is key to the success of nanofluids. The result is a matching set of brilliant thermal properties that have prompted students, experts and engineers all around the world to meet the challenge of exploring more. Many researchers have studied experimentally in this area and have reported that nanoparticles in the performance of fluid-enhanced heat transfer depend on some thermal properties. Nanofluid fluids seem to be very interesting for

their ability to heat more than normal liquids and can be used in many applications such as power generation, transport, or even electronics, renewable energy & space. In the light of these, a lot of literature was used to express thermophysical properties in terms of particles and they led to different results of promoting heat transfer in order to save cost and time compared to experimental devices.

### **1.3.1. Host liquid types**

Uddin et al. [6] suggest that familiar base fluids like water (H<sub>2</sub>O), ethylene glycol (EG), engine oil (EO), pump oil and glycerol have been appropriated as host liquids in nanofluids.

### **1.3.2. Nanoparticles material types**

Uddin et al. [6] state that the nanoparticles usually used in nano-fluids are made of many materials which are:

- ❖ Nitride ceramics like nitrides of silicon and aluminum.
- ❖ Metals like gold, Copper, and silver.
- ❖ Oxide ceramics like oxides of copper and aluminum.
- ❖ Carbide ceramics like carbides of silicon and titanium.
- ❖ Semiconductors like titanium dioxide and silicon carbide.
- ❖ Carbon nanotubes.
- ❖ Composite materials like nanoparticle alloys, Al<sub>70</sub>Cu<sub>30</sub> or nanoparticles basic polymer composite shell.

### 1.3.3. Application of nanofluids

Uddin et al. [6] also emphasize that promoting heat transfers is a really important topic. Many kinds of research and scientific papers have been focusing on a theme of nanofluids to comprehend the behavior of this unusual type of fluid and to benefit from it in many fields. Below is a simple list showing nanofluid applications:

- ❖ Biological and Biomedical.
- ❖ Cancer Therapeutics.
- ❖ Antibacterial Agent.
- ❖ Detergency.
- ❖ Solar Industry.
- ❖ Industrial Cooling.
- ❖ Smart Fluid.
- ❖ Nuclear Reactors.
- ❖ As Superconductor.
- ❖ Car Engine.
- ❖ As Fuel.
- ❖ As Brake Fluid.
- ❖ Microchips Electronic Industry.
- ❖ Microscale Fluidic.

### 1.4. Works established previously

Methods varied in past studies to support heat transfer where investigations gradually developed with the expansion of science. Initially, many researchers used air to conduct the practical and theoretical investigations, while others used the fluids like water, ethylene glycol, and glycerol, etc. In 1995, Cho developed a new term called nanofluid by putting small particles with big impacts inside the fluids to improve  $K$  (w/m.k) of liquids. After that period, the researchers developed the techniques by applying nanofluid instead of normal fluids as nanofluids contain a higher  $K$  than most familiar fluids. Nanofluids promote higher heat transfer, but the urgent need to increase heat transfer has to manage the researchers to think many times and use different techniques to increase heat transfer. Composite method is considered as a modern and

cheap technique which showed positive results for promoting the transfer of heat effectively and more than the results taken from nanofluid only.

#### **1.4.1. Airflow fitted with inserts**

Kalyani et al. [7] analyzed experimentally and numerically enhancement of heat transfer inside a circular tube using mesh inserts in the turbulent zone. The air was the working fluid used in this analysis. Reynolds numbers ranged from 7,000 to 14,000. Constant heated flux was applied to the horizontal tube. The configurations of tube and mesh were created using Gambit, and the fine meshing grid was applied using FLUENT. Firstly, CFD analysis was applied to the plain tube in order to make a comparison of the results obtained from the experimental analyses. For optimization purposes, numerical techniques were employed for the mesh inserts also. In the experiment, the values (twenty-two, eighteen, fourteen, and ten mm) were considered as screen diameters for mesh inserts. The results were compared with the normal flow case without using any material. The results showed that maximum increment in Nusselt number was 1.86 times observed at  $Re = 0.8$  and at 50mm distance between screens. Higher resistance to airflow was observed at pitches 2.5mm and 10mm for using mesh inserts. The maximum Nusselt number was 2.15 times of plain tube observed using CFD analysis at the 2.5mm (lowest pitch) and for the mesh diameter 26mm (biggest one). The numerical analyses were easier than experimental and it can be done at a short time. Pressure drop with mesh inserts was also higher than that was obtained from the plain tube, the maximum one was 1.23 times more than plain tube observed at  $Re = 0.9645$ . The total enhancement ratio was 2.006 for this study.

Liu et al. [8] investigated experimentally and numerically promoting heat transfer inside a tube using a permeable medium with the laminar and turbulent flow. Working fluid for this investigation was the air. Reynolds numbers in this investigation ranged from 1,000 to 19,000 changing from laminar to turbulent zone. Constant & the flux of heat applied on the surface was uniform. In the experiment, three different permeable media were considered with different porosity. There were three different permeable media which was used in the experiments with different porosity. The experimental & numerical investigations were determined to investigate the flow

resistance & heat transfer characteristics from laminar zone to fully turbulent regions and all depended on Reynolds number range. Numerical simulation was applied to find the effect of porous radius ratio on the performance of heat transfers. Both results for experimental and numerical showed that enhancement in convective heat transfer was achieved when using porous inserts with the approximate diameter of the tube. Also, in the laminar flow especially resistance increased in a sensible range. Finally, the results denoted that using a permeable medium inside the flow promoted heat transfer efficiency.

Liu et al. [9] investigated numerically the characteristics of heat transfer, flow resistance, and total hydraulic thermal performance of the turbulent airflow was studied in a circular tube by inserting the louver strip. Reynolds numbers in this analysis ranged from 10,000 to 45,000. The main interests in this investigation were the slant angle and the turbulators pitch effects. The Nusselt number was heightened from 2.75–4.05 times of smooth tube. The amount of the performance criterion ranged from 1.60 to 2.05, indicating that the inclusion of louver strip inserts has a very good overall thermal performance. Furthermore, the computational results showed that the best heat transfer rate was achieved using the largest slant angle and the smallest pitch, also indicating that there is an increase in flow resistance. The effect of the slanted angle was more than the effect of pitches for the "Nusselt number" and "friction factor". The total hydraulic thermal performance was observed at the median slant angle with the small pitch. All numerical investigation data showed that heat transfer enhancements were good using the louver strip, and it could be used in heat transfer applications.

Ahamed et al. [10] studied experimentally enhanced heat transfer in turbulent flow regime after adding triple helical tape inside a circular tube. Reynolds numbers in this study was  $22,000 \leq Re \leq 51,000$ . Mild steel was the material used for the triple helical tapes, and various helix angles were examined ( $\alpha=9^\circ, 13^\circ, 17^\circ, \text{ and } 21^\circ$ ). The experimental results were compared with the normal flow without any insert and it showed that increment for friction factor ranged from 3.0 to 4.5 times while the Nusselt number changed effectively. The maximum augmentation (3.7) was obtained by the insert when a steady blower power was used. At the final step, the correlations for friction factor and heat transfer were upgraded and it was valid to use with a circular tube under turbulent flow condition with inserts.

Vathare and Hebbal [11] analyzed numerically the enhancement of turbulent flow heat transfer in a horizontal tube with different inserts (cylinder, diamond and trapezoidal). The air was the working fluid used in this analysis, and the Reynolds number ranged from 6,000 to 14,000. The geometry of tube having inner diameter was 27.5 mm and length of the tube was 610 mm. The results showed that the increment in Nusselt Numbers was about 87% for cylinder inserted and was 85% with using diamond insert and 28% by trapezoidal insert, in a comparison with the plain tube. Friction factor of the tube with cylinder inserted was increased 600% compared to a normal tube. Enhancement ratio of cylinder inserts was 75% and the enhancement ratio for trapezoidal insert was 65%. Pressure drop was higher for all inserts types compared to the plain tube. And for cylinder insert was higher than the trapezoidal insert. All analysis results were compared with theoretical results obtained using a package of ANSYS version 12.0.

Tikhe [12] analyzed experimentally promotion of heat transfer in a circular tube when inserting a twisted-tape with different twist ratio and the flux of heat applied on the surface was constant. The ranges of Reynolds number ranged from 7,500 to 13,000. The values (0.35, 0.44, 0.53, 0.62 and 0.71) represented 5 different ratios of width employed in the experiment. For twisted tape inserts at twist ratio of 2.5, the results recorded that Nusselt numbers rose from 6.04% to 17.26% compared to the results of the plain tube with the increment of Reynolds number and increment width ratio of the swirl generators, and the friction factor decreased with the increment of Reynolds number and decreasing width ratio. The thermal performance factor was up to 1.17 times of those of the plain tube after using twisted tape inserts at the same pumping power. Finally, valid correlation for the Nusselt number was developed.

Dagdevir [13] investigated numerically the effect of adding 12 different configurations of sinusoidal conical-nozzle turbulators inside a circular tube and the flux of heat applied on the surface was uniform with turbulent airflow on heat properties, friction, and performance. Nine different Reynolds numbers ranging from 8,000 to 24,000 were utilized. Results showed that amplitude and period values had an effect on the increased turbulent near the nozzles, which caused increased both heat transfer and friction factor. The highest thermohydraulic performance was obtained for Type 11 model which was 2 mm wide and period 2.5. The highest Nusselt number was obtained



on half-tide period values. Increased amplitude values enhanced the Nusselt number in the same period, as well. It can be argued that the reason for promoting heat transfer in these differences was that lifting the surface area that occurred convection heat transfer and raised the turbulent beside the wall.

Sheikholeslami and Ganji [14] investigated both experimentally and numerically the forced convective heat transfer of turbulent flow, also heat transfer inside double pipe air to water heat exchanger, after adding two arrays, the first was a direct conical ring, and the second one was a reverse conical ring. Reynolds numbers ranged from 6,000 to 12,000. The effect (conical angle, Reynolds number, open area ratio and pitch ratio) was studied to improve heat transfer and pressure reduction. The numerical method was applied to show the physical phenomena, as showing the correlations of thermal performance, the Nusselt number, and the friction factor. Multi-goal optimization was used for a direct array. The results recorded that thermal achievement increased with the increment of open space and pitch ratio while decreasing with increasing Reynolds number. The use of conical rings enhanced the fluctuations of radial and tangential turbulence, thinning the boundary layer, thus made an increase in Nusselt number. Also, it can be said that the distribution of conical rings by direct array enhanced the thermal performance and increased by increasing the conical angle while the reverse effect was observed when the conical rings were distributed by a reverse array.

Uzagare and Bansod [15] investigated experimentally in circular tube enhanced heat transfer after inserting V-Jagged twisted strip. Cu and AL were the materials employed in this experiment for twisted tape. The working fluid used for practical investigation was air under constant heat flux & the variation of flow rate. The rate of heat transfers, f. factor, and Nu. number were specified and compared versus a normal tube. Width = 10mm with depth = 8mm and width = 10mm with depth = 10mm, representing the widths and depths of the twisted tapes used in the experiment, Reynolds numbers ranged from 6,000 to 13,000. The results showed that when using V-Jagged twisted tape the increment in Reynolds number increased heat transfer coefficient from 52% to 90% for copper and from 50% to 75% for aluminum and decrement in friction factor compared to the plain tube. The higher heat enhancement when using aluminum V-Jagged twisted tape with width = 10M and depth = 8mm was

75 % when comparing the results with the plain twisted-tape. V-Jagged Twisted Tape with 10mm width and 8mm depth gave 85% increment Nu & friction factor gave 2.0 lowest than other inserts when theoretical and experimental events were compared. It is noticeable that the aluminum with width = 10mm and depth = 8mm had a lower pressure drop as the friction factor was less and about 0.04 compared with other inserts.

Saroj and Mahendra [16] investigated experimentally transfer of heat and fluid flow features using s-shaped Inserts. The circular tube dimensions were 34 mm inner diameter and 38mm outer diameter with 3mm length and 2 mm thick. These inserts with different pitches were tested in a turbulent flow area of Reynolds numbers range from 4,000 to 20,000. The working fluid used in the experimental study was air. The comparisons of fluid flow characteristics of the plain tube and the inserted tube were studied. The results showed that the Nu for S-shaped copper inserts tube increased from 1.001 to 1.736 and f factor increment was from 1.006 to 1.26 higher than the plain tube. The friction factor for copper S-shape inserts was higher than f factor for a plain tube and that was observed for all configurations. The thermal performance factor for 90°, 120° and 180° S-shape copper insert was changed from 1 to 1.74 which means that the performance inside the tubes can be developed using inserts. This also manages liquid mixing and refines the thermal layers and also gives enhanced heat transfer.

#### **1.4.2. Water flow fitted with inserts**

Nagarajan and Sivashanmugam [17] investigated experimentally promoting heat transfer inside circular tube after adding 300 mm helical screw from left and right side with a spacer. The water was the working fluid used in this investigation. Reynolds numbers ranged from 1,000 to 10,000. The characteristics of friction factor and heat transfer were presented for a circular tube fitted with 300 mm helical screw from the right and left side with 100 mm space was left between the right and the left twist. Three various twist ratios were considered. The experimental outcomes were compared versus plain tube data, and the comparison showed that the coefficient of heat transfers had enhanced with the same effectivity for the two cases (right and left screw). The maximum heat transfer performance was observed at the lowest twist ratio and the highest Reynolds number. Also, the performance ratio of more than one indicated that

the type of twist inserts can be used effectively to develop heat transfer. Finally, the performance ratio was higher than one, which means twist inserts can be used effectively to develop the promotion of heat transfers.

Salman et al. [18] analyzed numerically the characteristics of heat transfer and friction factor inside a circular tube after inserting the horizontal baffles twisted tape. Swirl/vortex flow is one of the important methods of passive enhancement techniques. The twisted tape was used widely in heat exchangers and was considered as one of the important members of the passive model. Laminar flow under constant heat flux was considered in this CFD analyzes. Plain and baffled twisted tape was carried out using fluent program version 6.3.26. Two twist ratios were used for the plain twisted tape while one twist ratio was used for the baffled twisted tape. Good agreement with literature correlations for plain tube was seen with conflict lower than  $\pm 8$  %age for the Nusselt numbers and  $\pm 6.25$  for friction factor. Numerical analysis showed an increase in the Nusselt number with increasing Reynolds number and decrease of twist ratio. The maximum enhancements were observed at twist ratio equal 2.93 with baffling.

Oni and Paul [19] simulated numerically the thermal performance and heat transfer characteristics after inserting various twisted tapes inside various tubes designs of water turbulent flow. The aim was to find the best design to enhance heat transfer from compared the results with a plain tube. Reynolds numbers ranged from 5,000 to 20,000. Uniform wall flux was applied, the results showed that Nusselt number increased from 2.07 to 3.33 times and the friction factor from 10.65 to 13.1 higher than the plain tube and the thermal performance factor changed from 1.35 to 1.43 compared with plain twisted tape. When the alternate axis triangular with cut twisted tape was used, the better performance was obtained.

Patil et al. [20] studied experimentally the heat transfer enhancement in the circular tube after adding swirl flows generator under turbulent flow and uniform wall temperature. The water was the working fluid used in this studied. Two inserts were used in this study the first one was a wire coil and the second was screw-tape. The experimental results were compared with the plain tube and it showed enhanced heat transfer for all inserts. Increases of Nusselt numbers were related with the increment of Reynolds number and the highest one was 155 times bigger than that obtained in the plain tube and it was seen when a combination of screw-tape and wire coil was used

together. The friction factor decreased with increases in Reynolds number. Combined inserts gave the maximum Nu number and f factor at same Reynolds number.

Arulprakasajothi et al. [21] investigated experimentally the heat transfer influence after inserting conical strip inside a circular tube & laminar flow and two models of conical strips staggered and non-staggered were introduced as a turbulators in this investigation to look at behaviors with this change. Three various twist ratios (two, three and five) were carried out. The water was taken as the fluid used in this investigation. Two directions were used to distribute the conical strip; the first one was forward direction and the second was backward and both results were compared with a plain tube. The results showed that the conical strip inserts had contributed to increasing of the Nusselt number compared with a plain tube, and the best Nusselt number was recorded at twist ratio equal of 3 with staggered conical strip compared to the other strips.

Bhuyan et al. [22] investigated numerically the phenomena of heat transfer with and without rectangular inserts in a tubular shaped U-loop, finite element method was carried out in this investigation, and constant heat flux was taken. The water was considered as the working fluid. The dimensions of pipe were inner and outer diameter 26mm and 30mm respectively with the length of 1834mm. The rectangular inserts were coordinating on two models; the first was horizontal and the second was vertical. Firstly, the numerical simulation was carried out without insert, secondly, various combination of inserts (2, 4, 6, and 8) respectively were conducted. Two simulation methods (stationary, time-dependent) were carried out with total time of 180 s. The results showed that increasing the number of inserts led to the increment of transfer of heat at the same computational domain.

### **1.4.3. Nanofluids flow fitted with inserts**

Sundar & Sharma [23] determined experimentally the friction factor and the coefficient of convective heat transfer using  $\text{Al}_2\text{O}_3$ -water nanofluids in a smooth tube and with twisted tape insert with twist proportion bigger than 0, and less than 83. Under turbulent flow, Reynolds number values ranged ( $10000 \leq \text{Re} \leq 22000$ ) and different volume concentrations and temperatures were considered. The results indicated that at

0.5%  $\text{Al}_2\text{O}_3$ -Water nanofluid with twist ratio of five both of the (h) and (f) were higher than water results. At the end of the study, the regression equations of Nusselts number & friction factor were developed.

Eiamsa and Wongcharee [24] investigated experimentally the effects of used combined of CuO-water nanofluids with a micro-fin tube with double twisted-tapes (MF-DTs) on features: the rate of heat transfer, f. factor, and thermal performance. CuO-water volume concentrations were between 0.3 % and 1.0 %. Reynolds numbers ranged from 5,650 to 17,000. Also, an experiment was conducted for micro-fin tube alone (MF) and single twisted tape (MF-ST) for comparison purposes with results obtained. The results showed that the increase in heat transfers rate was comparatively proportional to the increased concentration of nanofluid volume fractions. When the working conditions were stable, thermal performance for micro-fin with double twisted tapes (MFDTs) was better than the thermal performance resulting from the use of one twisted tape (MF-ST). Finally, combined techniques could save energy with beneficial effect.

Saeedinia et al. [25] studied experimentally pressure drops and heat transfer features for CuO- Oil nanofluids flow in a tube with constant heat flux and laminar flow with five different coil wires inserted with pitches ranging from 25 to 35 mm. The volume concentrations range was from 0.07 % to 0.3 %. The results were 45% increment of heat transfers coefficient, and 63% pressure drop was obtained via highest Reynolds number with the highest wire diameter inside the tube. Because the heat transfer enhancement techniques were accompanied by the increase in flow pressure drop, the total performance of these ones was evaluated at several Re numbers. At the last, two empirical correlations with an error range ( $\pm 20$  %) were developed depending on the experimental data for predicting the Nusselt number and friction factor.

Kahani et al. [26] investigated experimentally the effect of both curvature ratio and the spacing of coil pitches on pressure drop and heat transfer behavior after using  $\text{Al}_2\text{O}_3$ /Water Nanofluid with helical coil insertion inside the tube under the laminar flow condition. In this study, ten and twenty were considered as the values of curvature ratio for coils while the coils pitch were 24 and 42 respectively. In the experiment, from 0.25 to 1 % was the varied ratio of nanoparticles. Nanofluids showed that when using any value from concentrations, the heat transfer rate was much higher, also, the same thing

happened to pressure drop compared with purified water. In addition, a significant improvement in the rate of heat transfers was observed when using curvature of coils as well as pressure drops when helical coils were used. The results recorded that the heat transfer rate improved proportionally to the increase of pitch coils and when the curvature ratio decreased.

Ramteke, and Ate [27] studied experimentally the heat transfer behavior of pure water and  $Al_2O_3$ -Water nanofluids in a circular tube with inserts (twisted tape with different twist ratios) and without inserts.  $Al_2O_3$ -Volume fractions was in the range of  $0 < \phi < 0.5$  % and twist ratio for the twisted tape was  $0 < H/D < 1$ . The results indicated an increment in the heat transfer coefficient at the higher volume concentration of nanofluids and lowest twist ratio of twisted tape.

Eiamsa-ard et al. [28] investigated experimentally and numerically promoted heat transfer when using titanium dioxide as a working fluid in heat exchangers tubes with overlapped double twisted strips. A combination of titanium dioxide and water was used with the addition of double overlapping twisted strips in order to promote heat transfer. The range used in the study for Reynolds Number was from 5400 to 15,200. The values (1.5), (2.0) and (2.5) represented overlapped twist ratios for the double twisted strips that were adopted in the experiment. In addition, the values (0.07%), (0.14%) and (0.21%) described the concentrations of  $TiO_2$  in this research. The empirical and numerical results recorded an increase in swirl intensity and turbulent kinetic energy when using overlapped double twisted tapes with the lowest overlapped twist ratio. When using overlapped double twisted strips with the overlapped twist ratio (1.5) and after comparing the consequences with those taken when using the plain tube, the comparison showed that heat transfers rate improved by 89%, friction factor increased by 5.43 times, and thermal performance increased by 1.13 times. In addition, the increase of heat transfer was proportional to the increased concentration of titanium dioxide in water due to the increased thermal conductivity.

Mirzaei, and Azimi [29] studied experimentally pressure drop and heat transfer characteristics of using graphene oxide-water nanofluids flow in a circular tube with wire coils. The range used in the experiment for Reynolds Number was between 600 and 7,000. All the tests were conducted on the basis that the pipe wall was under Constant heat flux. The performance of heat transfers, as well as the pressure drop, were

investigated when using the nanofluids depending on the design of the experimental settings. Graphite oxide was made using the Hummer method and identified by the immediate use of infrared spectroscopy, the diffraction in X-ray and electron microscopy. Three-volume concentrations (0.02%), (0.07%), and (0.12%) were equipped to separate graphene oxide in the water and nanofluids. Volumetric flow rate of nanofluids was arranged at 6, 8, and 10 liters/min. Appropriate equations based on average temperature were applied in order to calculate the physical thermal properties of water flow and nanofluids. These properties were employed for each experiment in order to calculate the coefficient of heat transfers and the Nusselt number as well as the factor of friction. In the end, depending on the results obtained from the practical experiment, the correlations were corrected for the Nusselt number and the friction factor. The empirical data have shown a good agreement with those expected. The results showed that mixing 0.12 % of water graphene oxide enhanced the heat transfer coefficient 77 %%. As a result, we can conclude that the use of graphite oxide with water achieved an increase in thermal efficiency and therefore can be used in heat transfer devices.

Sadeghi et al. [30] investigated numerically the heat transfer features when using nanofluids under laminar flow in the circular tube with helical wire inserts. The wall for test section was supported with a uniform flux of heat. Momentum, continuity, energy equations with SIMPLE algorithm were used to solve the coupling between pressure and velocity within the plain tube domain. From 1.95 to 4.89 representing the limitation of various twist ratios, various kinds of nanoparticles were used which include aluminum oxide ( $\text{Al}_2\text{O}_3$ ) and silicon dioxide ( $\text{SiO}_2$ ). In this study, three shapes of nanoparticles were adopted which were spherical, platelets and cylindrical. Also, nanoparticle concentrations ranging from 0.5 to 2.0 were applied for mixing with water to obtain nanofluid, while the diameter of nanoparticles ranged from 20 to 50 nm. All values above were employed to identify their influence on heat transfer features when using nanofluids under laminar flow in the circular tube with helical wire inserts. Results for all studied cases showed that the increase in the Nusselt numbers occurred whenever the Reynolds number increased and decreased the twist ratio.

Andreozzi et al. [31] investigated numerically the forced convection improvement after inserting the transverse ribs with nanofluids flow in a channel. A

combination of aluminum oxide and water under turbulent flow was used in a symmetrical hot channel fitted with ribbed. For rib designs, three geometric shapes (rectangle, triangle, and trapezoid) were adopted and examined. The variety utilized in the simulations for Reynolds Number was between 20,000 and 60,000. Various nanoparticle concentrations were used starting from 0% and ending at 4% for mixing with water to obtain nanofluid. The two-dimensional model of the channel and mixture model representing the behaviors was used in the governing equations in addition to the wall of the channel which was under the uniform flux of heat. FVM was used to set the model of equations. As a general conclusion, it was observed that the rate of heat transfers increased as the fraction of nanoparticle sizes increased and the Reynolds number but the larger pumping was required. A comparison of the results indicated that the performance of the triangular ribs was higher than that resulting from the use of trapezoidal but high-pressure losses was also observed. Finally, the rib shapes (rectangle and trapezoidal) gave the best thermal performance when the height of the pitch-rib was ten.

Vazifeshenas et al. [32] numerically investigated extremely turbulent flow heat transfer augmentation inside circular tube after adding adjusted shapes of twisted tape and nanofluid. The three-dimensional numerical simulation using FVM was carried out to cover the problem. In order to optimize the performance of the tape, the aluminum oxide particles were added in different concentrations to the water. The results revealed that only using center-cleared 14cm enhanced Nusselt number approximately 22 % and it made increment in friction factor about 13 %, also improvement happened after mixing 0.1 % of aluminum oxide with water and the increment in Nusselt number became 26 % instead of 22 %.

## 1.5. Thesis objectives

The objectives of three-dimensional, steady-state numerical investigation of turbulent flow inside a tube fitted with pentagon rings inserts are listed below:

- 1) To record geometrical parameter effects after using pentagon rings inserts with and without using ( $Al_2O_3$ -Water) nanofluids on thermal and flow field.



- 2) To record the difference in impacts from different distributions for Pentagon rings on thermal and flow field.
- 3) To record the difference in impacts from using three different concentrations of nanoparticles on the thermal and flow fields.
- 4) To record the effect of six different Reynold numbers on flow and thermal performance.

### **1.6. Thesis scope**

The three-dimensional numerical investigation examines the steady state of the turbulent flow of working fluids (water and nanofluid) inside a tube fitted with Pentagon inserts rings. The present study's scope is as follows:

- 1) Reviewing the literature on properties of nanofluid.
- 2) Reviewing the literature about heat transfers properties of various types of inserts with various geometric shapes.
- 3) Using the ANSYS Design Modeler for modeling and ANSYS Meshing for meshing the tube with Pentagon rings inserts.
- 4) Using (CFD) in ANSYS FLUENT 14.5 software to model the internal nanofluid flow in the tube with Pentagon rings insert.
- 5) Using different pitch length of  $d$ ,  $2d$ , and  $3d$ .
- 6) Using nanofluid type  $Al_2O_3$ .
- 7) Using three values of nanoparticle concentrations (1.5, 3.0, and 4.5 %).
- 8) Calculate Nusselt number, the factor of friction, and the performance evaluation analysis ( $\eta$ ) for all the problems in this study.

## CHAPTER 2

### MATERIALS AND METHODS

#### 2.1. Flow in circular tubes

In internal movement, however, the fluid was completely limited by the internal surfaces of the pipe, and therefore there's a limit how much the boundary layer can grow. Cengel [33]. You likely have pointed out that most essential fluids, especially liquids, are carried in round pipes. It is because pipes with a round cross-section can resist the large pressure dissimilarities between your inside and the exterior without starting any distortion. For a constant surface area, the circular pipe provides the highest heat transfer for minimal pressure drop, which points out the overwhelming level of popularity of circular pipes in heat transfer machines. In general, circular flow parts are referred to as cross-sectional tubing (especially when fluid is liquid). Small size pipes are usually known as tubes. Although the idea of the fluid motion is acceptable, well known theoretical alternatives are obtained limited to a few simple circumstances like the completely developed laminar circulation in a circular pipe. Therefore, we should count on the experimental results and the empirical relationships obtained for some fluid movement problems somewhat than closed-form analytical alternatives. Noting that the experimental outcomes details are obtained under carefully handled laboratory conditions which no two systems are exactly likewise, we should not be so naive with regard to viewing the results obtained as exact. One of 10 % (or even more) in friction or convection coefficient was determined using the relationships. Perhaps we have to discuss that the friction between your fluid layers in a pipe may cause the small rise in

substance temperature because of mechanical energy being changed to thermal energy. The generated heat via the friction was pretty small and there was no consideration for its value so that it was ignored. For example, in the absence of heat transfer, it would not be possible to detect the difference between entry and exit temperatures of liquids flowing in the tubes. The primary outcome of friction in fluid movement was the pressure drop. Thus, it was fair to expect that any temp change in the fluid was because of the heat transfer. Yet, frictional heat must be looked at for moves that require highly viscous liquids with large speed gradients. In most useful applications, the movement of a fluid through a tube or duct can be approximated to be one-dimensional, and so the properties can be assumed to alter in one way only. Because of this, in the uniform flow pointed out, all properties are consistent with any cross-section normal to the movement direction, and the properties are assumed to possess bulk average values within the cross-section Cengel [33].

### **2.1.1. Velocity profiles**

The streams in the internal flow were not free, so an alternative must be found. The velocity of the liquid changed from zero to maximum. Velocity value at the surface was zero because there was non-slip of liquid and at the center of the tube was a maximum value. It was convenient to work with the mean velocity ( $V_m$ ) for non-compressible liquids that flowed steadily within the cross-section of the fixed tube. In actual applications of heating and cooling, the average speed may change due to changing the density related to the temperature changes. In practice, there was little loss in accuracy due to the treatment of fluid properties as constants in some average temperature for the convenience of work Cengel [33].

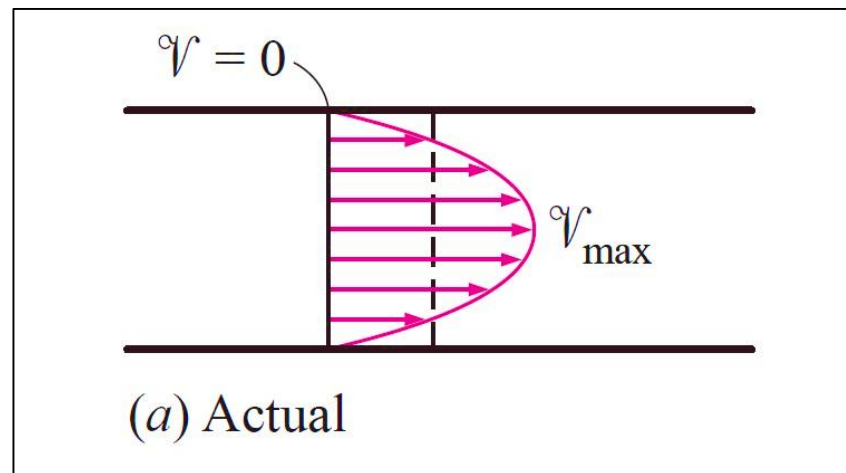


Figure 2. Actual velocity profiles for flow in a tube.

### 2.1.2. Temperature profiles

When a fluid is warmed or cooled as it moves through a pipe, the temps of the fluid at any combination section changes from  $(T_s)$  at the top of the wall for some maximum (or minimum in the state of heating) at the pipe center. In the fluid movement, it is convenient to work with the mean temperature  $(T_m)$  that remains uniform at a cross-section. Unlike the mean velocity, the mean temps  $(T_m)$  changes in the movement path whenever the fluid is warmed or cooled. Mean temperature  $(T_m)$  is defined from the demand that the conservation of energy basic principle is satisfied. That is, the vitality transferred by the fluid through a cross-section in actual circulation must match to the energy that might be transferred through the same cross-section if the substance were at a constant temperature  $(T_m)$  as outlined by Cengel [33].

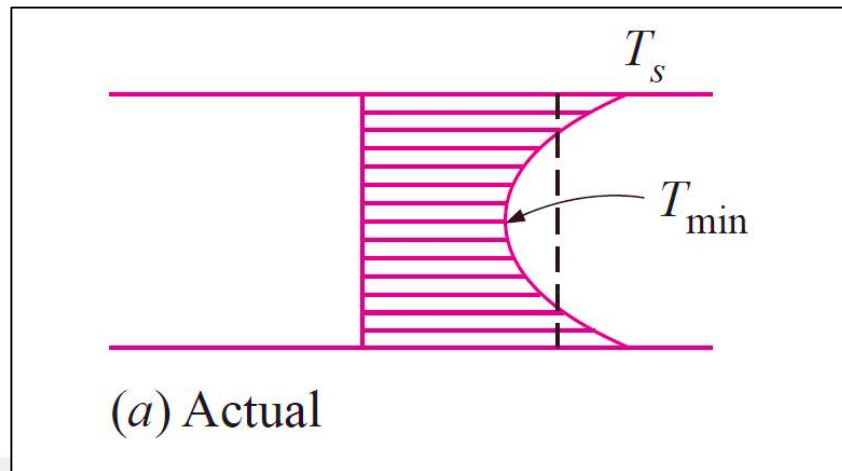


Figure 3. Actual temperature profiles for flow in a tube.

Internal flow characteristics resulting from fluid changes during heating and cooling are evaluated by calculating the mean temperature of the inlet and outlet.

$$T_b = \frac{T_{m,i} + T_{m,e}}{2} \quad (1).$$

### 2.1.3. Laminar and turbulent flow

The flow's conditions specifying the flow condition in the tube may be laminar or turbulent. The laminar flow is observed at low speeds, but turns into turbulent flow. If the liquid flow velocity exceeds the critical value, the shift to the disturbed state does not suddenly occur, but the flow begins to fluctuate between the laminar and the disturbance until achieving fully disturbed situation. On the practical side, most of the flows in the circular tubes are of the turbulent flow kind. The laminar flow is obtained by the flow of high viscosity liquids or fluid flow into narrow tubes, ducts or small diameters. Reynold's number to flow during the circular tube is described as:

$$Re = \frac{\rho V_m D}{\mu} = \frac{V_m D}{\nu} \quad (2).$$

Where  $V_m$  equals to mean fluid velocity,  $D$  equals to diameter of the tube, and  $\nu = \mu / \rho$  equals to kinematic viscosity of the fluid.

In most practical situations, the flow inside a tube is laminar if  $Re < 2300$  and it will be turbulent if  $Re > 10,000$  and the transitional region is between these limitations, which is outlined by Cengel [33] as shown below:.

$Re < 2300$

Laminar flow.

$2300 \leq Re \leq 10,000$

Transitional flow.

$Re > 10,000$

Turbulent flow.

In the case of the transition flow, the flow changes randomly between the laminar and turbulent, as presented in figure 4 below.

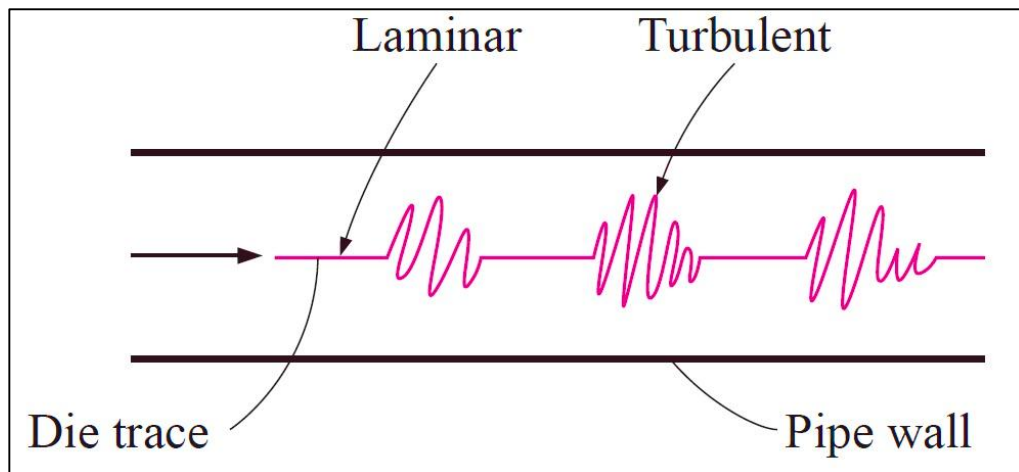


Figure 4. Transitional flow region.

### 2.1.4. Velocity boundary layer

The velocity of the boundary layer develops along the tube and increases in the direction of the flow until it reaches the center of the tube and thus fills the entire tube, as presented in figure 5 below.

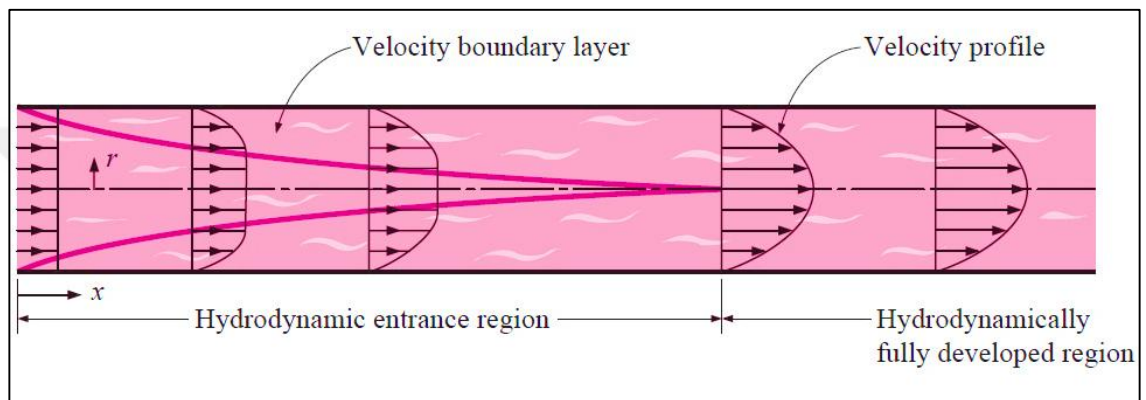


Figure 5. Velocity boundary layer.

The area from the pipe entrance to the point where the boundary layer is integrated into the center is called the hydrodynamic input area, and the length of this area is called the length of the hydrodynamic entry ( $L_h$ ). The flow in the input zone is called hydrodynamic flow development because this is the area where the speed profile develops. The area outside the entrance area where the speed profile is fully developed and remains unchanged is called the fully developed hydrodynamic zone. The velocity profile in the fully developed region is equivalent to the laminar flow and is somewhat flatter in the turbulent flow due to vortex movement in the radial direction [33].

### 2.1.5. Thermal boundary layer

Now, suppose that the liquid at a steady temperature coming into a circular pipe whose surface is preserved at a varying temperature. This time around the fluid particles in the level in touch with the top of the tube will consider the surface heat. This will start convection heat transfer in the pipe and the developed thermal boundary layer along the pipe. The thickness of the boundary layer also boosts in the movement direction till boundary layer extends to the tube center and so fills the complete pipe, as shown in figure 6 below [33].

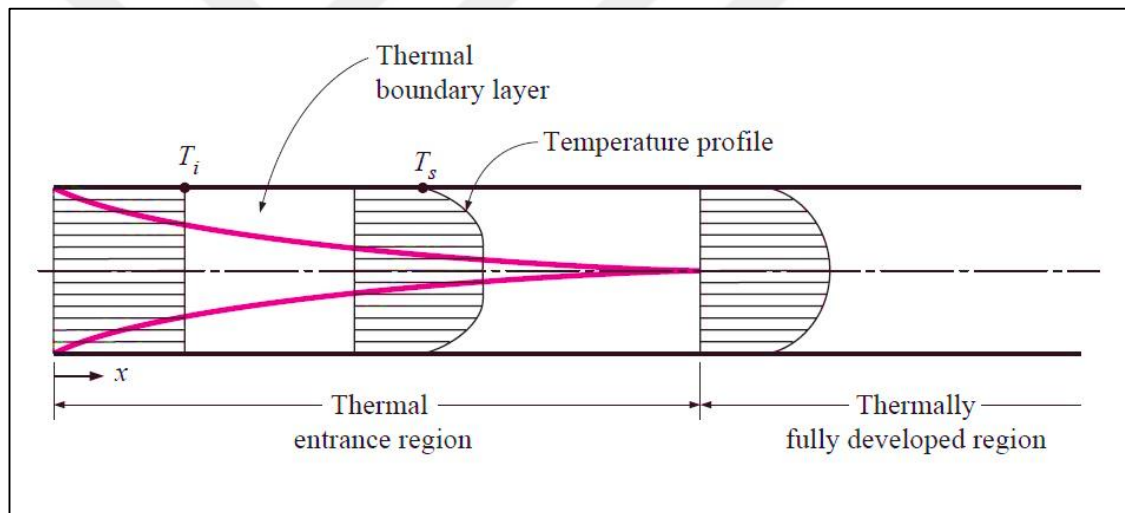


Figure 6. Thermal boundary layer.

The flow zone in which the thermal boundary layer develops and reaches the center of the tube is called the thermal input zone. The length of this zone is called the thermal input length ( $L_t$ ). The flow in the thermal input zone is called thermally developing flow because this is the area where the temperature profile develops. The area outside the thermal input area where the undetermined temperature expressed is called the fully developed zone as  $(T_s - T) / (T_s - T_m)$  is still unchanged [33].



### 2.1.6. Entry length in turbulent flow

In practice, it is generally agreed that the effects of the input are limited to the length of a 10-diameters tube, and the hydrodynamic and thermal input lengths are approximately taken to be as below [33].

$$L_{h, \text{ turbulent}} \approx L_{t, \text{ turbulent}} \approx 10D$$

The development of the turbulent flow in the input area, the lengths of entry to the turbulent flow are usually short, often only 10 diameters tube long, so the Nusselt number set for fully developed turbulent flow can be almost used for the entire tube. This easy approach provides logical outcomes for pressure drop and heat transfer for long pipes and stable outcomes for short ones. Correlations are available in the literature in order to obtain better accuracy when calculating heat transfer coefficient and friction. Cengel, 2003, page 463 [33].

### 2.1.7. Turbulent flow correlations for a smooth tube

We have already pointed out that fully turbulent in the smooth tubes occurs when Reynolds number is more than ten thousand. Due to existence of the difficulty in dealing with the turbulent flow theoretically, most of the correlations of friction and heat transfer in the turbulent flow are based on empirical studies. Also, the reason for the traditional use of turbulent flow in practice is due to the largest heat transfer coefficients observed when used [33].

#### 2.1.7.1. Pure fluids correlations

##### a. First Petukhov equation

The friction factor can be determined in the turbulent flow of the first explicit Petukhov equation [34] as shown below:

$$f = (0.790 \ln Re - 1.64)^{-2} \quad (3).$$

$$(10^4 < Re < 10^6)$$

The Nusselt number in the turbulent flow is linked to the friction factor by Chilton–Colburn measurement as follows:

$$Nu = 0.125 f Re Pr^{1/3} \quad (4).$$

If the friction factor is available, this equation allows utilizing appropriately to evaluate the Nusselt number for rough and smooth tubes.

### b. Colburn equation

For the turbulent flow that has been fully developed in the smooth tubes, a simple relationship can be reached for the Nusselt number by substituting the simple power law relationship ( $f = 0.184 Re^{-0.2}$ ) for the friction factor in the equation 4 given above.

$$Nu = 0.023 Re^{0.8} Pr^{1/3} \quad (5).$$

$$(0.7 \leq Pr \leq 160)$$

$$(Re > 10,000)$$

### c. Dittus -Boelter equation

$$Nu = 0.023 Re^{0.8} Pr^n \quad (6).$$

Where  $n = 0.3$  to cooling and  $0.4$  to heating for liquids flow into the tubes. This equation which is preferable to the Colburn equation is recognized as Dittus - Boelter [35]. Fluid properties are estimated depending on ( $T_b$ ). When the temperature variation between the liquid and the wall is very large, it may be necessary to use a correction factor to calculate the different viscosity near the wall and the center of the tube. The Nusselt number relationships above is somewhat simple, but they perhaps give as large errors as 25 %.

#### d. Second Petukhov equation

The error in the Dittus - Boelter equation can be greatly reduced to less than 10 % using more complex but precise relationships such as the second Petukhov equation expressed below:

$$Nu = \frac{\left(\frac{f}{8}\right) Re Pr}{1.07 + 12.7 \left(\frac{f}{8}\right)^{0.5} \left(Pr^{\frac{2}{3}} - 1\right)} \quad (7).$$

(0.5 ≤ Pr ≤ 2000)  
(10<sup>4</sup> < Re < 5 × 10<sup>6</sup>)

#### e. Gnielinski's equation

The accuracy of second Petukhov equation have been adjusted by Gnielinski [36] to suit with lower Reynolds numbers as shown below:

$$Nu = \frac{\left(\frac{f}{8}\right)(Re - 1000) Pr}{1.07 + 12.7 \left(\frac{f}{8}\right)^{0.5} \left(Pr^{\frac{2}{3}} - 1\right)} \quad (8).$$

(0.5 ≤ Pr ≤ 2000)  
(3 × 10<sup>3</sup> < Re < 5 × 10<sup>6</sup>)

#### f. Blasius equation

To measure the friction factor for pure fluids, Blasius [37] suggested the relationship below:

$$f = 0.316 Re^{-0.25} \quad (9).$$

(3000 < Re < 10<sup>5</sup>)

### 2.1.7.2. (AL<sub>2</sub>O<sub>3</sub>-Water) nanofluid correlations

#### A. Pak & Cho. [38] Experimental study

$$Nu = 0.021 Re^{0.8} Pr^{0.5} \quad (10).$$

(  $0 < \phi < 3.0 \text{ Vol } \%$  )  
 (  $10^4 < Re < 10^5$  )  
 (  $6.5 < Pr < 12.3$  )

#### B. Maiga et al. [39] numerical study

$$Nu = 0.085 Re^{0.71} Pr^{0.35} \quad (11).$$

(  $0 < \phi < 10.0 \text{ Vol } \%$  )  
 (  $104 < Re < 5 \times 10^5$  )  
 (  $6.6 < Pr < 13.9$  )

#### C. Vajjha et al.'s [40] experimental study

Three types of nanofluids experiments were conducted under constant heat flux, and the following heat transfer relationship was proposed for flow in a turbulent regime and this correlation is similar to a well-known Gnilinsky equation for a single phase as presented below.

$$Nu = 0.065(Re^{0.65} - 60.22)(1 + 0.0169 \phi^{0.15})Pr^{0.542} \quad (12).$$

(  $0 < \phi < 10.0 \text{ Vol } \%$  )  
 (  $3000 < Re < 1.6 \times 10^4$  )

To express the friction factor of nanofluids, they formed an equation that copied the well-known Blasius equation in the case of degeneration of the base fluid.

$$f_{nf} = 0.3164 Re_{nf}^{-0.25} \left( \frac{\rho_{nf}}{\rho_{bf}} \right)^{0.797} \left( \frac{\mu_{nf}}{\mu_{bf}} \right)^{0.108} \quad (13).$$

## 2.2. Useful parameters

In this section, some useful parameters for turbulent fluid flow in circular tubes such as (Prandtl number, turbulent intensity, heat transfer coefficient, pressure drop, Nusselt number, performance evaluation analysis) are defined and presented.

### 2.2.1. Prandtl number

It represents the better explanation of the relative thickness of the speed and thermal boundary layer, via dimensionless parameter, which is defined as follows:

$$Pr = \frac{\text{Molecular diffusivity of momentum}}{\text{Molecular diffusivity of heat}}$$

$$= \frac{\nu}{\alpha} = \frac{\mu C_p}{k} \quad (14).$$

### 2.2.2. Turbulent intensity

The intensity of the flow disturbance in the center of the tube within the fully developed zone is estimated as follows:

$$T.I = 0.16 Re^{-0.125} \quad (15).$$

### 2.2.3. Heat transfer coefficient.

The convective heat transfer coefficient ( $W/m^2.k$ ) through the tube is defined as:

$$h = \frac{\dot{q}}{T_w - T_b} \quad (16).$$

Where  $\dot{q}$  represents the uniform heat flux which is applied to the test section wall,  $T_w$  and  $T_b$  represent the wall temperature and bulk temperature of the fluid.

### 2.2.4. Pressure drop

The pressure drop ( $\Delta P$ ) is the pressure difference along the tube between the inlet and outlet pressure, and in fluid mechanics, the pressure drop is a positive value and can be defined as follows [33].

$$\Delta P = P_1 - P_2 \quad (17).$$

In practice, it was found appropriate to express pressure drop for all models of internal flows.

$$\Delta P = f \frac{L}{D} \frac{\rho v^2}{2} \quad (18).$$

### 2.2.5. Nusselt number

The Nusselt number can be calculated via:-

$$Nu = \frac{hD}{k} \quad (19).$$

### 2.2.6. Friction factor

Darcy friction factor presented by Kijjarvi [41] for turbulent flows in a circular pipe is defined as follows:-

$$f = \frac{2 D \Delta P}{\rho L v^2} \quad (20).$$

### 2.2.7. Performance evaluation analysis

The performance evaluation analysis ( $\eta$ ) introduced by Maddah et al. [42] is defined as the enhanced convective heat transfer coefficient ( $h_E$ ) to the non-enhanced one ( $h_{NE}$ ) at the same pumping power.

$$\eta = \left( \frac{h_E}{h_{NE}} \right) \quad (21).$$

### **2.3. Computational fluid dynamic (CFD)**

In order to save time and reduce the required effort in the laboratory, this program (CFD) is used to examine the systems including fluid flow such as heat transfer, chemical reactions, mass transfer, etc. by computer-based simulations and solving mathematical equations responsible for these processes using numerical methods as well as algorithms. This technology is very strong and extends a wide range. And also for the purpose of solving fluid flow problems easily all commercial packages of this program contain advanced user interfaces to introduce problem parameters and then obtain results and analysis in the form of engineering data which can be used in new studies or in redesigning the program for product development purpose and making it capable of troubleshooting. The mechanism of action of the CFD codes program is contained in three main steps outlined by Versteeg and Malalasekera [43].

#### **a) Pre-processor**

Pre-processing is summarized as follows: The program user enters the flow problem by using the software interface to create the geometrical form (the arithmetic field) and the establishment of the grid or what is known as the cell sub-division, and then defines the boundary conditions of the flow problem which include the characteristics of liquid, velocity, pressure and other conditions. The accuracy of the program depends on the number of cells in the grid so that the solution accuracy can be better if the number of cells are more and vice versa, also depends on the specifications of the computers used for this purpose, the high specifications of the computer are better because when using the high specifications, it can analyze the same problem with less time. Typically, unstructured grids are usually more accurate than structured ones, which is due to the possibility of dividing cells into areas where there is a significant change in flow in the case of unstructured grids. Actually, this depends mainly on user skills in grids design, 50% of the time is devoted to the definition of domain geometry and grids generation so great efforts are made by the software manufacturer to solve this problem and develop the program so that it is able to adapt to the problem and improve the grid automatically [43].

**b) Solver**

There are three main methods followed by the program in the numerical solution, namely the finite difference method, finite element method and spectral methods. Importance will be placed on the finite volume method only. This method differs from the other methods because it allows control of the level of integration. In addition, it has a simple concept to understand by engineers. Steps of the numerical algorithm are summarized as follows:

- 1) Integrating the governing equations of fluid flow.
- 2) Discretization - convert the integral equations to algebraic equations.
- 3) Algebraic equations are solved in a repetitive manner because underlying physical phenomena are complex and nonlinear so the approach of solution requires repetition.
- 4) Convergence in solution is important to ensure solving partial differential equations accurately [43].

**c) Post-processor**

It is used to show the results of numerical analysis in the form of images and diagrams. Vector or contour plots which can show many characteristics of flow such as the direction of speed or pressure or kinetic energy and other properties with the possibility of magnification and rotation and coloring and many advantages that will show the results clearly [43].



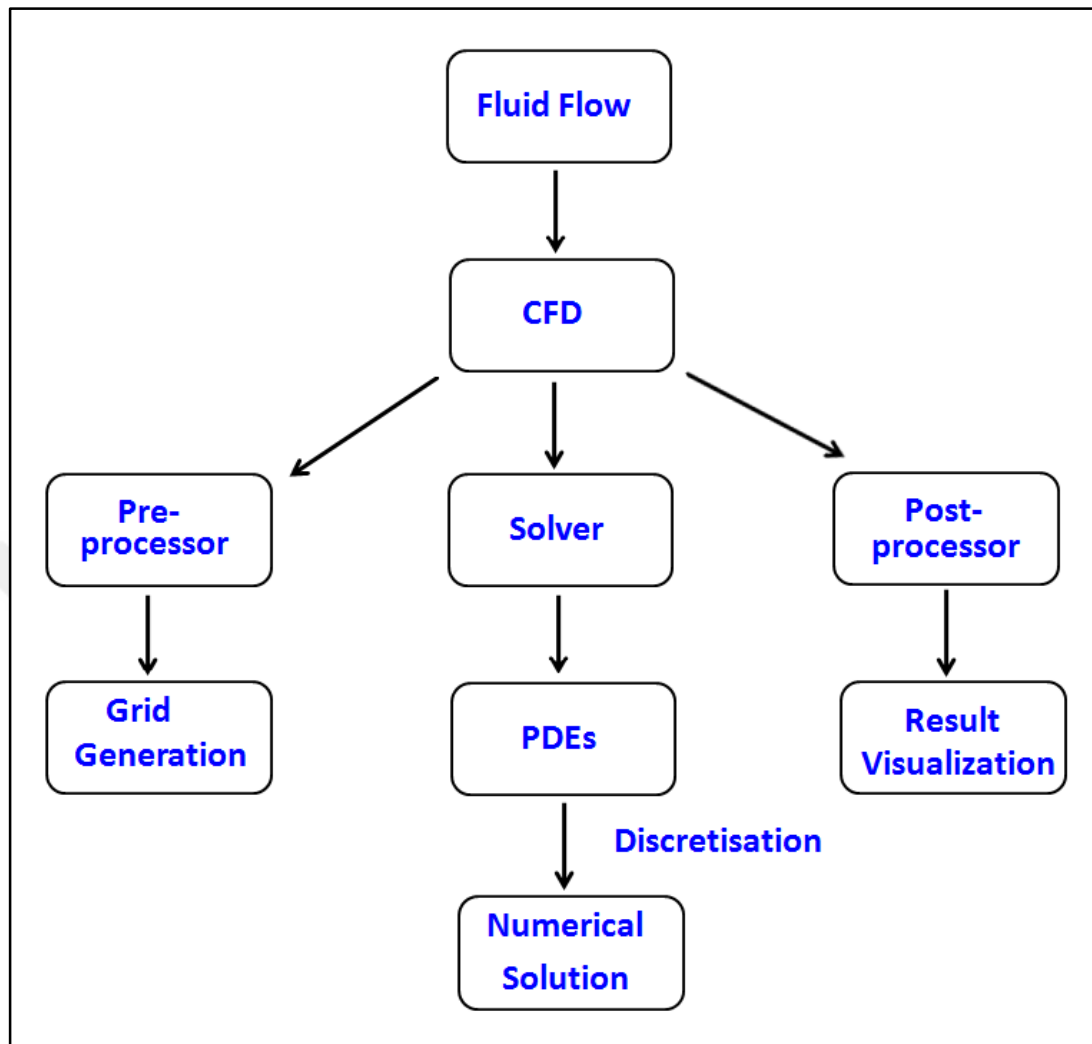


Figure 7. Overview of CFD [44]

### 2.3.1. Finite volume method (FVM)

In FVM, the arithmetic domain is separated into a limited number of items known as controllers. The governing equations for fluid flow are combined and resolved repeatedly based on the conservation laws of each control volume. The partitioning process produces a set of algebraic equations that solve the variables on a specified number of points within the controllers using the integration method. By integrating the control volumes, the flow around the domain can be quite modeled. This method can be used for structured and unstructured meshes. The style of this method of direct integration makes it more efficient and easy to program in terms of developing the CFD code.

As a result, the use of this method in CFD is common compared to other methods Suggested by Patel [44]. In the program CFD, there are two versions of FVM proposed by Stenmark [45] as follows:

### **2.3.1.1. Center node-based (FVM)**

At the node center on the VFM basis, the arithmetic domain is divided into a grid where each element in a grid forms the volume of the control. Integration of transport equations is performed above each controller volume and is calculated to obtain one set of algebraic equations for each controller cell. This method technique involves storing the variable value in a node located in the center of the cell. In addition, the discretization of equations also includes the cell face. Therefore, we use interpolation methods to get approximate values in these positions. The selection of interpolation approach has an important impact on numerical stability, Convergence rate, and accuracy according to Stenmark [45].

### **2.3.1.2. Vertex-based FVM**

In a vertex based FVM, control volumes are built around each grid vertex, that is, every cell corner. The grid vertices are additionally used to store the variables. Similarly, as inside the vertex-based approach, the governing equations are integrated over each control volume. Be that as it may, since a control volume exists in a few grid elements, discretization is done inside every element and afterward the properties are allocated to the similar control volume. To determine the discretized equations features are required for other positions than the grid vertices. Approximations are required and in the vertex-based approach, the idea of finite element shape functions is utilized to acquire these approximations. The presence of the shape capacities relies upon the element sort [45].

## 2.4. Configuration and assemblification of shapes

In this part, the figures configuration of current study model was simply described. The pre-processor SOLIDWORKS 2017 student version was used to create the geometry and for models assembly. Three typical formations of pentagon rings fitted with three different pitch lengths combined with ( $\text{Al}_2\text{O}_3$  - water) nanofluids flow were studied in a hot horizontal circular tube. The tube has diameter ( $D$ ) mm, and the length of the tube was ( $L$ ) mm. An entrance section length ( $L_1$ ) mm was modeled as a ( $10D$ ) to supply fully developed flow at the inlet of the test region, the test section length was considered as a ( $L_2$ ) mm, and an exit section length ( $L_3$ ) mm was selected as a ( $5D$ ) to defect the reverse flow effect in the numerical study. Tube dimensions were diameter = 50 mm, entrance section = 500 mm, test section length = 1500 mm and exit section = 250 mm. Figures 8 and 9 schematic diagrams of the problem statement depicted the dimensions of the tube used in this research.

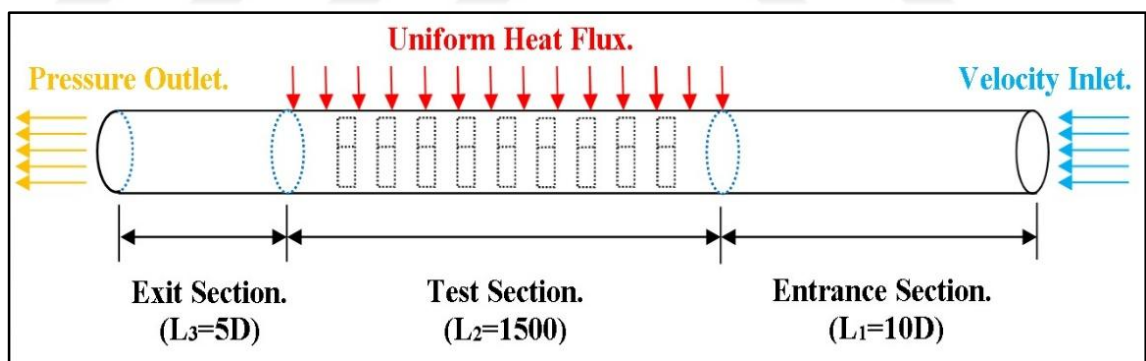


Figure 8. Schematic diagrams of the problem statement.

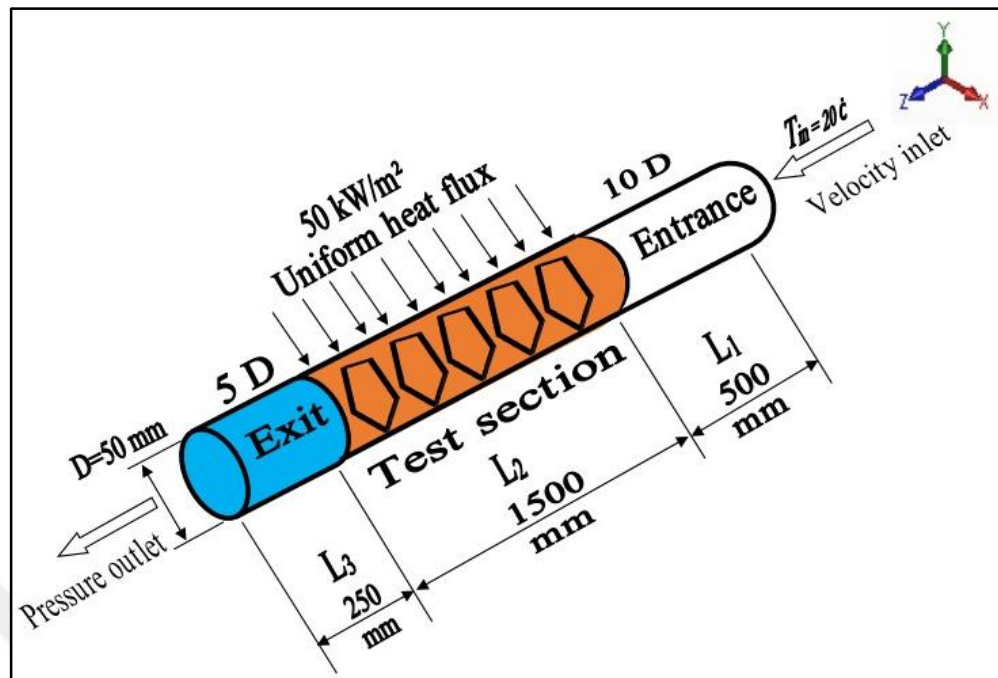


Figure 9. Schematic diagrams showing the dimensions of tube sections.

The pentagon ring had five sides, the outer and inner circumscribed circles dimensions were described for drawing purpose with SolidWorks program. The Pentagon ring also had a width (W), figure 10 shows the dimensions of pentagon ring used in this research.

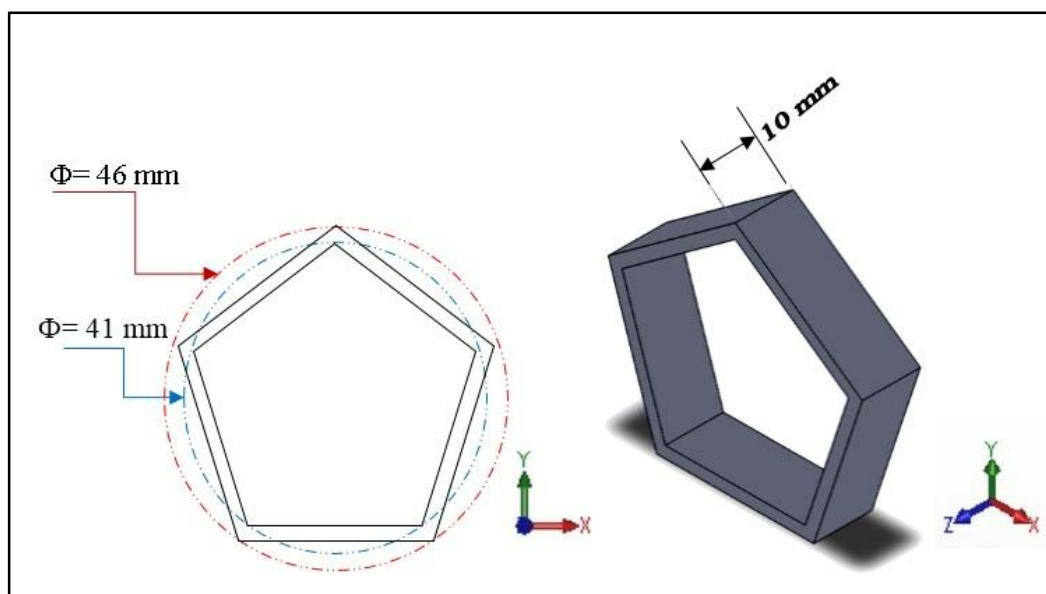


Figure 10. 3D view shows the dimensions of pentagon ring.

For the purpose of assembling shapes, the Solidworks 2017 program was used to distribute pentagon rings inside smooth tube test section. Pentagon rings were inserted according to three pitch lengths ( $d$ ,  $2d$ ,  $3d$ ), and the observed numbers of pentagon rings inside test section were 29, 14, 9 respectively, as shown in figure 11 below. The pitch length (PL) is defined as the axial length (Z) or space between pentagon rings that is assumed to find distributing range, distributing range is defined as the number of space between pentagon rings, distributing range (DR) = full test section length / PL.

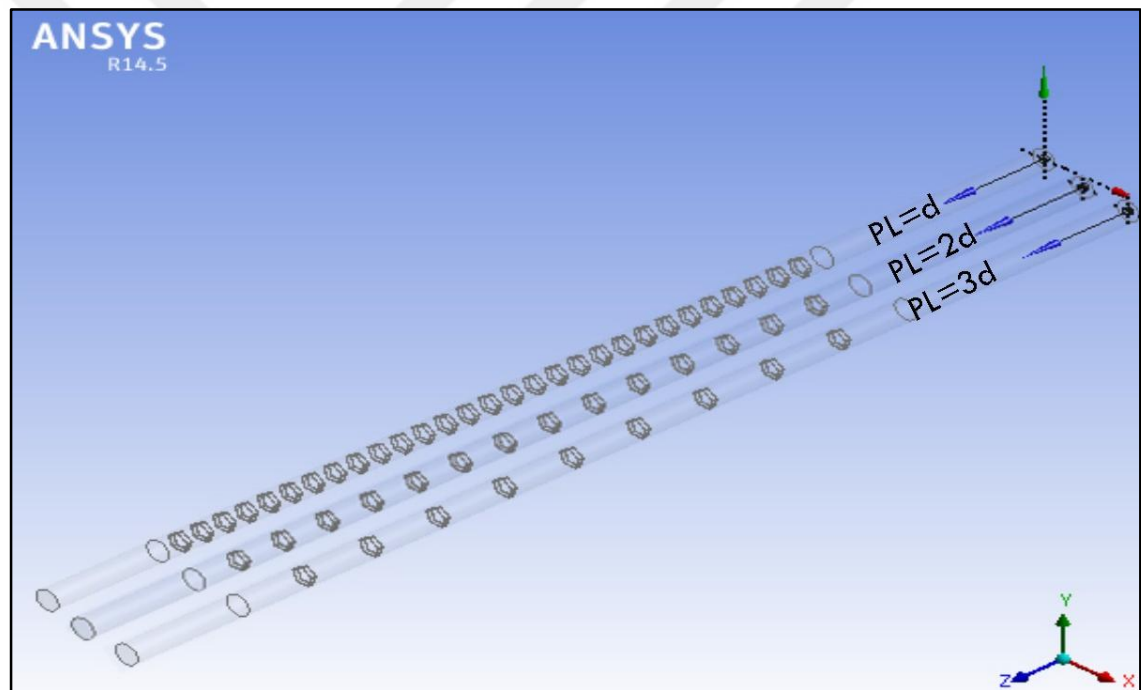


Figure 11. 3D view showing distribution of the pentagon rings.

The distribution method is detailed as follows:

1) When  $PL = d = 50$  mm.

$DR = \text{full test section length} / PL.$

$$= 1500 / 50 = 30.$$

Length from Entrance to first pentagon ring (LFE) = entrance length + (full test section length –  $DR * 0.5$  pentagon ring width) /  $DR.$

$$LFE = 500 + (1500 - 30 * 5) / 30.$$

$$= 500 + 45 = 545 \text{ mm}$$

Number of pentagon rings (NOPR) =  $DR - 1$

$$= 30 - 1$$

$$= 29$$

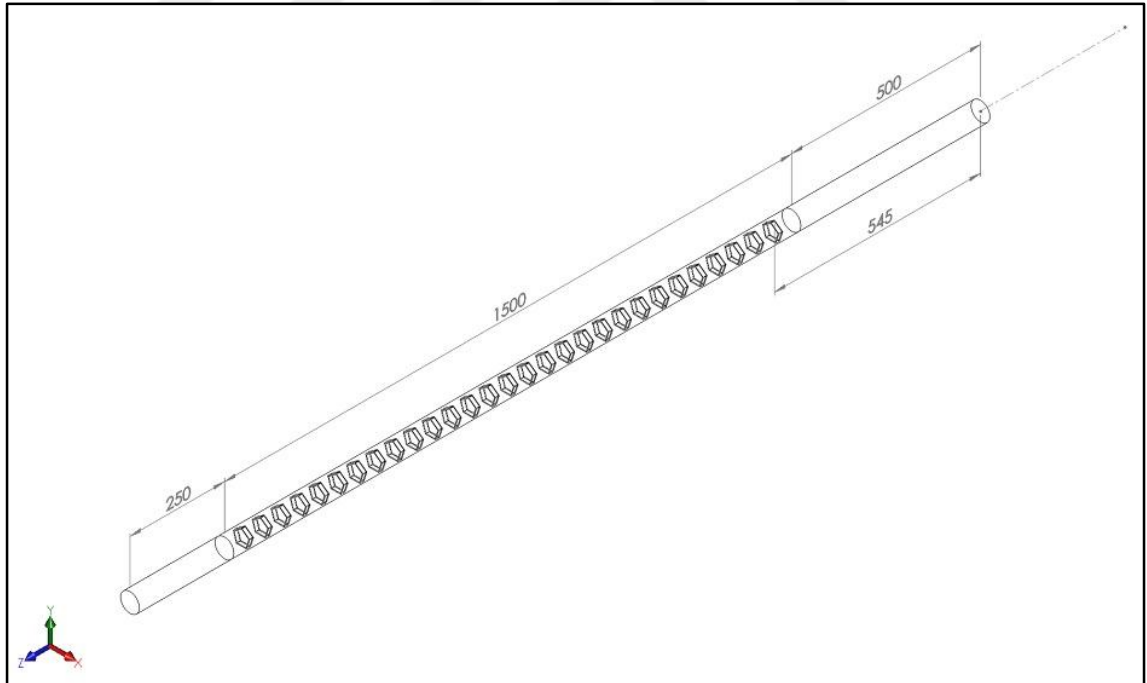


Figure 12. 3D view showing the distribution of 29 of pentagon rings inside test section.

2) When  $PL = 2d = 100$  mm.

$DR = \text{full test section length} / PL$ .

$$= 1500 / 100 = 15$$

Length from entrance to first pentagon ring (DFE) = entrance length + (full test section length –  $DR * 0.5$  pentagon ring width) /  $DR$ .

$$LFE = 500 + (1500 - 15 * 5) / 15.$$

$$= 500 + 95 = 595 \text{ mm}$$

(NOPR) =  $DR - 1$

$$= 15 - 1$$

$$= 14$$

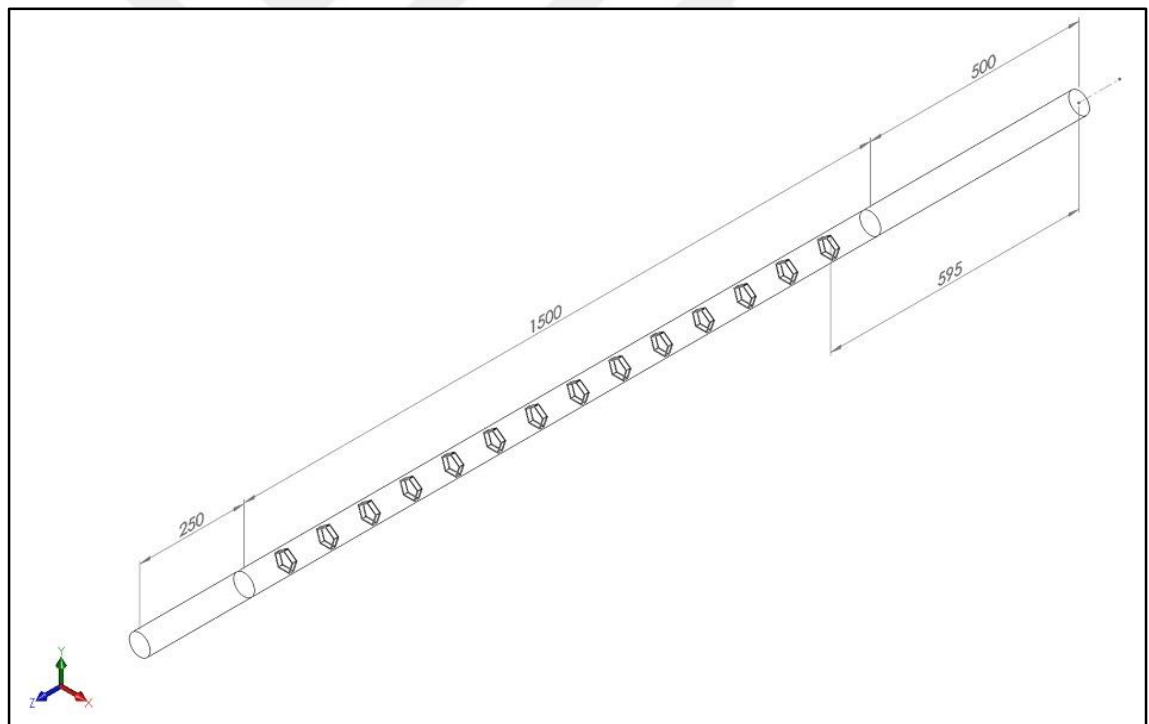


Figure 13. 3D view showing the distribution of 14 of pentagon rings inside test section.

3) When  $PL = 3d = 150$  mm.

$DR = \text{full test section length} / PL$ .

$$= 1500 / 150 = 10.$$

Length from entrance to first pentagon ring (DFE) = entrance length + (full test section length –  $DR * 0.5$  pentagon ring width) /  $DR$ .

$$LFE = 500 + (1500 - 10 * 5) / 10.$$

$$= 500 + 145 = 645 \text{ mm.}$$

(NOPR) =  $DR - 1$

$$= 10 - 1$$

$$= 9$$

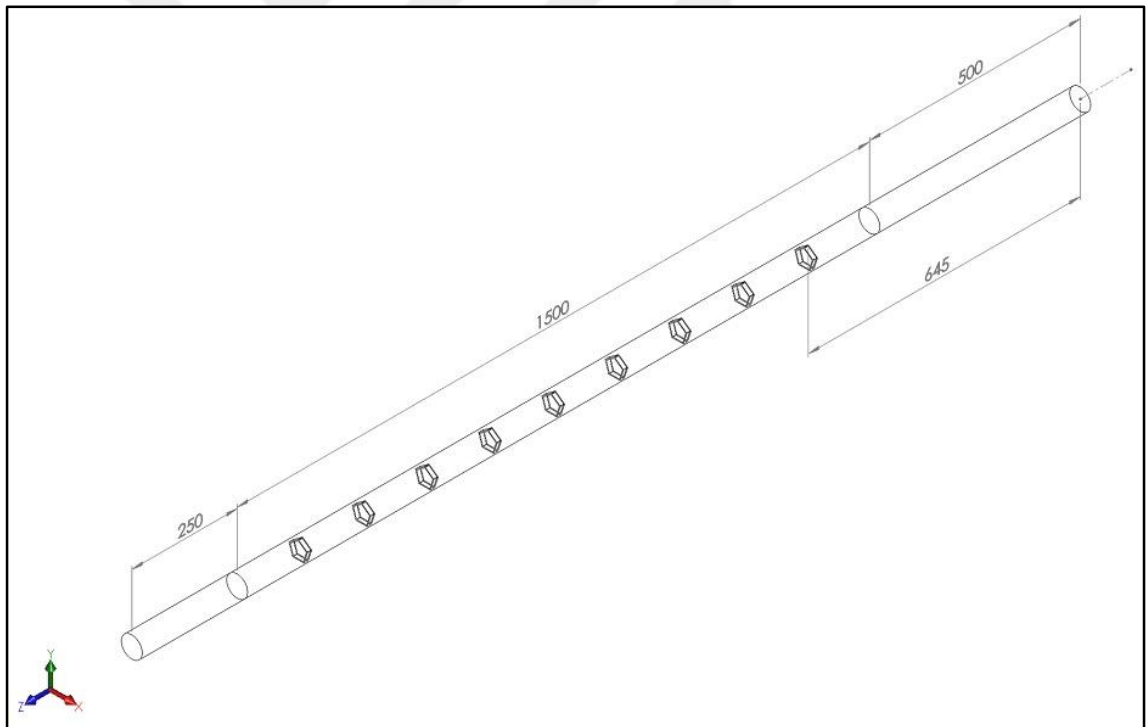


Figure 14. 3D view showing the distribution of 9 of pentagon rings inside test section.



## 2.5. Boundary conditions

The method of solving non-linear partial differential equations depended on the boundary conditions imposed to solve the problem. Below, we summarized the boundary conditions that were adopted in this study:

- At the pipe entrance, the velocity and temperature of the fluid were assumed as uniform, the velocity ( $V_z$ , in) was in the direction of the z-axis, the velocity values were based on Reynolds numbers and also on the thermophysical properties of the fluid. The fluid entry temperature was  $T_{in}=293.15$  K. The intensity of the disturbance was calculated from equation 15 previously mentioned in the subheading in 2.2.2. The hydraulic diameter was equal to the inner diameter of a tube ( $D=0.05$ m) because the outer diameter of tube was neglected in this study. All thermal properties were calculated based on the fluid temperature at the inlet section and, ( $T_{in}$ ) was considered as the reference temperature for this study.
- In the pipe exit, gauge pressure=zero was specified, and the analyzer extracted the other quantities of flow and measurement such as temperature and turbulent quantities from the internal domain.
- The length of entrance section ( $L1$ ) was assumed to be equal to  $10 \times$  of the diameter of the tube to provide a fully developed flow, the length of the test section ( $L2 = 1.5$  m) was assumed as in the previous experiment to ensure the solution methodology. Also, the length of exit section ( $L3$ ) was assumed to be equal to  $5 \times$  the diameter of the tube to prevent reverse flow.
- On the pipe wall, a non-slip boundary condition with uniform heat flux,  $\dot{q} = 50$  KW/m<sup>2</sup> was performed.
- Turbulent flow with Reynolds numbers ranging from 5000 to 15000 was performed.
- The ( $Al_2O_3$ -water) nanofluid volume fractions were assumed as  $\phi=1.5, 3,$  and  $4.5\%$ .
- Three different pitch lengths of pentagon rings ( $d, 2d,$  and  $3d$ ) were investigated.
- In addition, the inlet temperature of the fluid was used in all calculations in order to calculate the thermophysical properties of water and nanoparticles as well as nanofluids.

### 2.5.1. Governing equations

Nanofluid was treated as single-phase fluids, and all energy and motion equations for the pure liquid could be used directly to nanofluid. We just need to change the thermophysical properties. The steady state-dimensional governing equations for heat transfer by fluid flow within the one-phase model can include the following assumptions:

- Fluid flow was non-compressible, Newtonian with turbulent motion.
- The circular horizontal tube was placed under uniform heat flux and the Boussinesq approximation was also neglected due to horizontal tube placement.
- Particles' shape was spherical and regular in size.
- Fluid phase including nanoparticles was in thermal stability and no-slip among them and both flow with the same velocity.
- The impacts of radiation and viscous consumption were negligible.

For 3D model, the governing equations for fluid flow and heat transfer of a dimensional steady-state can be expressed for a single phase model as shown below [46], [47]:

Continuity equation:

$$\nabla \cdot (\rho \vec{v}) = 0 \quad (22).$$

Momentum equation:

$$\nabla \cdot (\rho \vec{v} \vec{v}) = -\nabla p + \nabla \cdot \left[ \mu (\nabla \vec{v} + \nabla \vec{v}^T) - \frac{2}{3} \nabla \cdot \vec{v} I \right] + \rho \vec{g} \quad (23).$$

Energy equation:

$$\nabla \cdot (\rho \vec{v} C_p T_{nf}) = \nabla \cdot (\lambda \nabla T_{nf}) \quad (24).$$

$\vec{v}$  is the velocity vector,  $T_{nf}$  is the temperature,  $\vec{g}$  is the gravitational body force,  $I$  is the unit tensor,  $\rho$  is the density,  $p$  is the pressure,  $\mu$  is the dynamic viscosity and  $\lambda$  is the thermal conductivity of nanofluid.

### 2.5.2. Numerical method

Initially, 3D- Geometry model and collecting shapes were created using the program of SolidWorks 2017 student version, three cases of pentagon rings depending on three pitch lengths fitted inside horizontal heated tube were studied. Full details of the geometry and collection of shapes were mentioned in the subheading under 2.2.2. Then, a commercial version of the ANSYS 14.5 Workbench program was used to conduct the investigation of the specific problem, which is summarized as follows:

- To ensure the accuracy of using numerical methods and procedure, firstly, a previous experimental study was followed to guarantee the solution methodology.
- CFD simulations of 3-dimensions were formed by using FVM with high computer specifications Core(TM) i7-7500U CPU 2.70 GHz (double precision and four processes parallel-local machine options).
- Constructing the grid of the geometry and converting grid domain to polyhedra and this field was used because of the number of cells which was greatly reduced and also these elements might get good computational results without losing more time.
- Single-phase with enabled energy equation and using of a standard k-Omega as a viscous model was set as models.
- Water and (AL<sub>2</sub>O<sub>3</sub>-Water) nanofluid were selected as working fluids.
- Water-liquid was created as a material of fluid (fluent fluid materials).
- Fluid properties (density, specific heat, thermal conductivity, and viscosity) were assumed constant (depending on fluid inlet temperature).
- Cell zone conditions were defined as water-liquid.
- Definition of inputs and outputs according to boundary conditions were mentioned in the subheading under 2.5.
- The solution methods were implemented with the following options:
  - ❖ Pressure-velocity coupling scheme was simple.
  - ❖ Least squares cell-based method was selected as a gradient solver method.
  - ❖ Spatial discretization of (pressure, momentum, and energy) equation was chosen as second-order upwind.
  - ❖ Spatial discretization of turbulent Kinetic energy and specific dissipation rate was chosen as the first-order upwind.

- ❖ The high order term was used and the relaxation factor was set as default value 0.25 for all variables as a relaxation option for the stability of the converged solutions.
- Residual monitor's values were set to  $10^{-3}$  for all variables, except for energy for which  $10^{-7}$  was used, turbulent kinetic (k) and turbulent dissipation energies ( $\omega$ ) for which  $10^{-4}$  was used.
- The standard methods were set as the initialization method for the solution and computing from the inlet was selected.
- All equations were solved sequentially and iteratively so as to obtain a converged numerical solution.
- The reports of total pressure (P1, P2) and total temperature (T2, Tw) were acquired from surface integrals option to the area weighted average from the program.

### **2.5.3. Grid independence study**

An accurate test was needed for grid independence to ensure the accuracy of the solution and validity of numerical methodology. Thus, the grid independence check was carried out by using six different grid cells with 0.6, 0.9, 1.7, 2.5, 3.8 and 4.2 million total cells. Each grid case was created with the same mesh topology. The study showed that the solution was grid-independent beyond the 2.5 million cells case, where the predicted Nusselt number was nearly identical to the predicted value from the 3.8 million cells as presented in figures (15, 16, and 17) below. Therefore, the CFD Simulations were performed by the 2.5 million cells. In addition, if a large number of cells was selected, this would increase the needed time to analyze the problem only without any significant improvement in the Nusselt number.

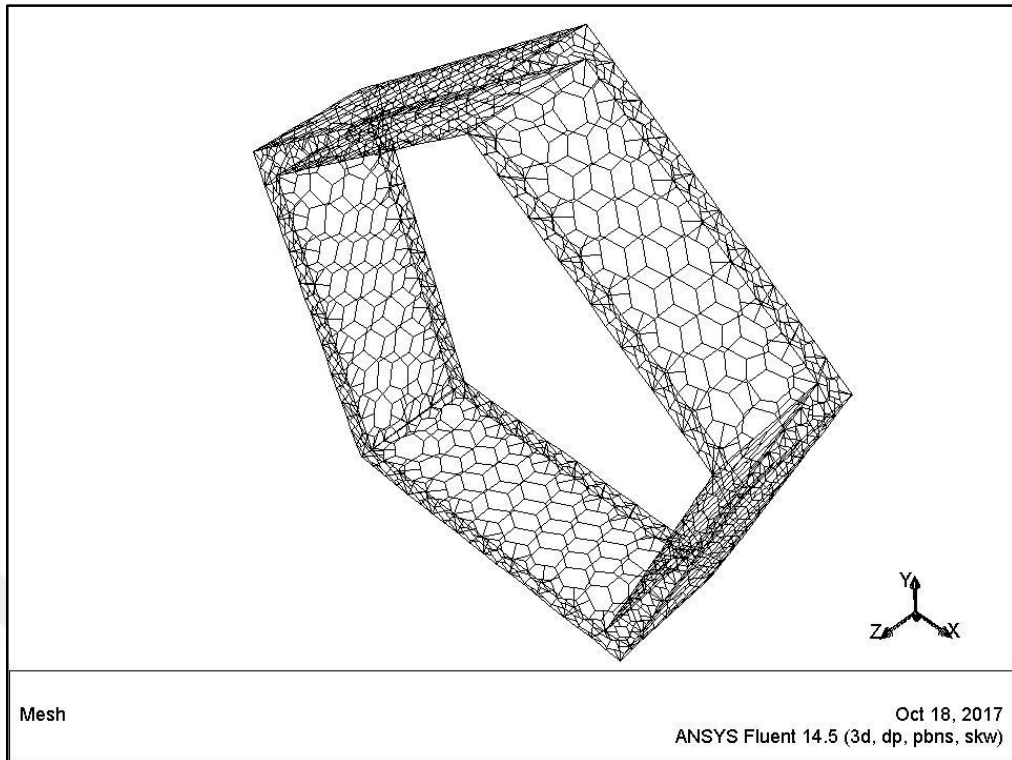


Figure 15. 3D view mesh models for the pentagon ring.

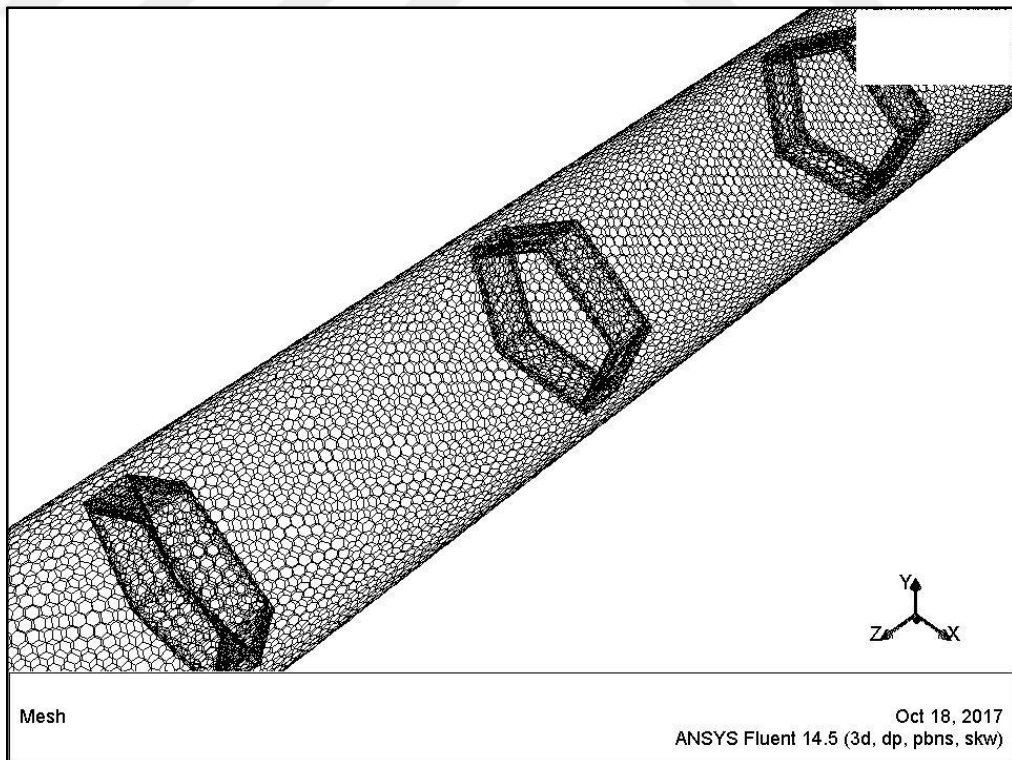


Figure 16. 3D view mesh models for the tube fitted with pentagon rings.

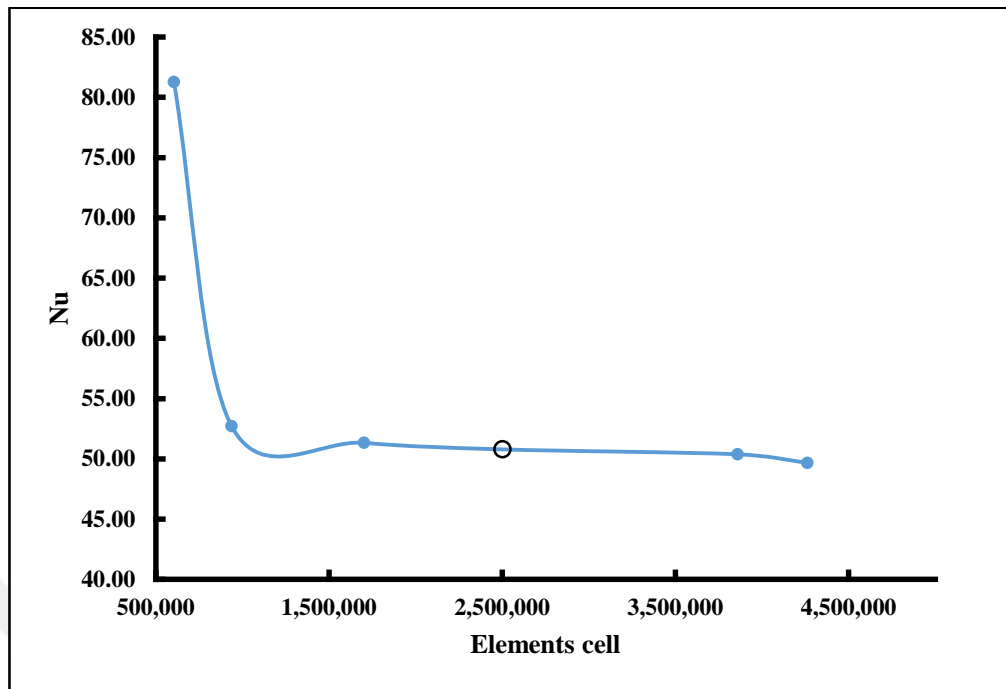


Figure 17. Study of independence check.

## 2.6. Thermophysical properties of water, nanoparticles, and nanofluids

Finding thermophysical properties at a certain temperature for water and for nanoparticles was very easy, but the difficulty lied in finding the appropriate and efficient equations for calculating the properties of nanofluids. Many previous published researches had offered many ways to calculate the thermophysical properties for nanofluids and this topic is still a matter of discussion and until this time no fixed and ensured method is available to calculate these characteristics.

### 2.6.1. Properties of water

The physical properties of saturated water at 20 °C (SI Units) were used which was outlined in Table A-9 in property tables and charts (SI Unit), by Cengel [48]. As listed below in (Table 3).

Table 3. Properties of saturated water at 20 °C (SI Units).

$\rho$ (kg/m <sup>3</sup> )	$C_p$ (j/kg.k)	$K$ (w/m.k)	$\mu$ (kg/m.s)	Pr
998	4182	0.598	0.001002	7.01

### 2.6.2. Properties of nanoparticles

Figure 18 below shows a comparison of the thermal conductivity between nanoparticles, liquids and polymers commonly used. The comparison showed that nanoparticles have higher thermal conductivity than liquids and polymers, so they are mixed with liquids to enhance the heat transfer coefficient.

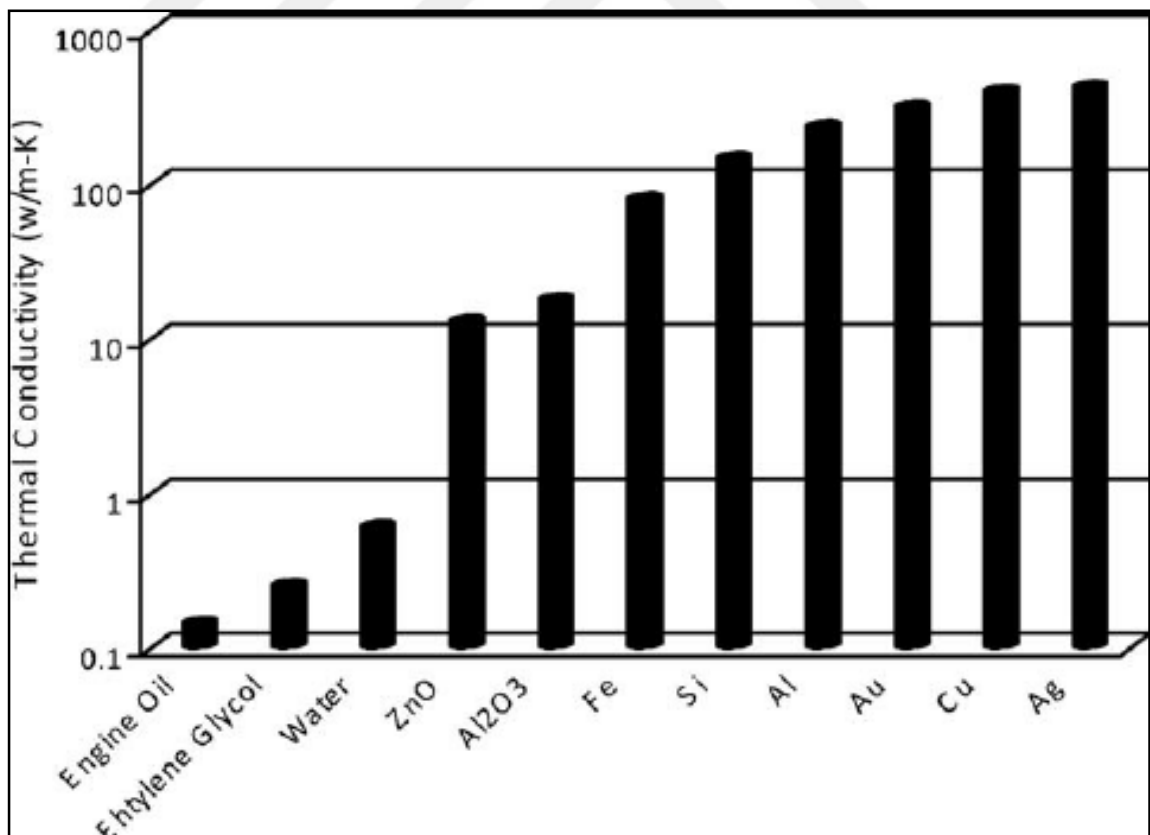


Figure 18. Comparison of the thermal conductivity of common liquids, polymers and solids.

The physical properties of Al<sub>2</sub>O<sub>3</sub> nanoparticles at T<sub>in</sub>=293.15 K used in this research were assumed as presented in Masuda et al. [49] as outlined in Table (4) below:

Table 4: Properties of nanoparticles (AL<sub>2</sub>O<sub>3</sub>).

Density ρ (kg/m <sup>3</sup> )	Specific Heat Cp (j/kg.k)	Thermal conductivity K (w/m.k)
3880	773	36

### 2.6.3. Thermophysical properties of nanofluids

#### 2.6.3.1. Density

The density of nanofluid (kg/m<sup>3</sup>) was calculated by the following equation:-

$$\rho_{nf} = \{\varphi \times \rho_{np}\} + \{(1 - \varphi) \times \rho_{water}\} \quad (25).$$

#### 2.6.3.2. Specific heat

The specific heat of nanofluid (kJ/kg.K) was calculated by the following equation:-

$$Cp_{,nf} = \frac{[\varphi x \{ \rho_{np} x Cp_{np} \} + (1 - \varphi) x \{ \rho_{water} Cp_{,water} \}]}{\rho_{nf}} \quad (26).$$

#### 2.6.3.3. Thermal conductivity

Thermal conductivity of nanofluid (w/m. k) was calculated according to Yu & Choi [50] which is defined as follows:

$$k_{nf} = \left[ \frac{k_{np} + 2k_w + 2\varphi(k_{np} - k_w)(1 + \beta)^3}{k_{np} + 2k_w - \varphi(k_{np} - k_w)(1 + \beta)^3} \right] k_w \quad (27).$$



### 2.6.3.4. Dynamic viscosity

Dynamic Viscosity of nanofluid (kg/m. s) was calculated according to general Einstein's formula as presented in Santra et al. [51] which is defined as follows:

$$\mu_{nf} = \mu_w(1 + 2.5\varphi) \quad (28).$$

Table 5 below shows the thermophysical properties of the nanofluids measured using the above equations.

Table 5: Thermophysical properties of (AL<sub>2</sub>O<sub>3</sub>/Water) nanofluids at T<sub>in</sub>=293.15 K

$\varphi$ (%)	$\rho$ (kg/m <sup>3</sup> )	C <sub>p</sub> (j/kg.k)	K (w/m.k)	$\mu$ (kg/m.s)	Pr
1.5%	1041	3991	0.632750	0.001040	6.56
3%	1084	3816	0.668873	0.001077	6.15
4.5%	1128	3654	0.706452	0.001115	5.77

## CHAPTER 3

### RESULTS AND DISCUSSION

#### 3.1. Validation of the current numerical results

For the purpose of verifying the validity of the numerical results, the results obtained should be compared with the previous research correlations, which was appropriate for the boundary conditions of the current study.

##### 3.1.1. Water flow in a smooth tube

The Nusselt number results of the water flow in a smooth tube were compared with the correlations (Colburn, Dittus-Boelter, Petukhov, and Gnielinski) which were previously mentioned in Chapter II under 2.1.7.1. It was found that the two correlations (Colburn and Petukhov) corresponded to the obtained results with a deviation ratio of less than 10 % which showed quite good agreement with these correlations. The maximum deviation ratio differed from the first correlation by ( $\mp 4$  %) and ( $\mp 3$  %) from the second correlation recorded. The Chart (1) below shows the representation of all correlations mentioned above.

The friction factor results of the water flow in a smooth tube were compared with Blasius correlation which was previously mentioned in Chapter II under 2.1.7.1.f. It was found that the correlation above corresponds to the obtained results with a deviation ratio of less than ten % which showed good agreement with this correlation. The maximum deviation ratio differed by 9.83%. Chart 2 below shows the representation of Blasius correlation vs. with numerical result.

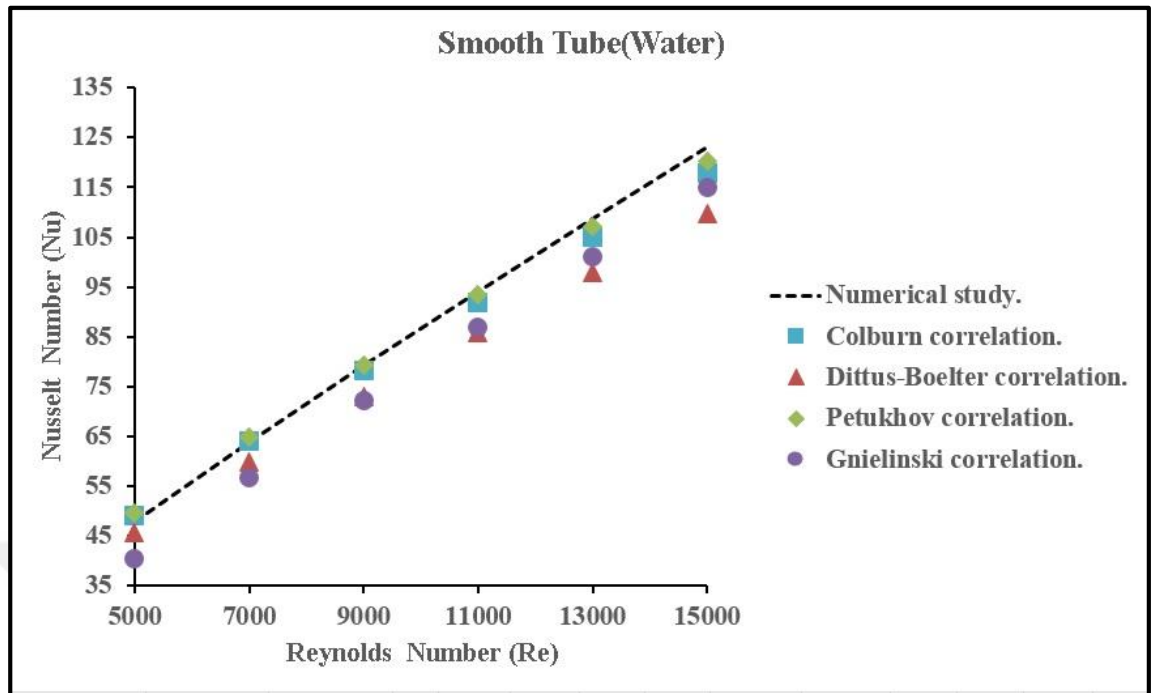


Chart 1. Nu correlations vs. numerical result.

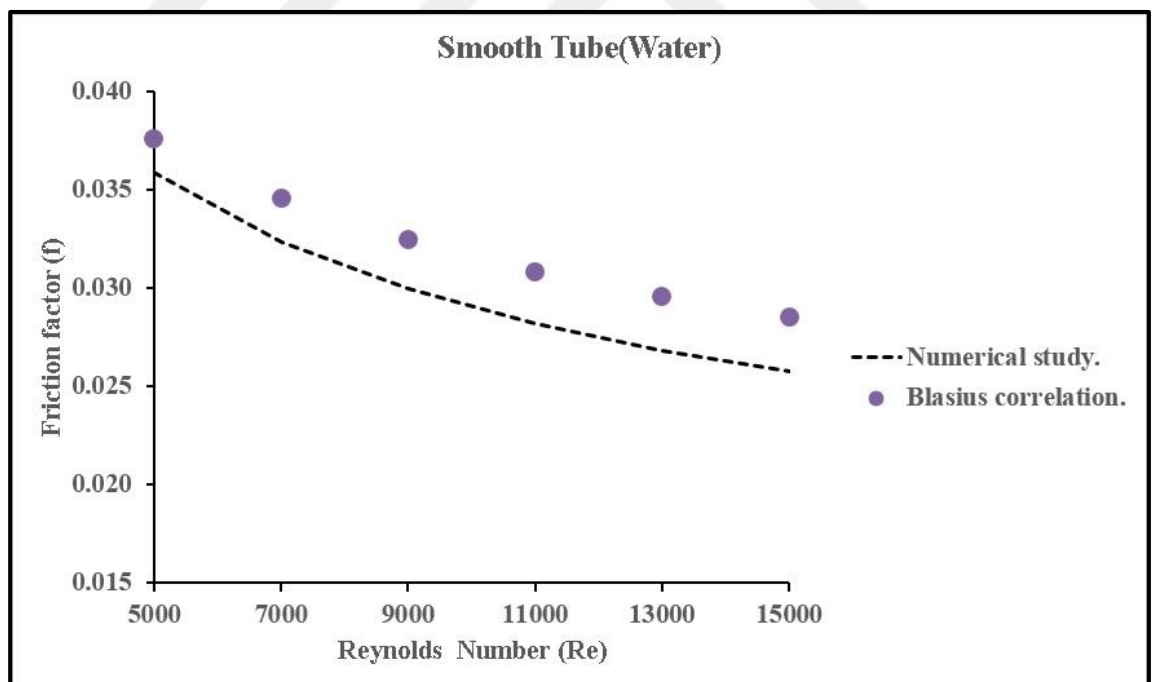


Chart 2. Blasius correlation vs. numerical result.

### 3.1.2. (AL<sub>2</sub>O<sub>3</sub>-Water) nanofluid flow in a smooth tube

The Nusselt number results of the (Al<sub>2</sub>O<sub>3</sub>-water) nanofluid flow in a smooth tube were compared with the correlations (Pak & Cho, Maiga, and Vajjha) which were previously mentioned in Chapter II under 2.1.7.2. It was found that the correlation (Pak & Cho) corresponds to the obtained results for all used volume fractions (1.5, 3 and 4 %) with a deviation ratio less than 10 % which shows quite good agreement with this correlation. Chart 3 below shows the representation of all correlations mentioned above observed at volume fraction 1.5%.

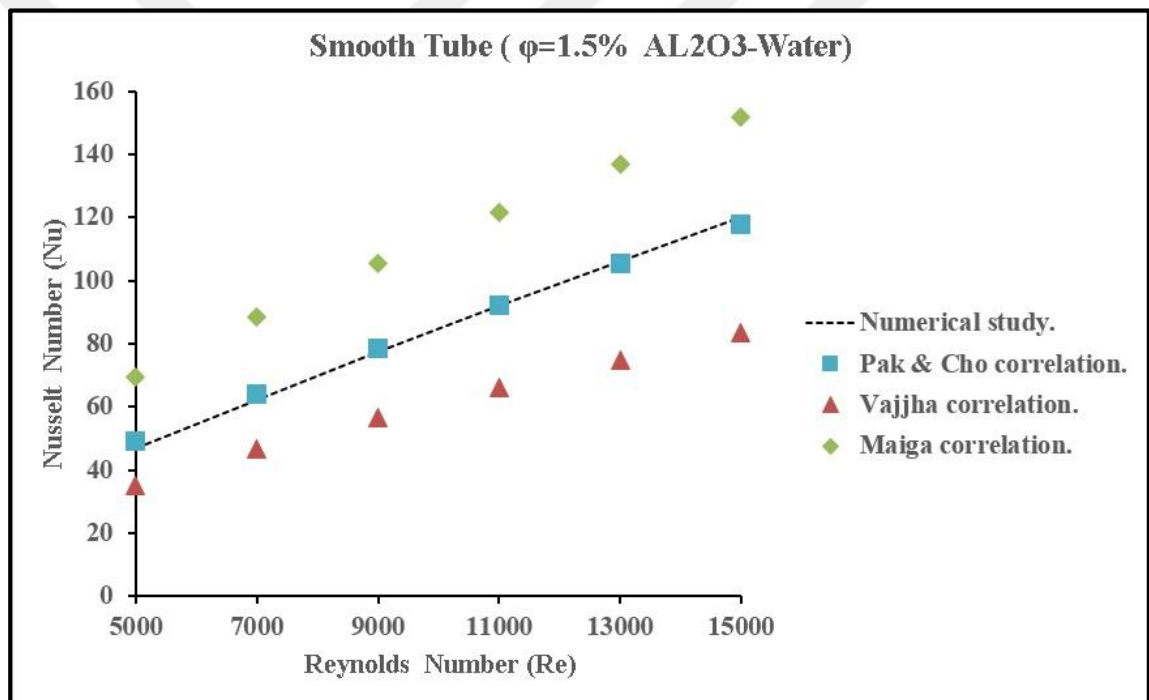


Chart 3. (Al<sub>2</sub>O<sub>3</sub>-water) nanofluid correlations vs. numerical result.

Chart 4 below shows the representation of the correlation Pak & Cho with numerical results for the volume fractions (1.5, 3 and 4 %).

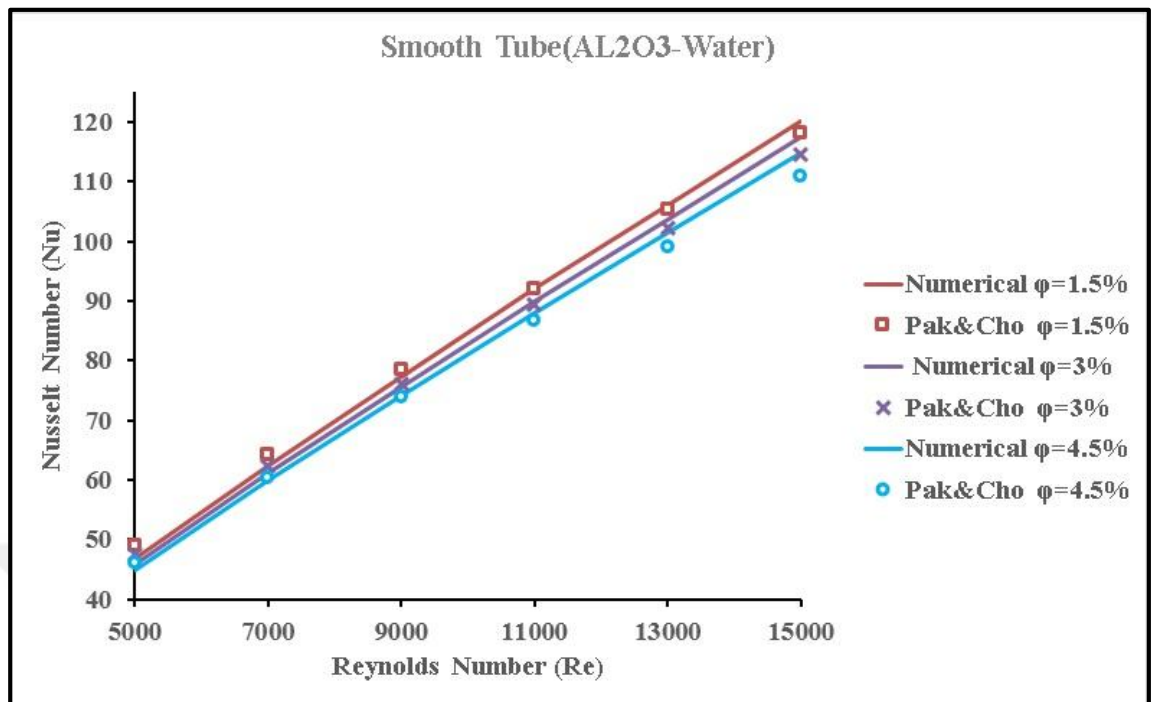


Chart (4). Pak & Cho correlation vs. numerical result

Heat transfer coefficient increased with the increase of (AL<sub>2</sub>O<sub>3</sub>-Water) nanofluids concentration and also with the increase of the Reynolds number as shown below in chart 5.

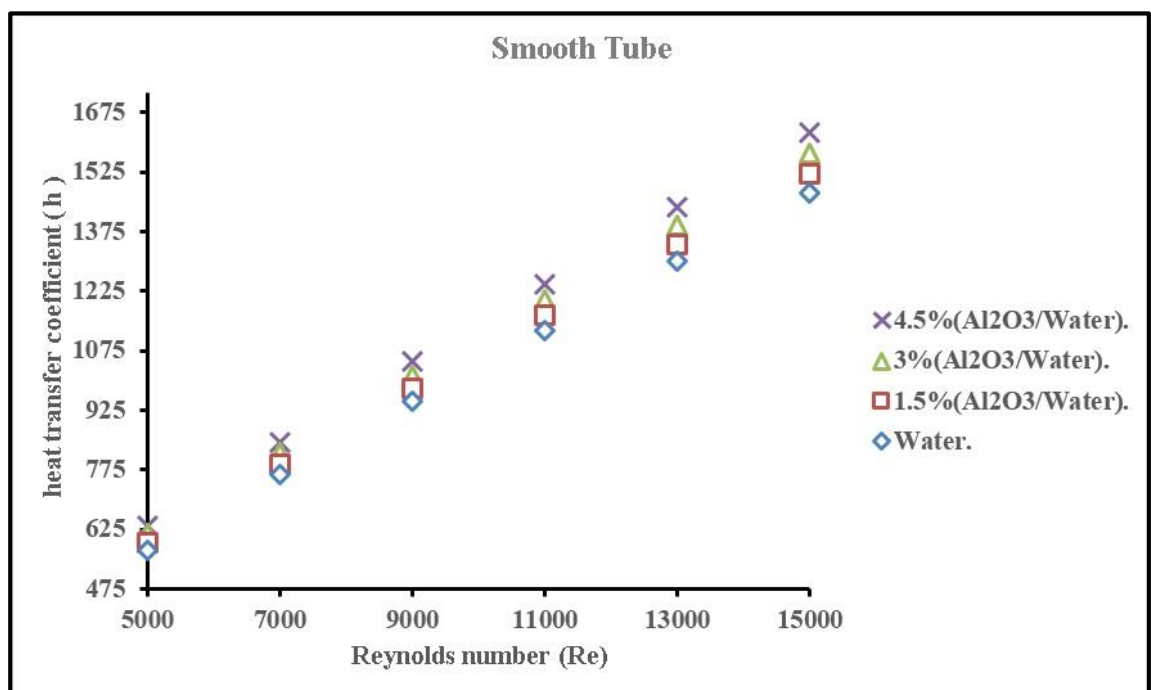


Chart (5). Heat transfer coefficient vs. Reynolds number.

As in the water flow, the friction factor decreased with the increase of the Reynolds number, but the addition of  $Al_2O_3$  nanoparticles with the concentrations (1.5, 3 and 4.5%) to water did not change the friction factor effectively from the recorded results in the case of water flow only as shown below in Chart (6).

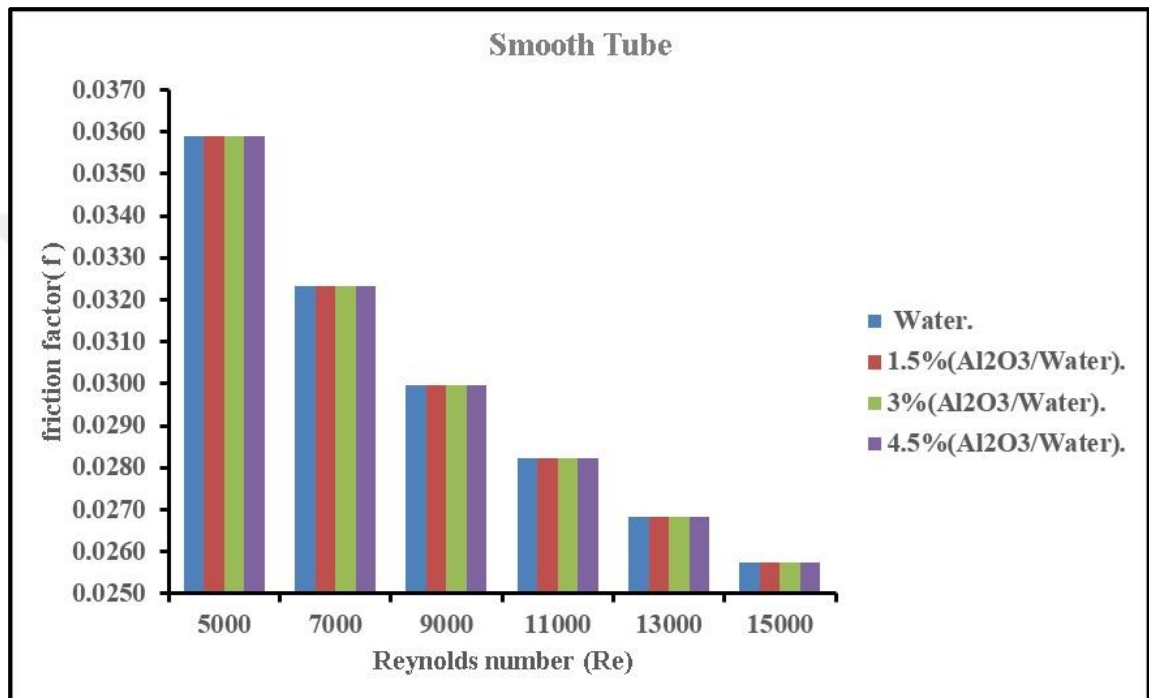


Chart 6. Friction factor vs. Reynolds number.

We can conclude from this that it is possible to treat the fluid ( $Al_2O_3$ -water) nanofluid as a pure liquid as long as the added concentrations from nanoparticles has not achieved any significant change in the friction factor.

The pressure drop per unit length (Pa/m) increased effectively with the increase of Reynolds number as well as with the increase of ( $Al_2O_3$ -water) nanofluid concentrations (1.5, 3 and 4.5%) as shown below in Chart 7.

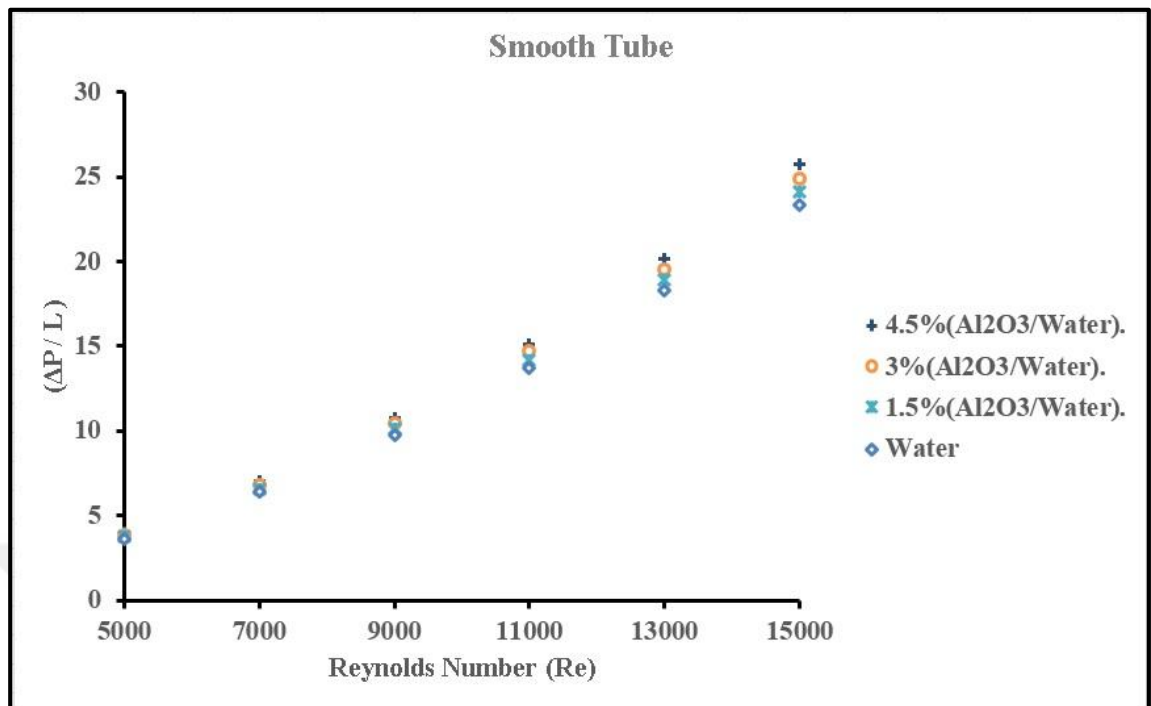


Chart 7. Pressure drop vs. Reynolds number.

The surface temperature (K) decreased with the increase of Reynolds number as well as with the increase of (Al<sub>2</sub>O<sub>3</sub>-water) nanofluid concentrations in water as shown below in Chart 8.

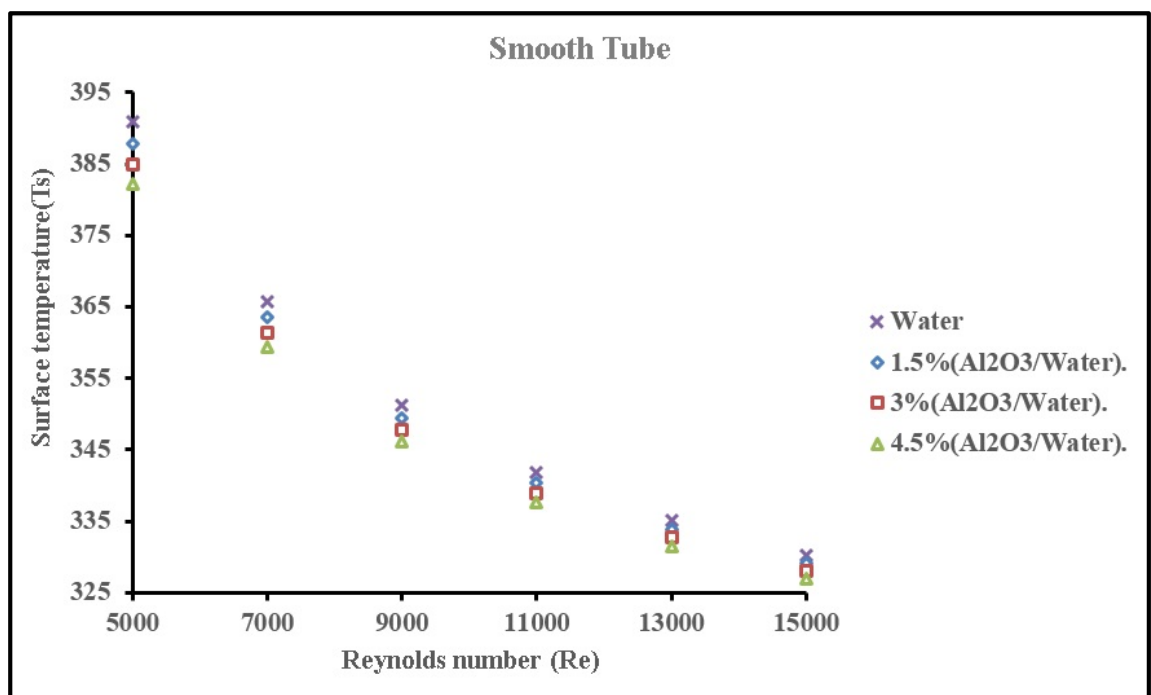


Chart 8. Surface temperature vs. Reynolds number.

## **3.2. The effect of addition 9 of pentagon rings on the heat transfer characteristics for water flow and (AL<sub>2</sub>O<sub>3</sub>-water) nanofluid flow**

### **3.2.1. On the (h)**

The value of the heat transfer coefficient increased after inserting nine of the pentagon rings from the recorded values when using water or nanofluids flow only. The increment was directly proportional to increase in in the Reynolds number and also to increase the concentration of nanofluids.

- The highest increment value was 2149 w/m<sup>2</sup>.k. It was recorded at Reynolds number of 15000 when 4.5% of Al<sub>2</sub>O<sub>3</sub>-water nanofluids with insert of nine of the Pentagon rings were used. While the highest increment value was 1623 w/m<sup>2</sup>.k when 4.5% of (AL<sub>2</sub>O<sub>3</sub>-water) nanofluids flow was only used, and the highest increment value was 1472 w/m<sup>2</sup>.k when water flow was only used.
- The lowest increment value was 765 w/m<sup>2</sup>.k. It was recorded at Reynolds number of 5000 when water flow with insert of nine of the Pentagon rings were used. While the lowest increment value was 593 w/m<sup>2</sup>.k when 1.5% of (Al<sub>2</sub>O<sub>3</sub>-water) nanofluids flow was only used, and the lowest increment value was 572 w/m<sup>2</sup>.k when the water flow was only used as shown below in Chart 9.



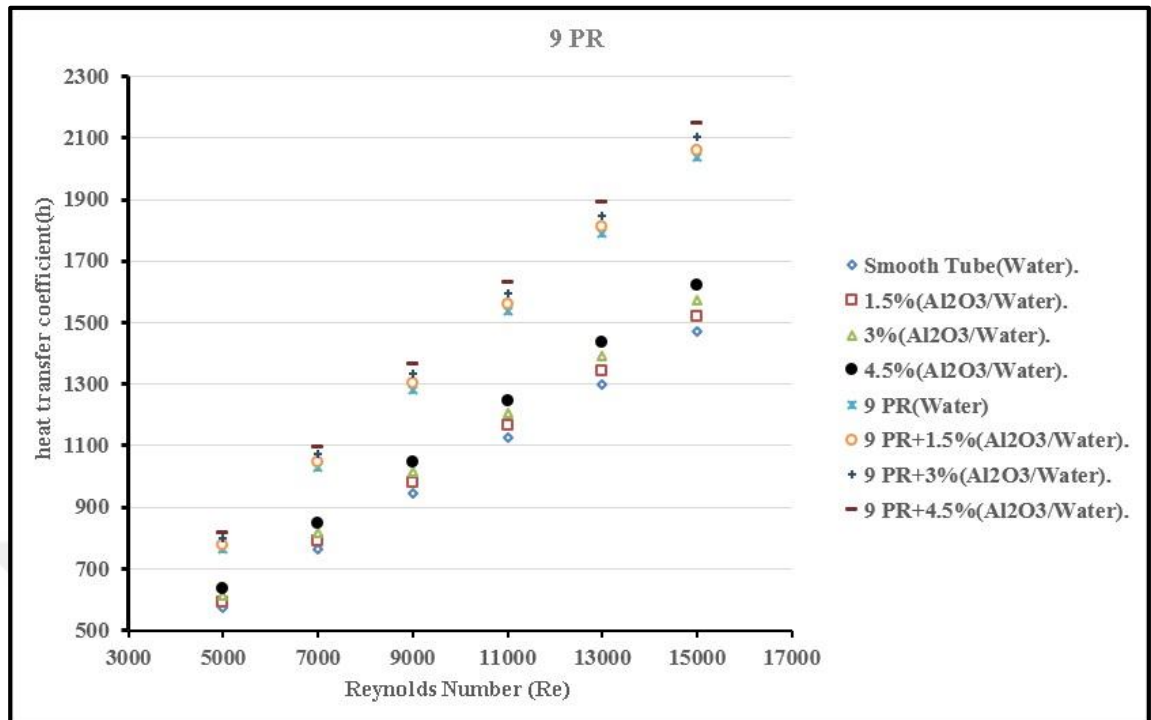


Chart 9. Heat transfer coefficient vs. Reynolds number.

### 3.2.2. On the (Nu)

The value of the Nusselt number increased after inserting nine of the pentagon rings from the recorded values when using water or nanofluids only. The increment was directly proportional to increase in the Reynolds number and inversely proportional to increase in the concentration of nanofluids.

- The highest increment value was 170. It was recorded at Reynolds number of 15000 when water flow with insert nine of the pentagon rings were used. While the highest increment value was 123 when the water flow was only used, and the highest increment value was 120 when 1.5% of (Al<sub>2</sub>O<sub>3</sub>-water) nanofluids flow was only used.
- The lowest increment value was 58. It was recorded at Reynolds number of 5000 when 4.5% of (Al<sub>2</sub>O<sub>3</sub>-water) nanofluid flow with insert of nine of the pentagon rings were used. While the lowest increment value was 48 when the water flow was only

used, and the lowest increment value was 45 when 4.5% of (Al<sub>2</sub>O<sub>3</sub>-water) nanofluids flow was only used as shown below in Chart 10.

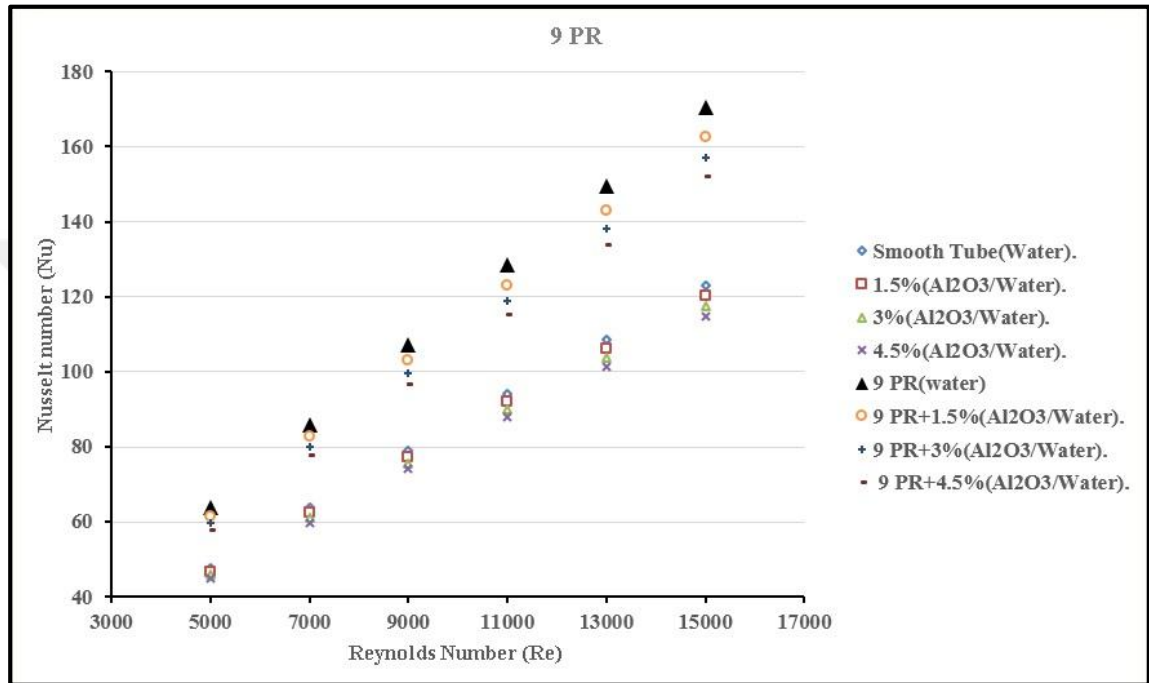


Chart 10. Nusselt number vs. Reynolds number.

### 3.2.3. On the (f)

The value of the friction factor increased after inserting nine of the pentagon rings from the recorded values when using water or nanofluids only. The increment was inversely proportional to increase in in the Reynolds number and approximately constant to increase the concentration of nanofluids at the same Reynolds number.

- The highest increment value was 0.11. It was recorded at Reynolds number of 5000 when the flow of water or all concentrations of (Al<sub>2</sub>O<sub>3</sub>-water) nanofluids with insert of nine of the Pentagon rings were used. While the highest increment value was 0.04

when the water or all concentration of ( $\text{Al}_2\text{O}_3$ -water) nanofluids flow were only used.

- The lowest increment value was 0.09. It was recorded at Reynolds number of 15000 when the flow of water or all concentrations of ( $\text{Al}_2\text{O}_3$ -water) nanofluids with insert of nine of the pentagon rings were used. While the lowest increment value was 0.03 when water or all concentration of ( $\text{Al}_2\text{O}_3$ -water) nanofluids flow were only used as shown below in Chart 11.

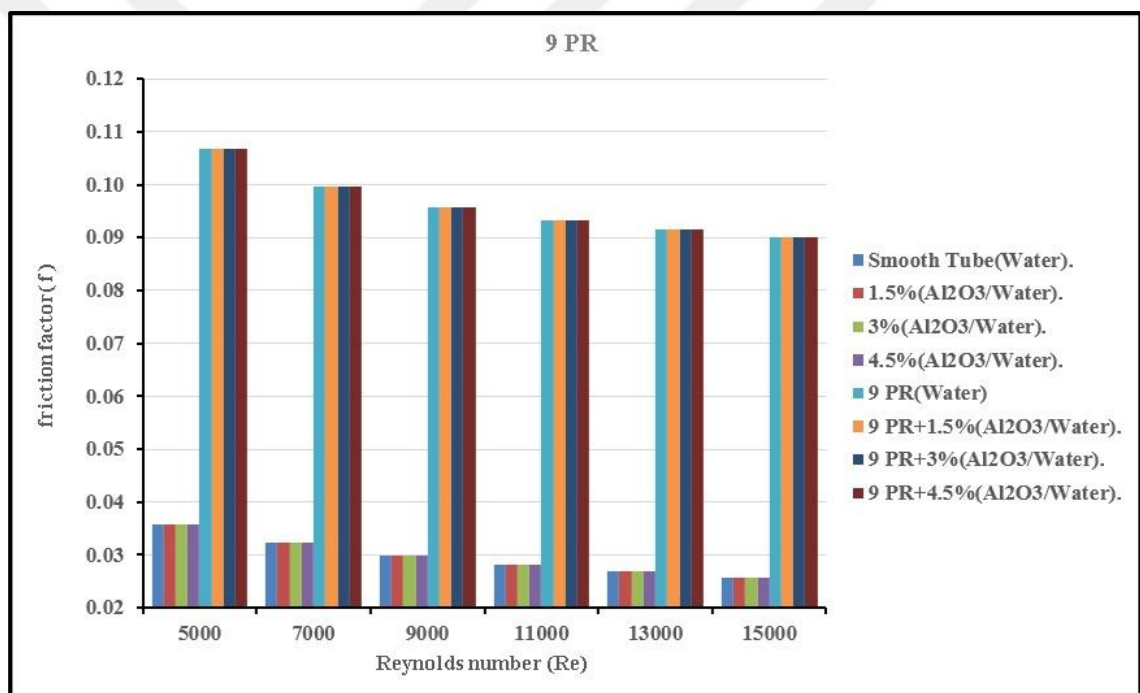


Chart 11. Friction factor vs. Reynolds number.

### 3.2.4. On the ( $T_s$ )

The value of the surface temperature decreased after inserting nine of the pentagon rings from the recorded values when using water or nanofluids only. The decrement was directly proportional to increase in in the Reynolds number and also to increase the concentration of nanofluids.

- The highest decrement value was 322 K. It was recorded at Reynolds number of 15000 when 4.5% of (Al<sub>2</sub>O<sub>3</sub>-water) nanofluids flow with insert of nine of the Pentagon rings were used. While the highest decrement value was 327 K when 4.5% of (Al<sub>2</sub>O<sub>3</sub>-water) nanofluids flow was only used, and the highest decrement value was 330 K when water flow was only used.
- The lowest decrement value was 377 K. It was recorded at Reynolds number of 5000 when water flow with insert of nine of the Pentagon rings were used. While the lowest decrement value was 387 K when 1.5% of (Al<sub>2</sub>O<sub>3</sub>-water) nanofluids flow was only used, and the lowest decrement value was 390 K when water flow was only used as shown below in Chart 12.

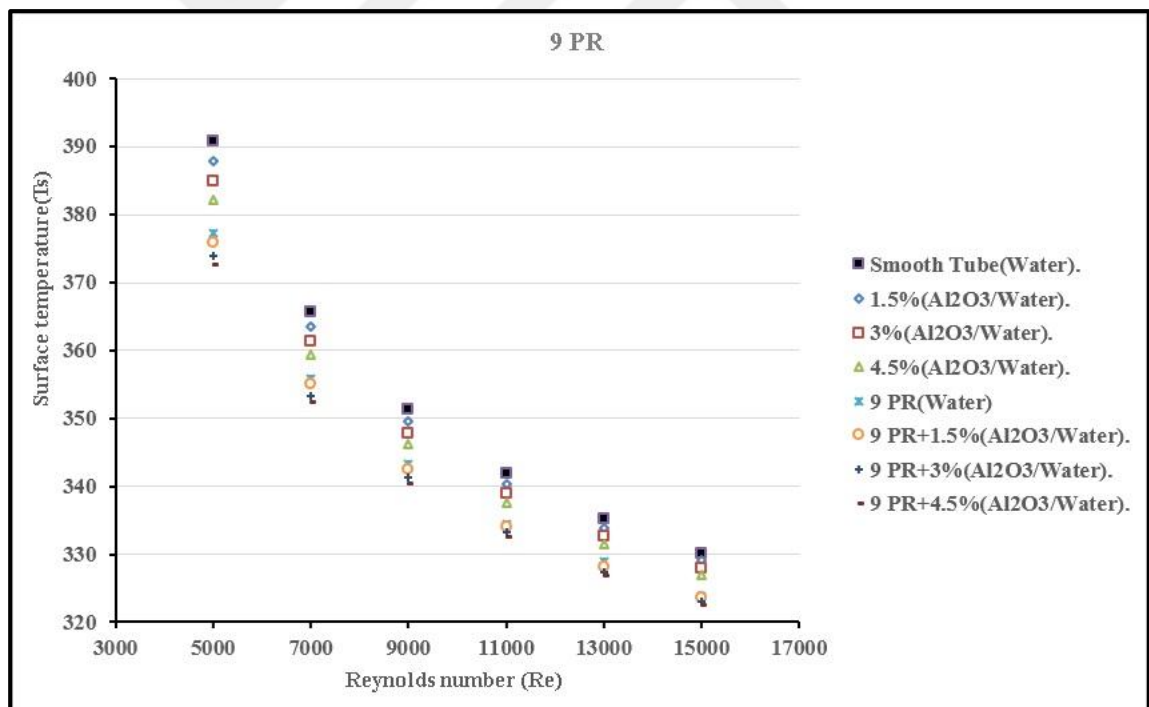


Chart 12. Surface temperature vs. Reynolds number.

### 3.2.5. On the ( $\Delta p$ )

The value of the pressure drop per unit length (Pa/m) increased after inserting nine of the pentagon rings from the recorded values when using water or nanofluids only. The increment was directly proportional to increase in in the Reynolds number and also to increase the concentration of nanofluids.

- The highest increment value was (89.87 Pa/m). It was recorded at Reynolds number (15000) when 4.5% of ( $\text{Al}_2\text{O}_3$ -water) nanofluids flow with insert of nine of the Pentagon rings were used. While the highest increment value was (25.71 Pa/m) when 4.5% of ( $\text{Al}_2\text{O}_3$ -water) nanofluids flow was only used, and the highest increment value was (23.31 Pa/m) when the water flow was only used.
- The lowest increment value was (10.74 Pa/m). It was recorded at Reynolds number (5000) when water flow with insert of nine of the Pentagon rings were used. While the lowest increment value was (3.73 Pa/m) when 1.5% of ( $\text{Al}_2\text{O}_3$ -water) nanofluids flow was only used, and the lowest increment value was (3.61 Pa/m) when the water flow was only used. As shown below in chart (13).

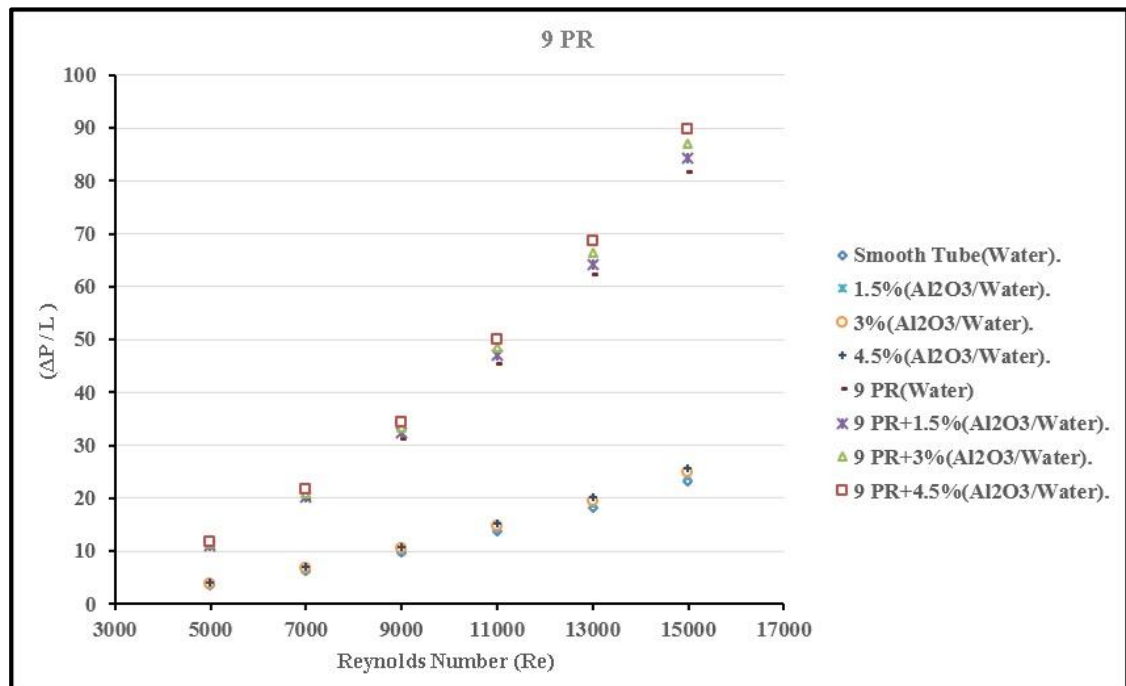


Chart 13. Pressure drop vs. Reynolds number.

### **3.3. The effect of addition (14) of pentagon rings on the heat transfer characteristics for water flow and (AL<sub>2</sub>O<sub>3</sub>-water) nanofluid flow**

#### **3.3.1. On the (h)**

The value of the heat transfer coefficient increased after inserting fourteen of the pentagon rings from the recorded values when using water or nanofluids flow only. The increment was directly proportional to increase in in the Reynolds number and also to increase the concentration of nanofluids.

- The highest increment value was 2386 w/m<sup>2</sup>.k. It was recorded at Reynolds number of 15000 when 4.5% of (Al<sub>2</sub>O<sub>3</sub>-water) nanofluids with insert of fourteen of the Pentagon rings were used. While the highest increment value was 1623 w/m<sup>2</sup>.k when 4.5% of (AL<sub>2</sub>O<sub>3</sub>-water) nanofluids flow was only used, and the highest increment value was 1472 w/m<sup>2</sup>.k when water flow was only used.
- The lowest increment value was 829 w/m<sup>2</sup>.k. It was recorded at Reynolds number of 5000 when water flow with insert of fourteen of the Pentagon rings were used. While the lowest increment value was 593 w/m<sup>2</sup>.k when 1.5% of (Al<sub>2</sub>O<sub>3</sub>-water) nanofluids flow was only used, and the lowest increment value was 572 w/m<sup>2</sup>.k when the water flow was only used as shown below in Chart 14.

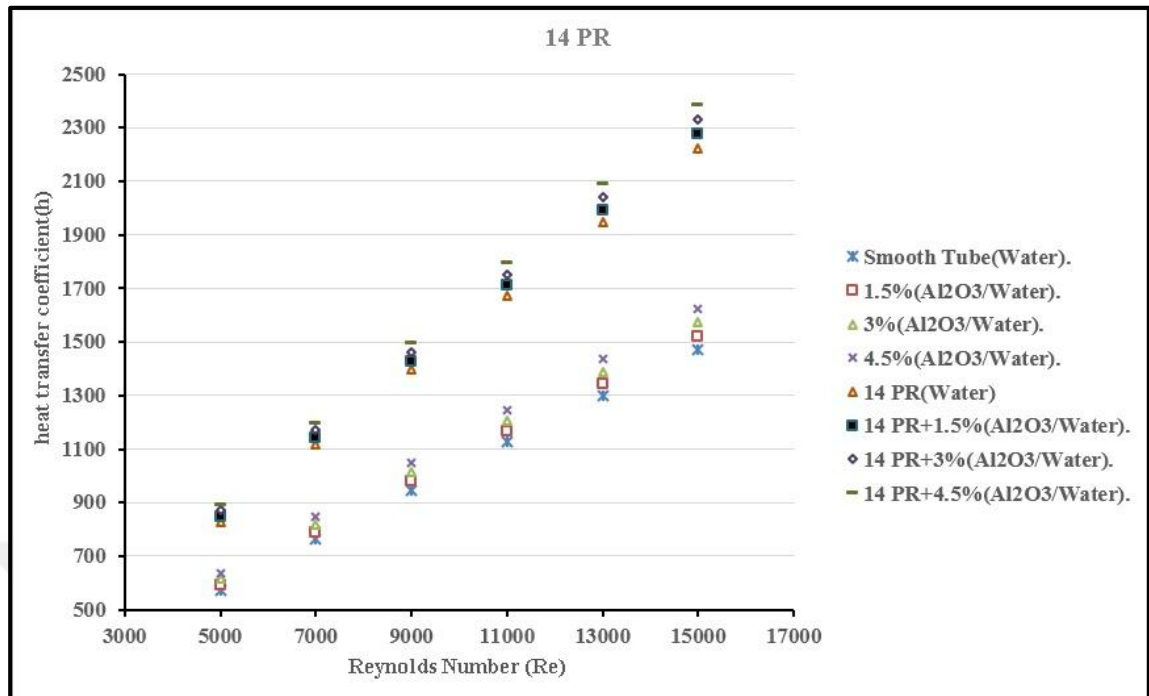


Chart 14. Heat transfer coefficient vs. Reynolds number.

### 3.3.2. On the (Nu)

The value of the Nusselt number increased after inserting fourteen of the pentagon rings from the recorded values when using water or nanofluids only. The increment was directly proportional to increase in the Reynolds number and inversely proportional to increase in the concentration of nanofluids.

- The highest increment value was 186. It was recorded at Reynolds number of 15000 when water flow with insert of fourteen of the Pentagon rings were used. While the highest increment value was 123 when the water flow was only used, and the highest increment value was 120 when 1.5% of (Al<sub>2</sub>O<sub>3</sub>-water) nanofluids flow was only used.
- The lowest increment value was 63. It was recorded at Reynolds number of 5000 when 4.5% of (Al<sub>2</sub>O<sub>3</sub>-water) nanofluid flow with insert of fourteen of the Pentagon rings were used. While the lowest increment value was 48 when the water flow was

only used, and the lowest increment value was 45 when 4.5% of (Al<sub>2</sub>O<sub>3</sub>-water) nanofluids flow was only used as shown below in Chart 15.

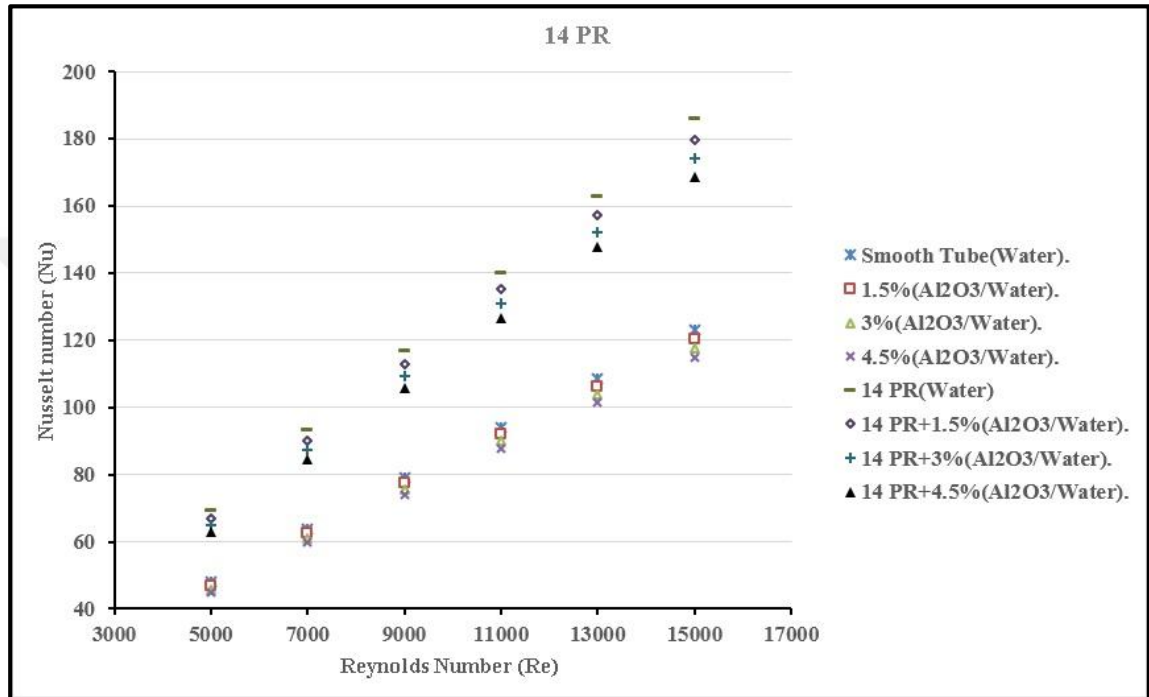


Chart 15. Nusselt number vs. Reynolds number.

### 3.3.3. On the (f)

The value of the friction factor increased after inserting fourteen of the pentagon rings from the recorded values when using water or nanofluids only. The increment was inversely proportional to increase in in the Reynolds number and approximately constant to increase the concentration of nanofluids at the same Reynolds number.

- The highest increment value was 0.15. It was recorded at Reynolds number 5000 when the flow of water or all concentrations of (Al<sub>2</sub>O<sub>3</sub>-water) nanofluids with insert of fourteen of the pentagon rings were used. While the highest recorded



increment value was 0.04 when the water or all concentration of (Al<sub>2</sub>O<sub>3</sub>-water) nanofluids flow were only used.

- The lowest increment value was 0.12. It was recorded at Reynolds number of 15000 when the flow of water or all concentrations of (Al<sub>2</sub>O<sub>3</sub>-water) nanofluids with insert of fourteen of the pentagon rings were used. While the lowest recorded increment value was 0.03 when water or all concentration of (Al<sub>2</sub>O<sub>3</sub>-water) nanofluids flow were only used as shown below in Chart 16.

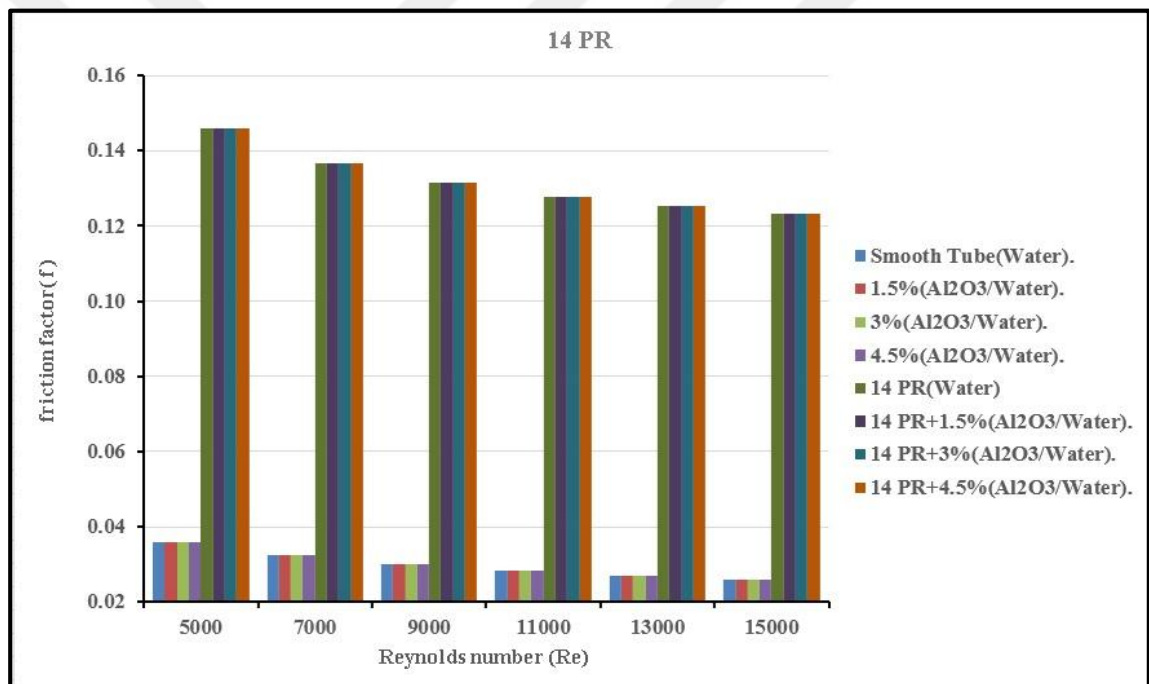


Chart 16. Friction factor vs. Reynolds number.

### 3.3.4. On the (T<sub>s</sub>)

The value of the surface temperature decreased after inserting fourteen of the pentagon rings from the recorded values when using water or nanofluids only. The decrement was directly proportional to increase in in the Reynolds number and also to increase the concentration of nanofluids.

- The highest decrement value was 319 K. It was recorded at Reynolds number of 15000 when 4.5% of (Al<sub>2</sub>O<sub>3</sub>-water) nanofluids flow with insert of fourteen of the pentagon rings were used. While the highest recorded decrement value was 327 K when 4.5% of (Al<sub>2</sub>O<sub>3</sub>-water) nanofluids flow was only used, and the highest recorded decrement value was 330 K when water flow was only used.
- The lowest decrement value was 372 K. It was recorded at Reynolds number of 5000 when water flow with insert of fourteen of the pentagon rings were used. While the lowest recorded decrement value was 387 K when 1.5% of (Al<sub>2</sub>O<sub>3</sub>-water) nanofluids flow was only used, and the lowest recorded decrement value was 390 K when water flow was only used as shown below in Chart 17.

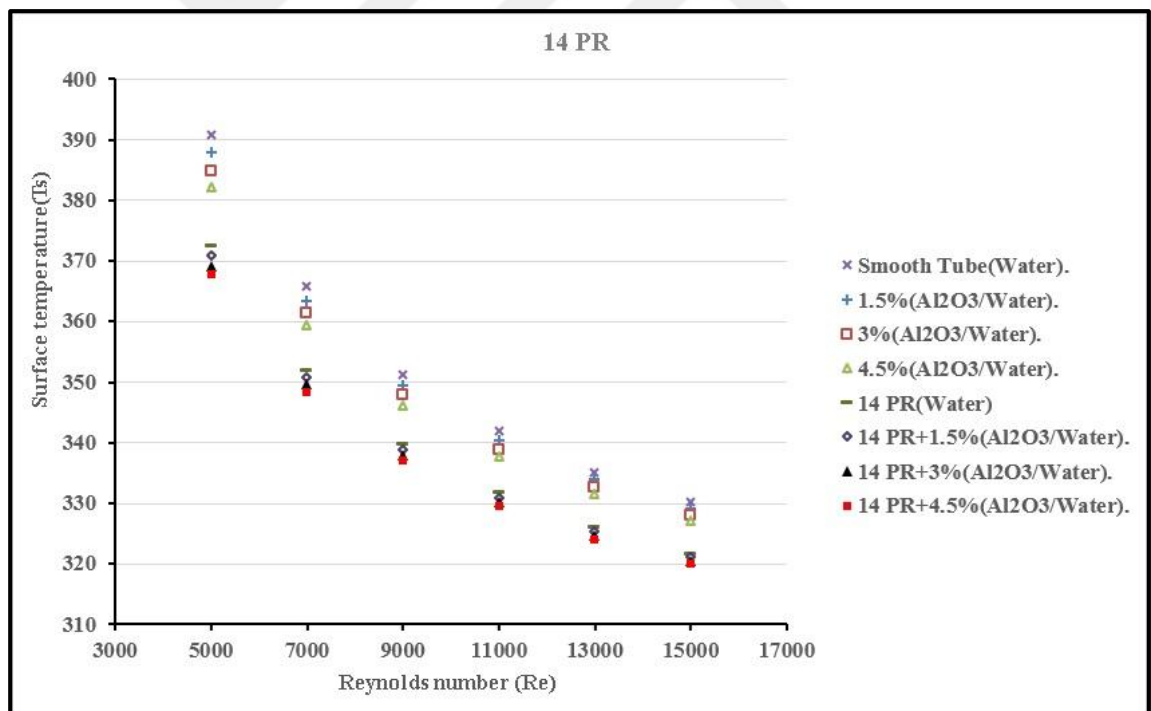


Chart 17. Surface temperature vs. Reynolds number.

### 3.3.5. On the ( $\Delta p$ )

The value of the pressure drop per unit length (Pa/m) increased after inserting fourteen of the Pentagon rings from the recorded values when using water or nanofluids only. The increment was directly proportional to increase in in the Reynolds number and also to increase the concentration of nanofluids.

- The highest increment value was 123.11 Pa/m. It was recorded at Reynolds number of 15000 when 4.5% of ( $\text{Al}_2\text{O}_3$ -water) nanofluids flow with insert of fourteen of the pentagon rings were used. While the highest recorded increment value was 25.71 Pa/m when 4.5% of ( $\text{Al}_2\text{O}_3$ -water) nanofluids flow was only used, and the highest recorded increment value was 23.31 Pa/m when the water flow was only used.
- The lowest increment value was 14.68 Pa/m. It was recorded at Reynolds number of 5000 when water flow with insert of fourteen of the pentagon rings were used. While the lowest recorded increment value was 3.73 Pa/m when 1.5% of ( $\text{Al}_2\text{O}_3$ -water) nanofluids flow was only used, and the lowest recorded increment value was 3.61 Pa/m when the water flow was only used as shown below in Chart 18.

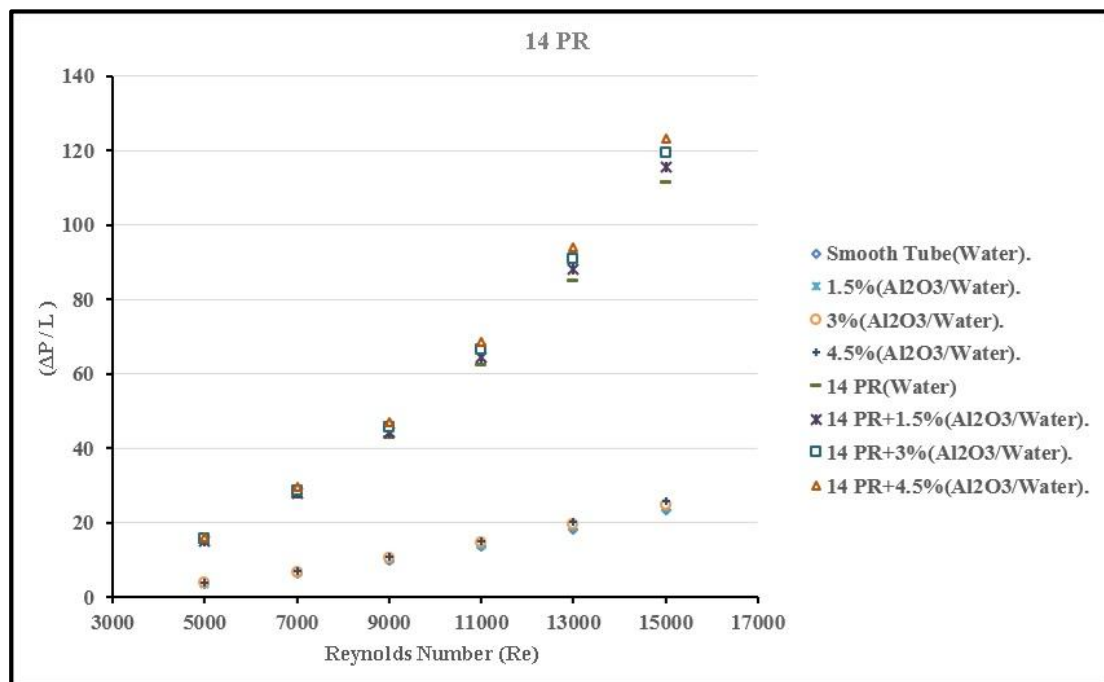


Chart 18. Pressure drop vs. Reynolds number.

### **3.4. The effect of addition (29) of pentagon rings on the heat transfer characteristics for water flow and (AL<sub>2</sub>O<sub>3</sub>-water) nanofluid flow**

#### **3.4.1. On the (h)**

The value of the heat transfer coefficient increased after inserting twenty nine of the pentagon rings from the recorded values when using water or nanofluids flow only. The increment was directly proportional to increase in in the Reynolds number and also to increase the concentration of nanofluids.

- The highest increment value was 3018 w/m<sup>2</sup>.k. It was recorded at Reynolds number of 15000 when 4.5% of (AL<sub>2</sub>O<sub>3</sub>-water) nanofluids with insert of twenty nine of the pentagon rings were used. While the highest increment value was 1623 w/m<sup>2</sup>.k when 4.5% of (AL<sub>2</sub>O<sub>3</sub>-water) nanofluids flow was only used, and the highest increment value was 1472 w/m<sup>2</sup>.k when water flow was only used.
- The lowest increment value was 986 w/m<sup>2</sup>.k. It was recorded at Reynolds number of 5000 when water flow with insert of twenty nine of the pentagon rings were used. While the lowest increment value was 593 w/m<sup>2</sup>.k when 1.5% of (AL<sub>2</sub>O<sub>3</sub>-water) nanofluids flow was only used, and the lowest increment value was 572 w/m<sup>2</sup>.k when the water flow was only used as shown below in Chart 19.

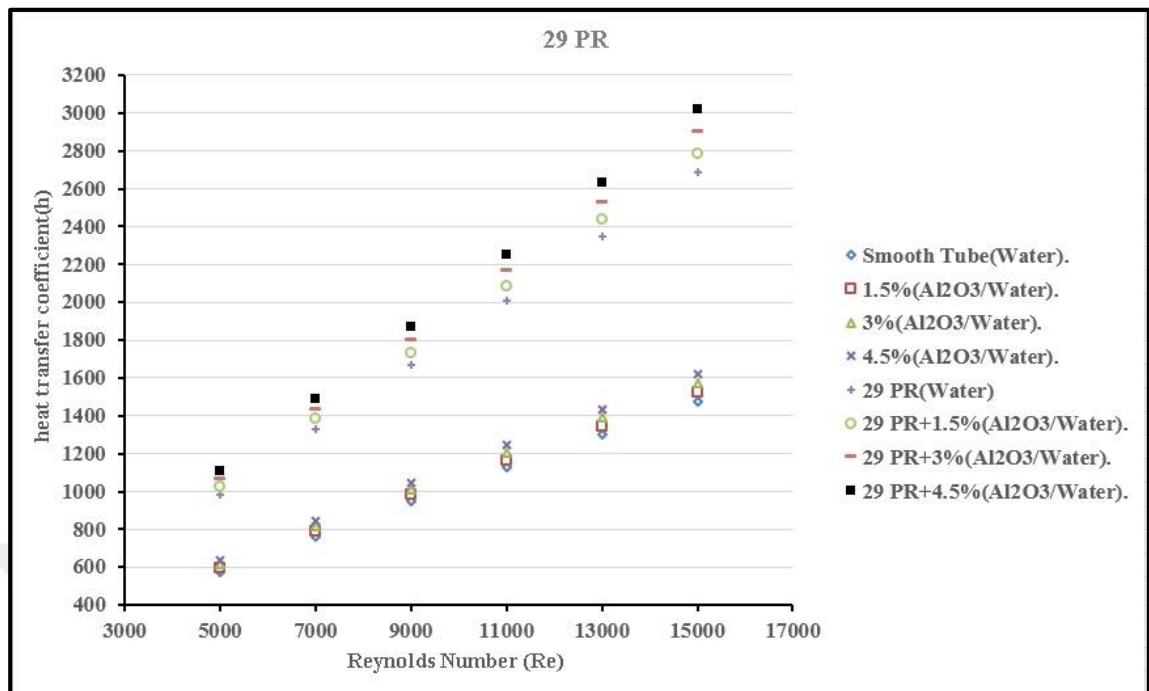


Chart 19. Heat transfer coefficient vs. Reynolds number.

### 3.4.2. On the (Nu)

The value of the Nusselt number increased after inserting twenty-nine of the Pentagon rings from the recorded values when using water or nanofluids only. The increment was directly proportional to increase in in the Reynolds number and inversely proportional to increase in the concentration of nanofluids.

- The highest increment value was 225. It was recorded at Reynolds number of 15000 when water flow with insert of twenty nine of the Pentagon rings were used. While the highest increment value was (123) when the water flow was only used, and the highest increment value was (120) when 1.5% of (Al<sub>2</sub>O<sub>3</sub>-water) nanofluids flow was only used.
- The lowest increment value was (78). It was recorded at Reynolds number (5000) when 4.5% of (Al<sub>2</sub>O<sub>3</sub>-water) nanofluid flow with insert of twenty nine of the pentagon rings were used. While the lowest increment value was 48 when the water

flow was only used, and the lowest increment value was 45 when 4.5% of (Al<sub>2</sub>O<sub>3</sub>-water) nanofluids flow was only used as shown below in Chart (20).

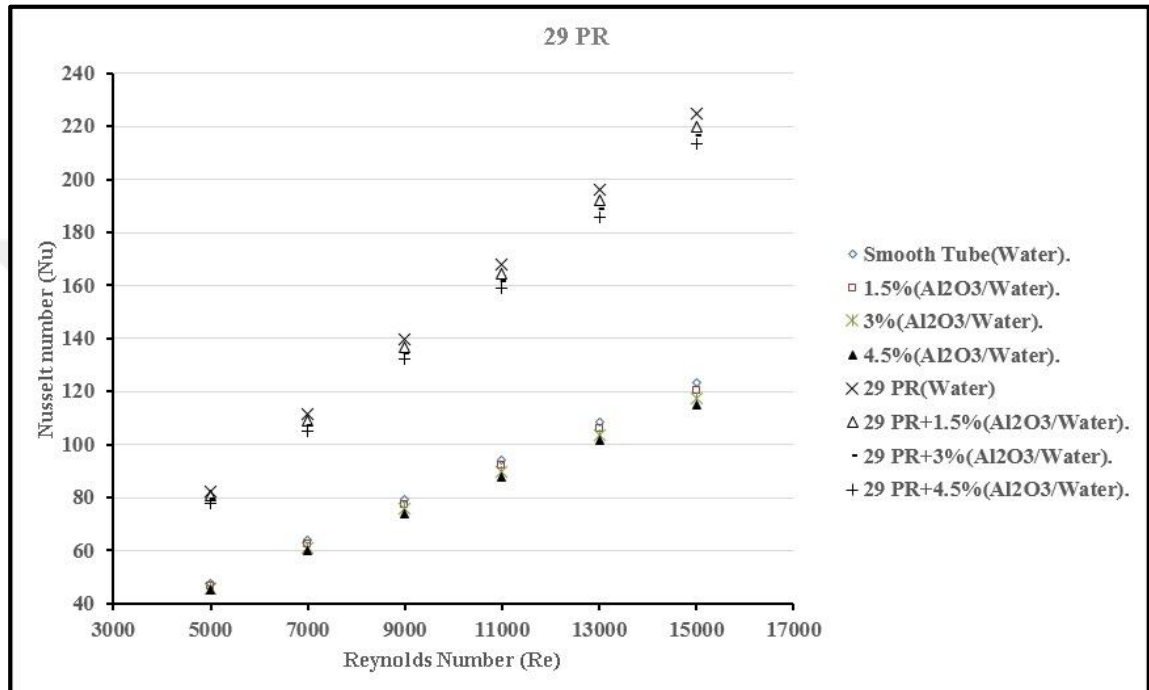


Chart 20. Nusselt number vs. Reynolds number.

### 3.4.3. On the (f)

The value of the friction factor increased after inserting twenty-nine of the pentagon rings from the recorded values when using water or nanofluids only. The increment was inversely proportional to increase in in the Reynolds number and approximately constant to increase the concentration of nanofluids at the same Reynolds number.

- The highest increment value was 0.23. It was recorded at Reynolds number of 5000 when the flow of water or all concentrations of (Al<sub>2</sub>O<sub>3</sub>-water) nanofluids with insert of twenty nine of the pentagon rings were used. While the highest recorded

increment value was 0.04 when the water or all concentration of ( $\text{Al}_2\text{O}_3$ -water) nanofluids flow were only used.

- The lowest increment value was 0.19. It was recorded at Reynolds number of 15000 when the flow of water or all concentrations of ( $\text{Al}_2\text{O}_3$ -water) nanofluids with insert of twenty nine of the pentagon rings were used. While the lowest recorded increment value was 0.03 when water or all concentration of ( $\text{Al}_2\text{O}_3$ -water) nanofluids flow were only used as shown below in Chart 21.

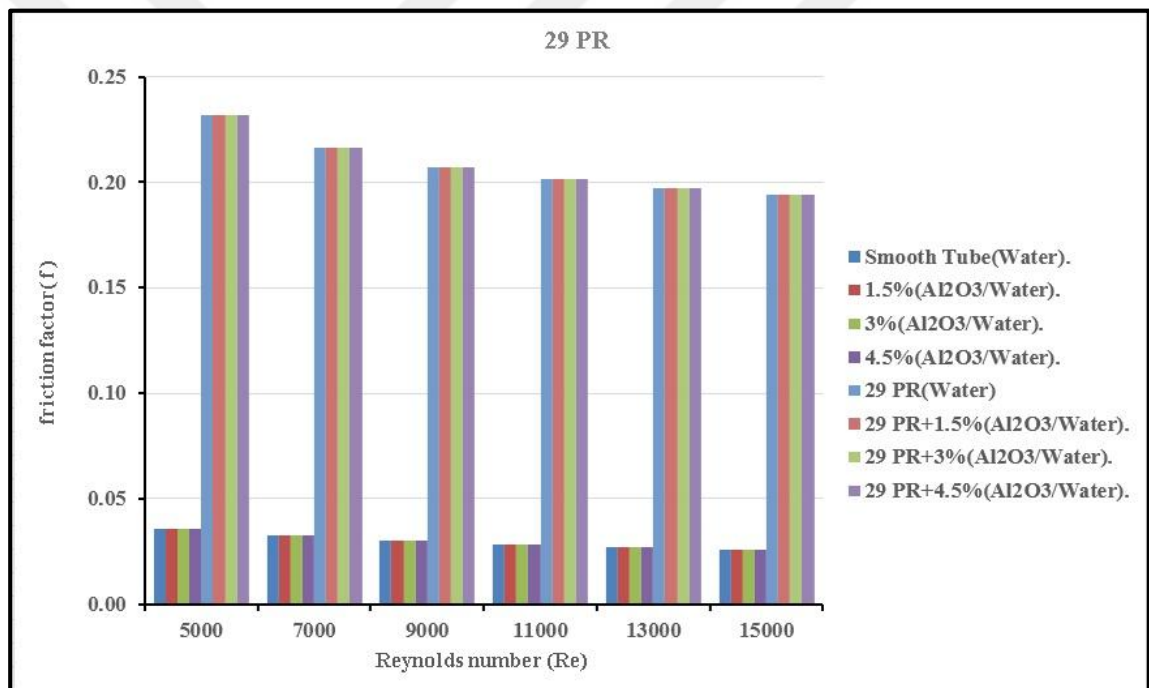


Chart 21. Friction factor vs. Reynolds number.

#### 3.4.4. On the ( $T_s$ )

The value of the surface temperature (K) decreased after inserting twenty-nine of the pentagon rings from the recorded values when using water or nanofluids only. The decrement was directly proportional to increase in in the Reynolds number and also to increase the concentration of nanofluids.

- The highest decrement value was 315 K. It was recorded at Reynolds number of 15000 when 4.5% of ( $\text{Al}_2\text{O}_3$ -water) nanofluids flow with insert of twenty nine of the Pentagon rings were used. While the highest recorded decrement value was (327 K) when 4.5% of ( $\text{Al}_2\text{O}_3$ -water) nanofluids flow was only used, and the highest recorded decrement value was (330 K) when water flow was only used.
- The lowest decrement value was (363 K). It was recorded at Reynolds number of 5000 when water flow with insert of twenty nine of the Pentagon rings were used. While the lowest recorded decrement value was 387 K when 1.5% of ( $\text{Al}_2\text{O}_3$ -water) nanofluids flow was only used, and the lowest recorded decrement value was 390 K when water flow was only used as shown below in Chart 22.

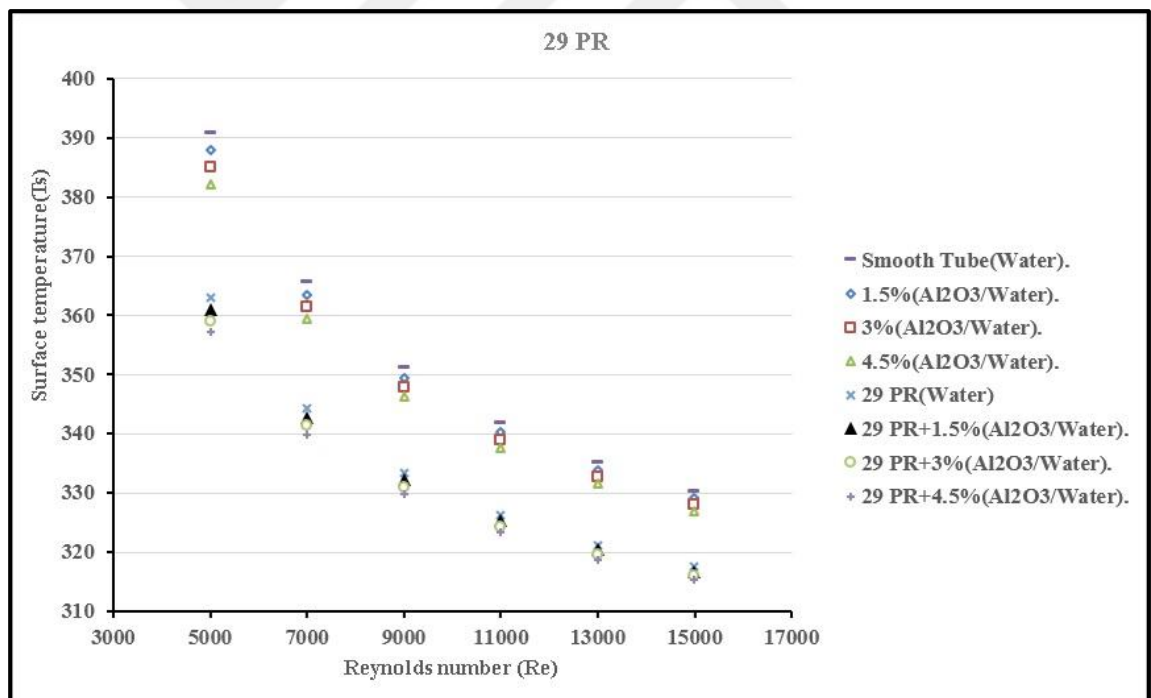


Chart 22. Surface temperature vs. Reynolds number.



### 3.4.5. On the ( $\Delta p$ )

The value of the pressure drop per unit length (Pa/m) increased after inserting twenty-nine of the pentagon rings from the recorded values when using water or nanofluids only. The increment was directly proportional to increase in in the Reynolds number and also to increase the concentration of nanofluids.

- The highest increment value was 193, 58 Pa/m. It was recorded at Reynolds number of 15000 when 4.5% of ( $\text{Al}_2\text{O}_3$ -water) nanofluids flow with insert of twenty nine of the pentagon rings were used. While the highest recorded increment value was 25.71 Pa/m when 4.5% of ( $\text{Al}_2\text{O}_3$ -water) nanofluids flow was only used, and the highest recorded increment value was 23.31 Pa/m when the water flow was only used.
- The lowest increment value was 23.31 Pa/m. It was recorded at Reynolds number of 5000 when water flow with insert of twenty nine of the Pentagon rings were used. While the lowest recorded increment value was 3.73 Pa/m when 1.5% of ( $\text{Al}_2\text{O}_3$ -water) nanofluids flow was only used, and the lowest recorded increment value was 3.61 Pa/m when the water flow was only used as shown below in Chart 23.

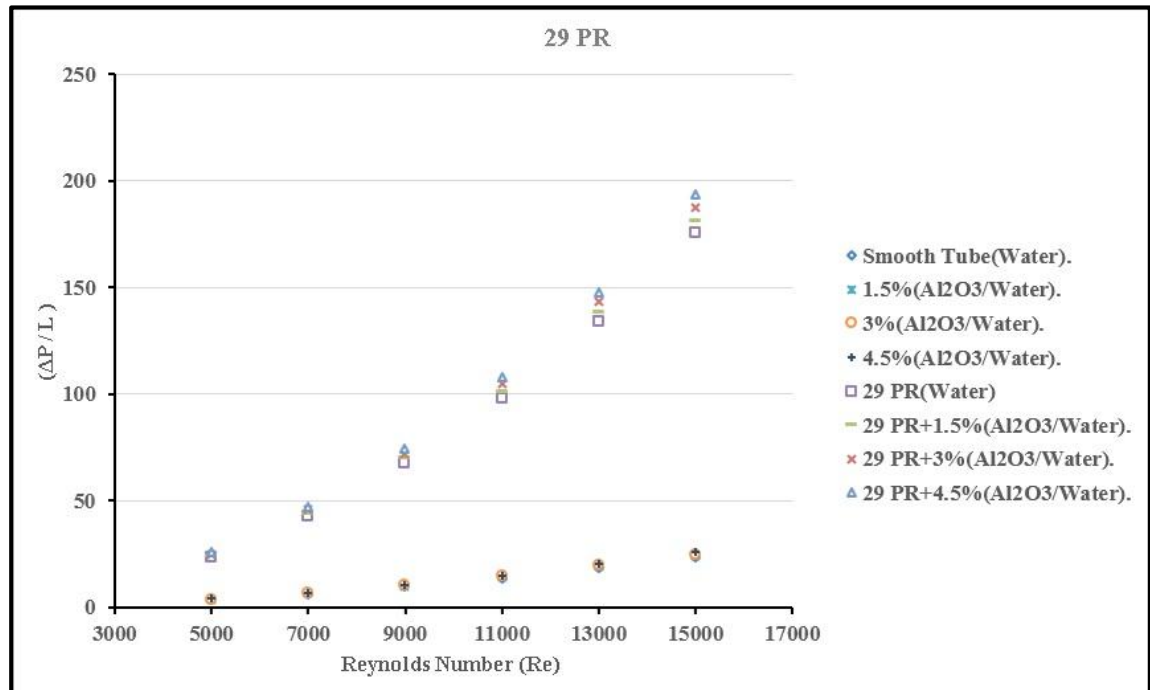


Chart 23. Pressure drop vs. Reynolds number.

### 3.5. The effects comparison of addition (9, 14, and 29) of pentagon rings on the heat transfer characteristics for water flow only

#### 3.5.1. On the (h)

The value of the heat transfer coefficient was increased after inserting 9, 14, and 29 of the pentagon rings from the recorded values when using water flow only. The increment was directly proportional to increase in in the Reynolds number and also to increase in a number of Pentagon rings into the tube.

- The highest increment values were 2686, 2222 and 2038 w/m<sup>2</sup>.k. It was recorded at Reynolds number of 15000 when water flow with insert of 29, 14, and 9 of the pentagon rings were used respectively, while the highest value was 1472 w/m<sup>2</sup>.k when the water flow was only used.
- The lowest increment values were 765, 829 and 986 w/m<sup>2</sup>.k. It was recorded at Reynolds number of 5000 when water flow with insert of 9, 14, and 29 of the Pentagon rings were used respectively, while the lowest value was 572 w/m<sup>2</sup>.k when the water flow was only used as shown below in Chart 24.

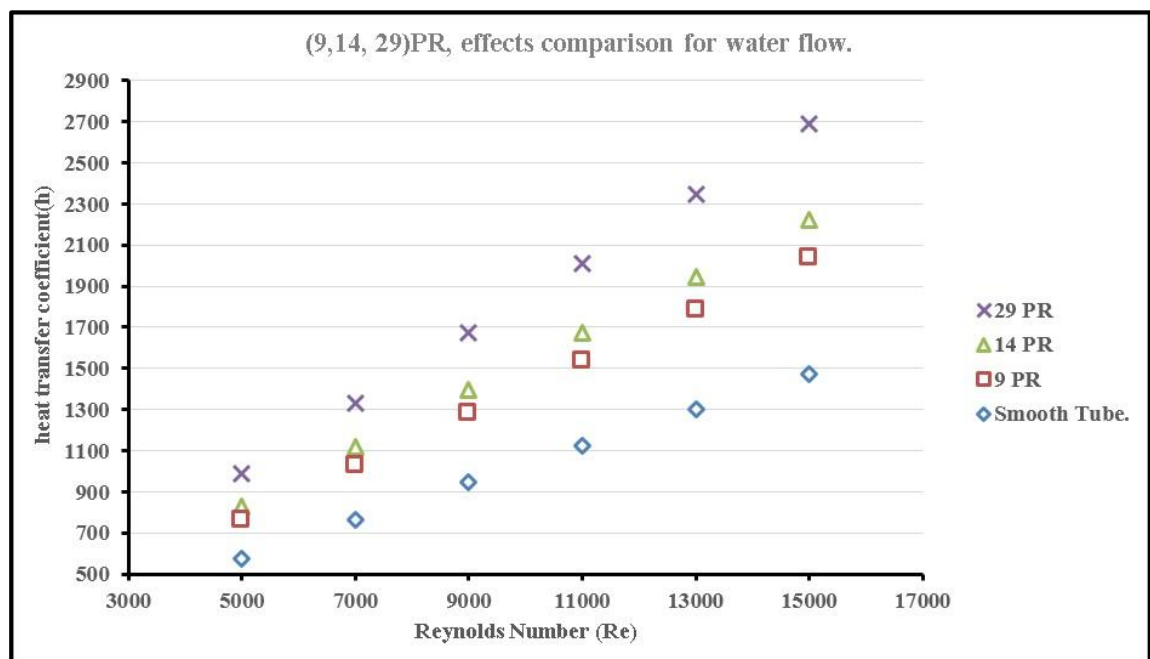


Chart 24. Heat transfer coefficient vs. Reynolds number.

### 3.5.2. On the (Nu)

The values of the Nusselt number increased after inserting 9, 14, and 29 of the pentagon rings from the recorded values when using water flow only. The increment was directly proportional to increase in in the Reynolds number and also to increase in a number of pentagon rings inserted into the tube.

- The highest increment values were 225, 186 and 170. It was recorded at Reynolds number of 15000 when water flow with insert of 29, 14, and 9 of the pentagon rings were used respectively, while the highest value was 123 when the water flow was only used.
- The lowest increment values were 64, 69 and 82. It was recorded at Reynolds number of 5000 when water flow with insert of 9, 14, and 29 of the pentagon rings were used respectively, while the lowest value was 48 when the water flow was only used as shown below in Chart 25.

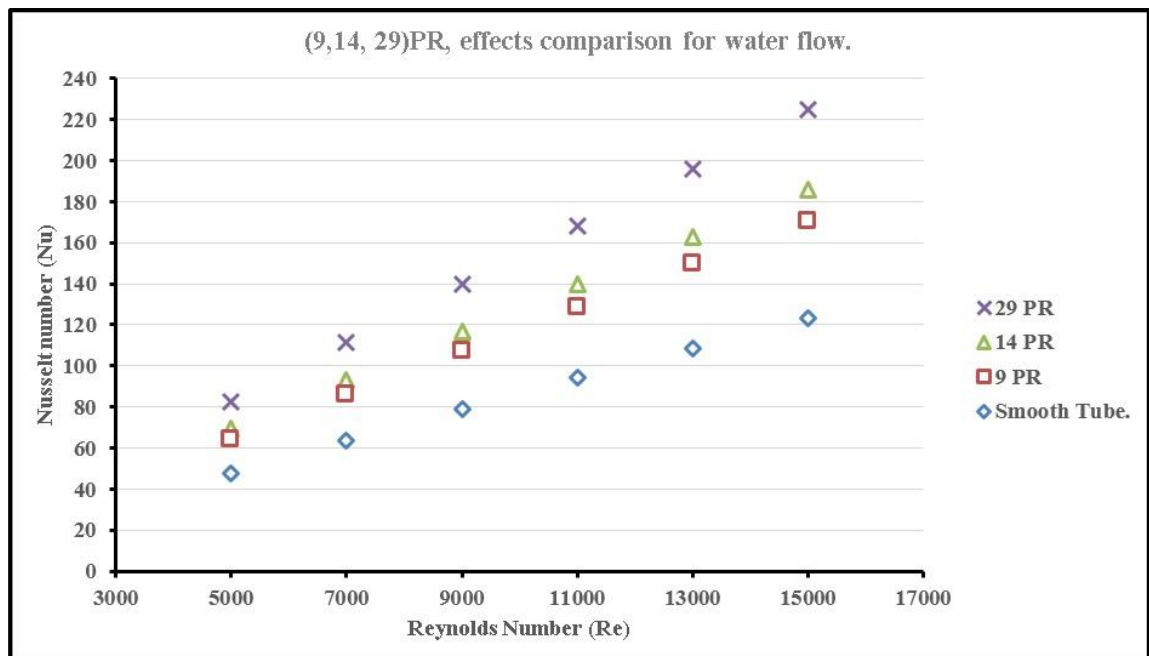


Chart 25. Nusselt number vs. Reynolds number.

### 3.5.3. On the (f)

The values of the friction factor increased after inserting 9, 14, and 29 of the pentagon rings from the recorded values when using water flow only. The increment was inversely proportional to increase in in the Reynolds number and also to increase in a number of Pentagon rings inserted into the tube.

- The highest increment values were 0.23, 0.15 and 0.11. It was recorded at Reynolds number of 5000 when water flow with insert of 29, 14, and 9 of the pentagon rings were used respectively, while the highest value was 0.04 when the water flow was only used.
- The lowest increment values were 0.09, 0.12 and 0.19. It was recorded at Reynolds number of 15000 when water flow with insert of 9, 14, and 29 of the pentagon rings were used respectively, while the lowest value was 0.03 when the water flow was only used as shown below in Chart 26.

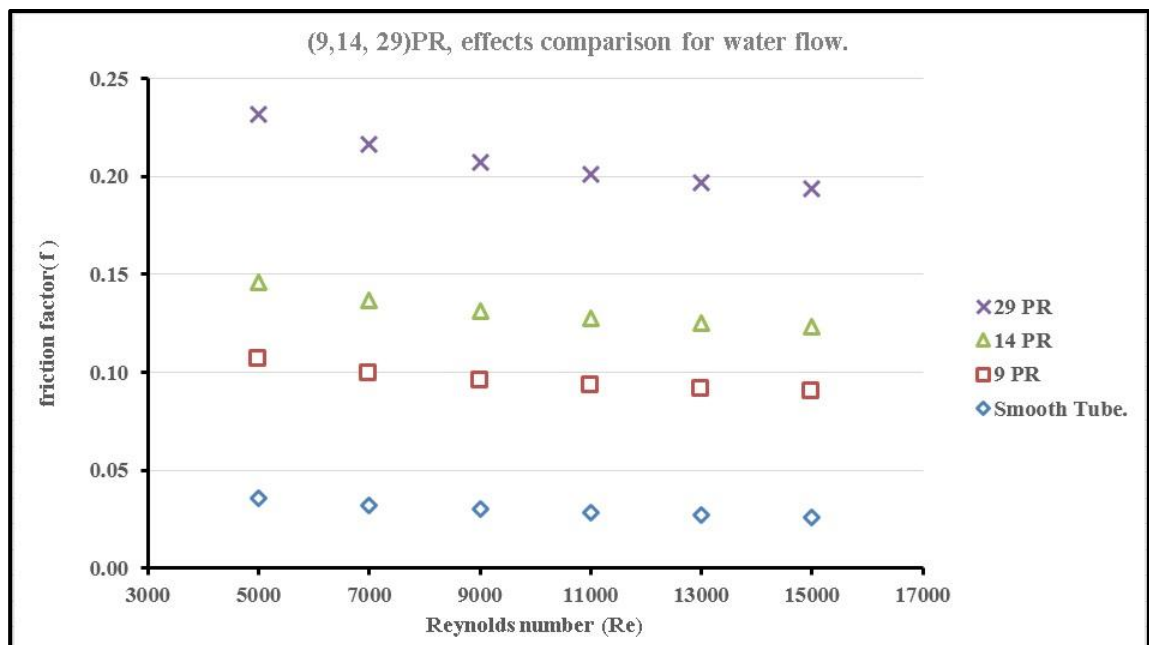


Chart 26. Friction factor vs. Reynolds number.

### 3.5.4. On the ( $T_s$ )

The values of the surface temperature (K) decreased after inserting 9, 14, and 29 of the pentagon rings from the recorded values when using water flow only. The decrement was directly proportional to increase in in the Reynolds number and also to increase in a number of Pentagon rings inserted into the tube.

- The highest decrement values were 317, 321 and 323 K. It was recorded at Reynolds number of 15000 when water flow with insert of 29, 14, and 9 of the pentagon rings were used respectively, while the highest value was 330 K when the water flow was only used.
- The lowest decrement values were 377, 372, and 363 K. It was recorded at Reynolds number of 5000 when water flow with insert 9, 14, and 29 of the Pentagon rings were used respectively, while the lowest value was 390 K when the water flow was only used as shown below in Chart 27.

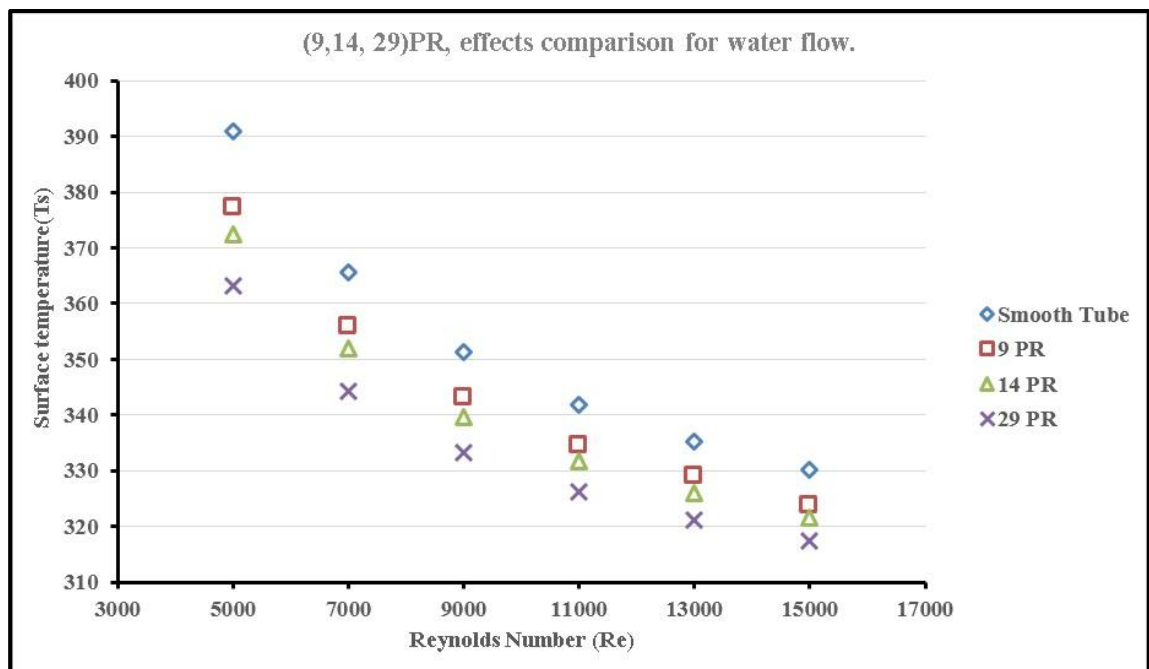


Chart 27. Surface temperature vs. Reynolds number.

### 3.5.5. On the ( $\Delta p$ )

The values of the pressure drop per unit length (Pa/m) increased after inserting 9, 14, and 29 of the pentagon rings from the recorded values when using water flow only. The increment was directly proportional to increase in in the Reynolds number and also to increase in a number of Pentagon rings inserted into the tube.

- The highest increment values were 175.46, 111.58 and 81.46 Pa/m. It was recorded at Reynolds number of 15000 when water flow with insert of 29, 14, and 9 of the Pentagon rings were used respectively, while the highest value was 23.31 Pa/m when the water flow was only used.
- The lowest increment values were 10.74, 14.68, and 23.31 Pa/m. It was recorded at Reynolds number of 5000 when water flow with insert 9, 14, and 29 of the Pentagon rings were used respectively, while the lowest value was 3.6 Pa/m when the water flow was only used as shown below in Chart 28.

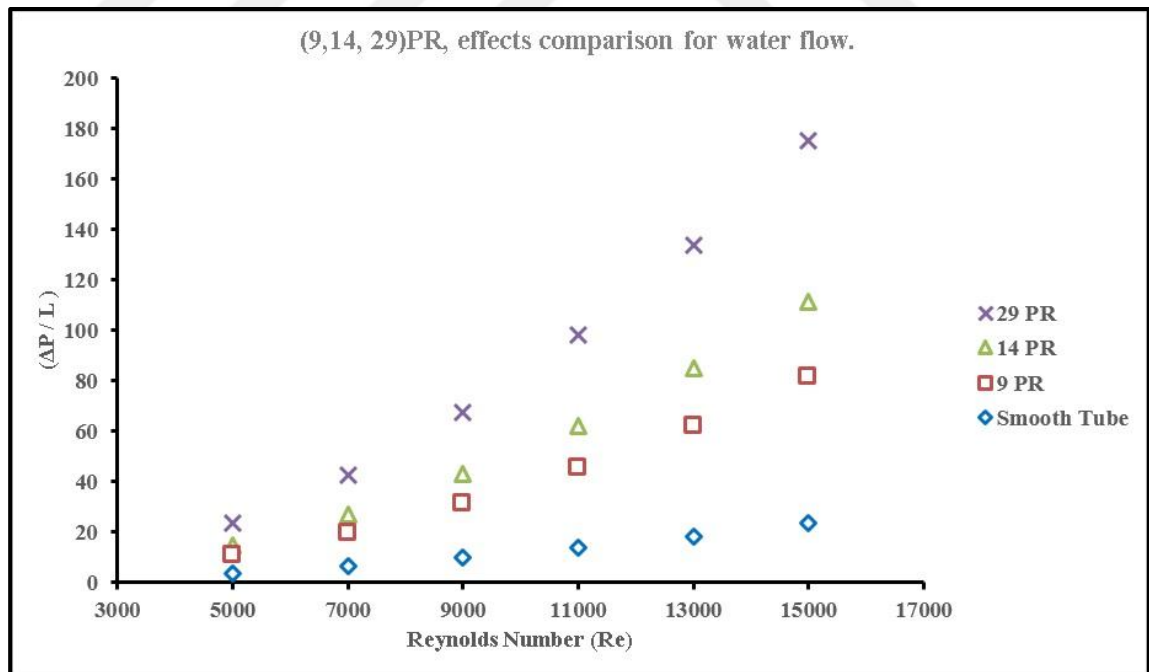


Chart 28. Pressure drop vs. Reynolds number.

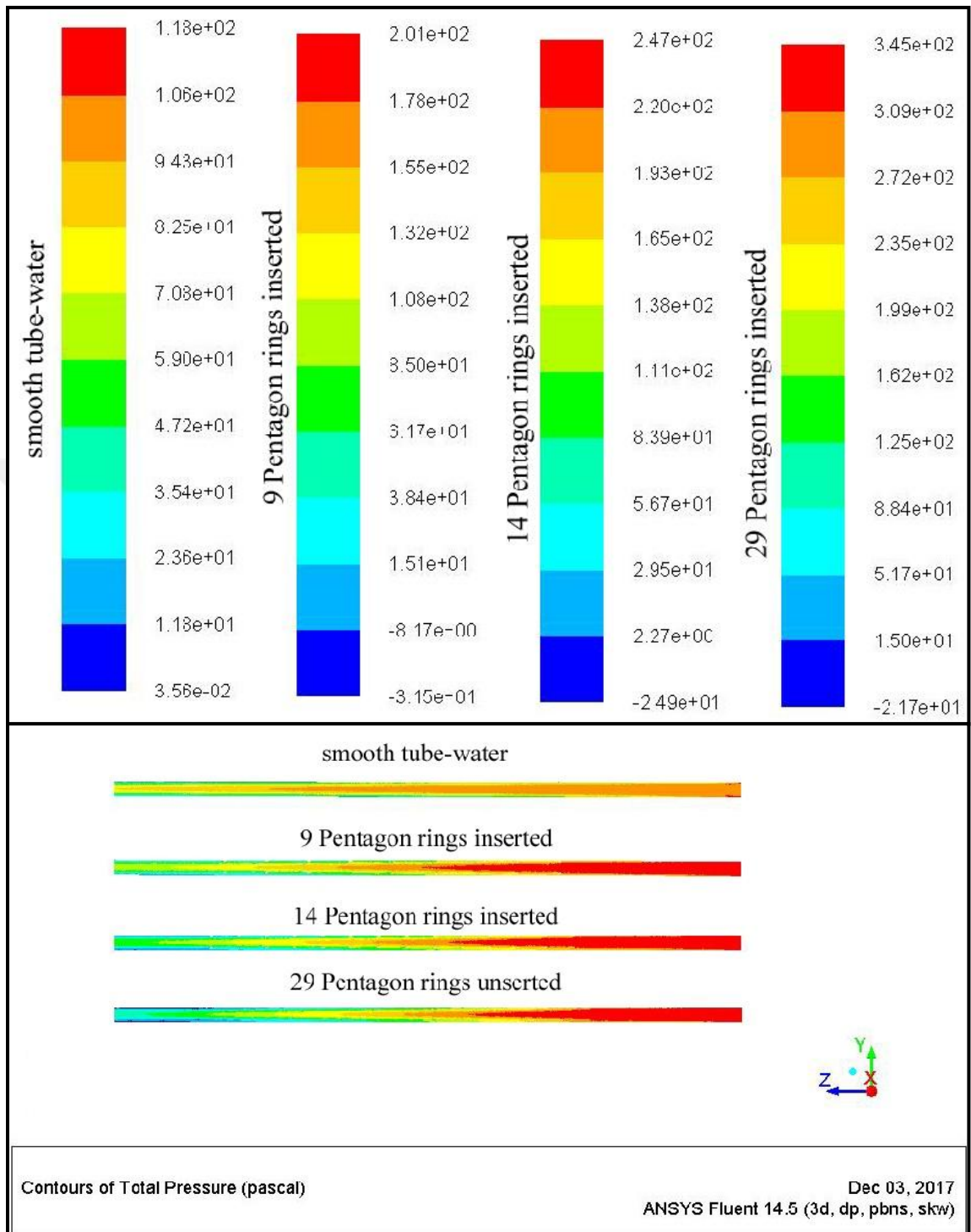


Figure 19. Comparison of total pressure counters between water flow in the smooth tube and water flow in a tube fitted with 9, 14, and 29 pentagon rings observed at Reynolds number of 15,000.

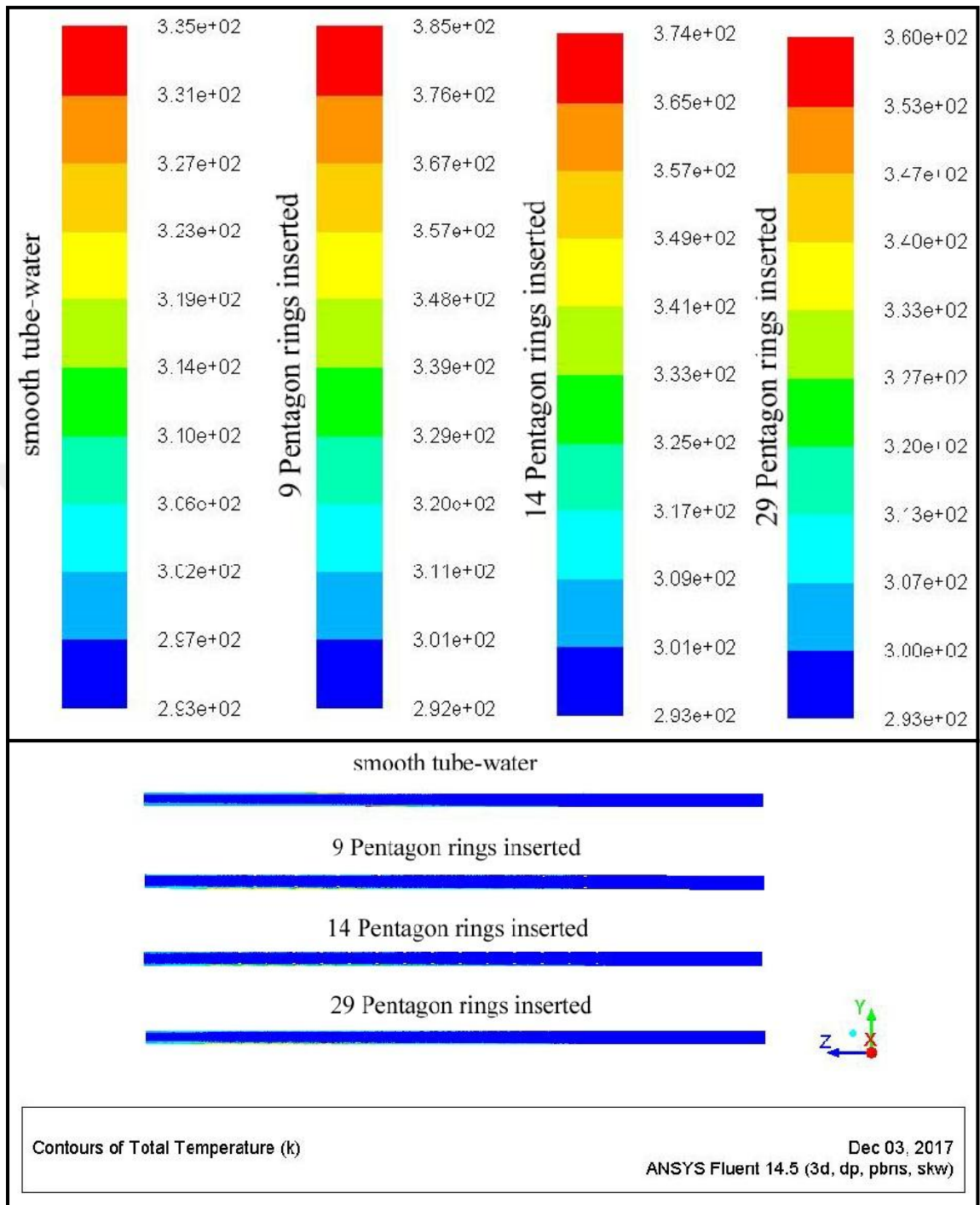


Figure 20. Comparison of total temperature counters between water flow in the smooth tube and water flow in a tube fitted with 9, 14, and 29 pentagon rings observed at Reynolds number of 15,000.



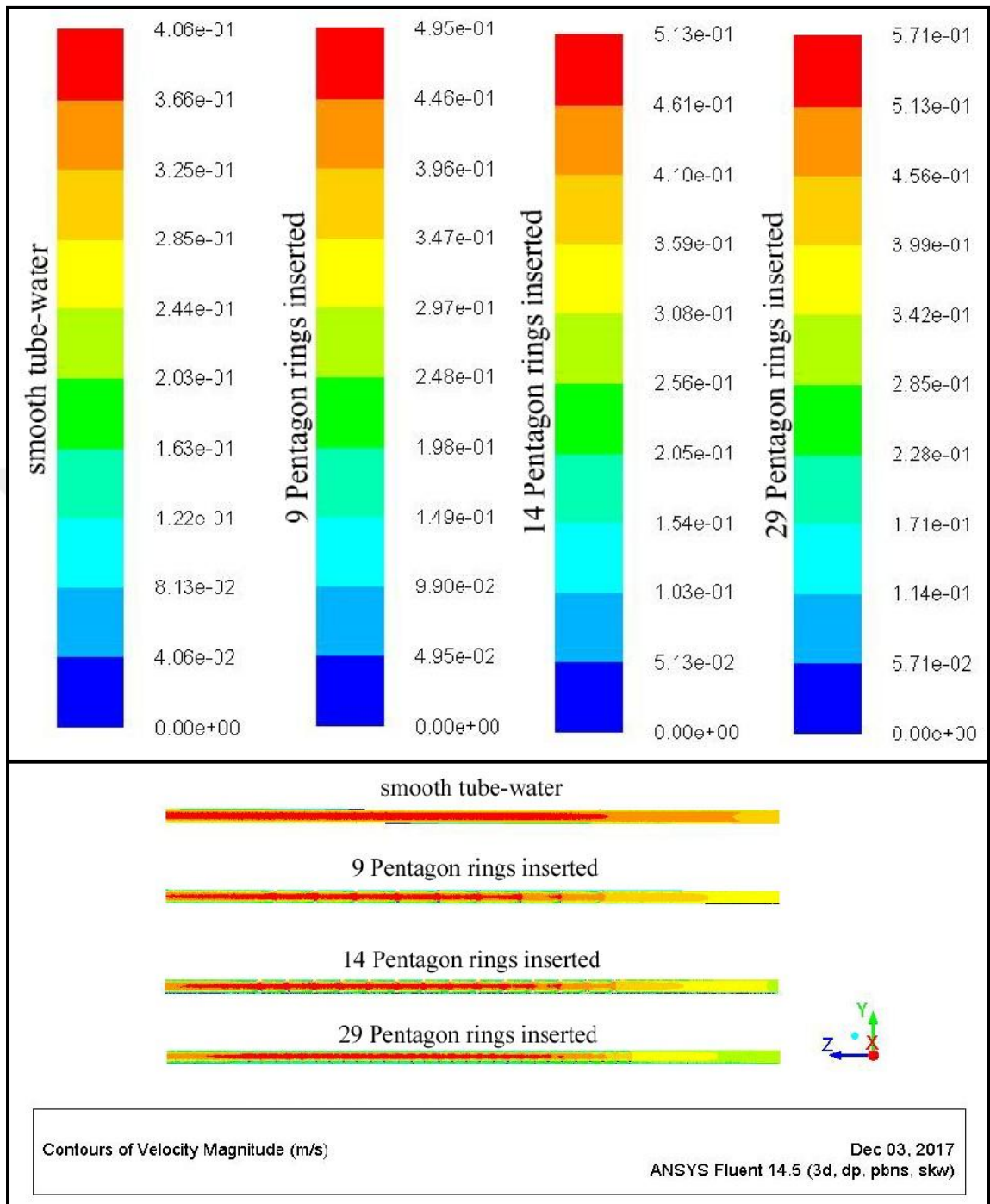


Figure 21. Comparison of velocity magnitude counters between water flow in the smooth tube and water flow in a tube fitted with 9, 14, and 29 pentagon rings observed at Reynolds number of 15,000.

### **3.6. The effects comparison of addition of 9, 14, and 29 of pentagon rings on the heat transfer characteristics for (AL<sub>2</sub>O<sub>3</sub>-water) nanofluids flow only**

#### **3.6.1. On the (h)**

The values of the heat transfer coefficient increased after inserting 9, 14, and 29 of the pentagon rings from the recorded values when using nanofluids only. The increment was directly proportional to increase in in the Reynolds number, nanofluids concentration, and a number of Pentagon rings inserted into the tube.

- The highest increase obtained values were 3018, 2386 and 2149 w/m<sup>2</sup>.k. It was recorded at Reynolds number of 15000 when 4.5% of (AL<sub>2</sub>O<sub>3</sub>-water) nanofluids flow with insert of 29, 14, and 9 of the pentagon rings were used respectively. While the highest increment value was 1623 w/m<sup>2</sup>.k when 4.5% of (AL<sub>2</sub>O<sub>3</sub>-water) nanofluids flow was only used.
- The lowest increase obtained values were 779, 847and 1024 w/m<sup>2</sup>.k. It was recorded at Reynolds number of 5000 when 1.5% of (Al<sub>2</sub>O<sub>3</sub>-water) nanofluids flow with insert 9, 14, and 29 of the Pentagon rings were used respectively. While the lowest increment value was 593 w/m<sup>2</sup>.k when 1.5% of (Al<sub>2</sub>O<sub>3</sub>-water) nanofluids flow was only used as shown below in Chart 29.

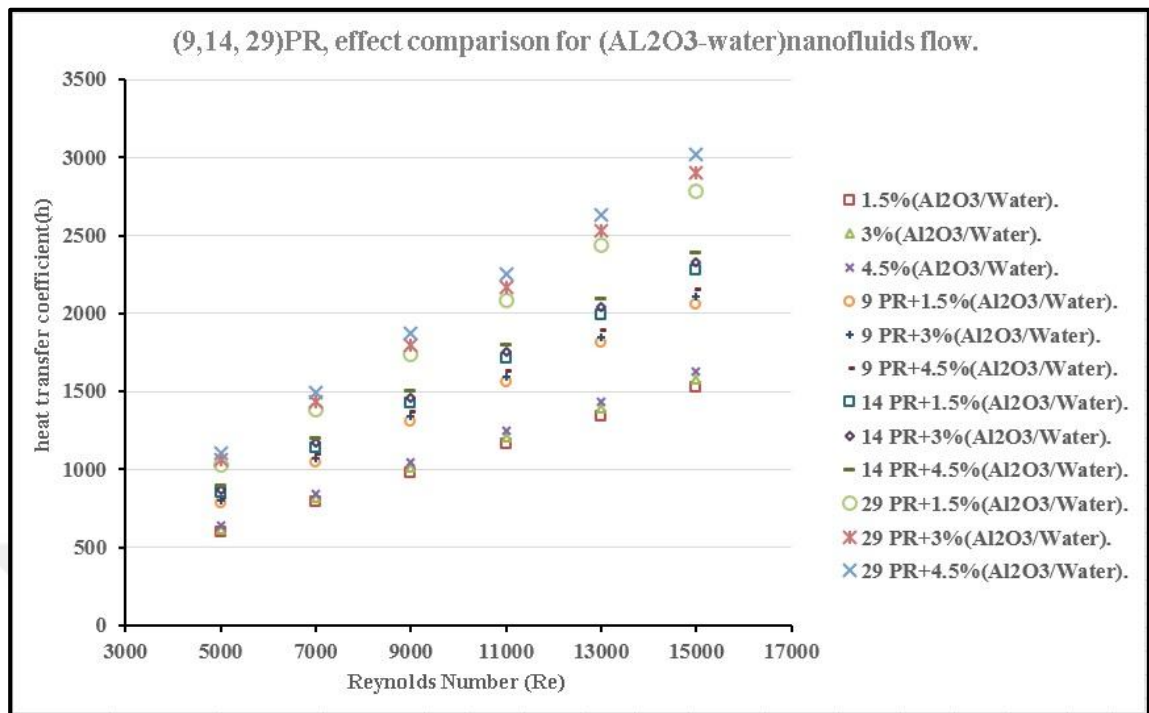


Chart 29. Heat transfer coefficient vs. Reynolds number.

### 3.6.2. On the (Nu)

The values of the Nusselt number increased after inserting 9, 14, and 29 of the Pentagon rings from the recorded values when using nanofluids only. The increment was directly proportional to increase in in the Reynolds number and a number of pentagon rings inserted into the tube, and inversely proportional to increase in nanofluids concentration.

- The highest increase obtained values were 220, 180 and 163. It was recorded at Reynolds number of 15000 when 1.5% of (AL<sub>2</sub>O<sub>3</sub>-water) nanofluids flow with insert of 29, 14, and 9 of the pentagon rings were used respectively. While the highest increment value was 120 when 1.5% of (AL<sub>2</sub>O<sub>3</sub>-water) nanofluids flow was only used.
- The lowest increase obtained values were 58, 63 and 78. It was recorded at Reynolds number of 5000 when 4.5% of (AL<sub>2</sub>O<sub>3</sub>-water) nanofluids flow with insert of 9, 14, and 29 of the pentagon rings were used respectively. While the lowest

increment value was 45 when 4.5% of (Al<sub>2</sub>O<sub>3</sub>-water) nanofluids flow was only used as shown below in Chart 30.

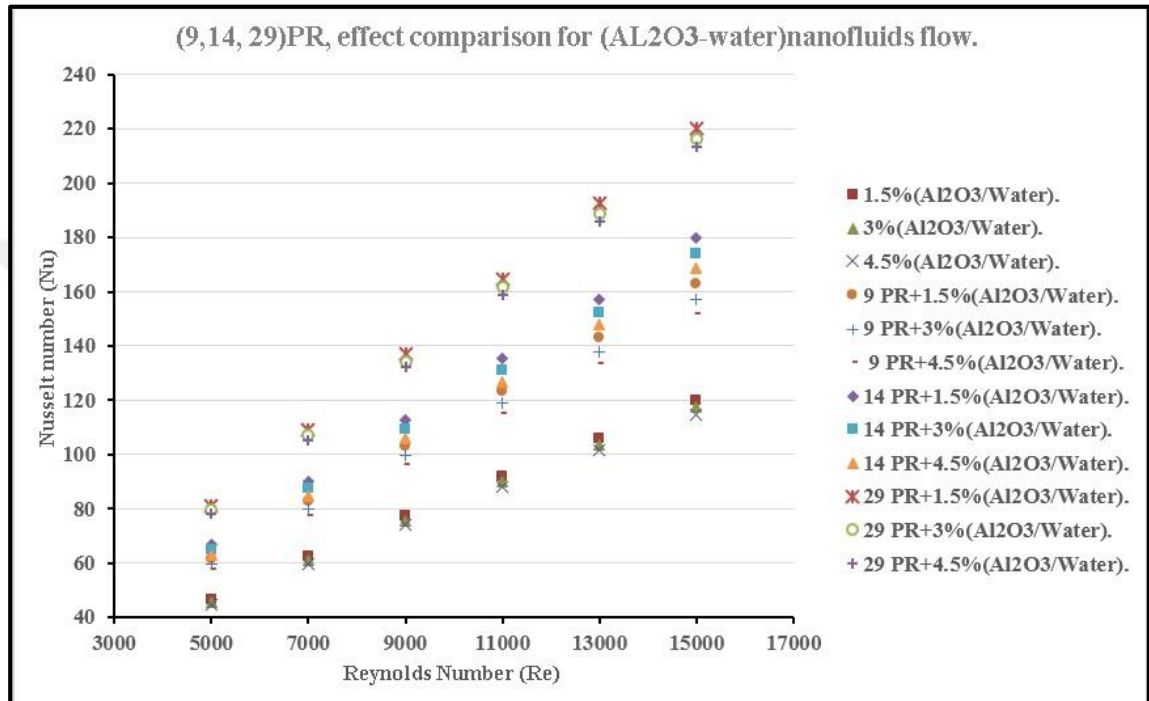


Chart 30. Nusselt number vs. Reynolds number.

### 3.6.3. On the (f)

The values of the friction factor increased after inserting 9, 14, and 29 of the pentagon rings from the recorded values when using nanofluids only. The increment was directly proportional to increase in a number of pentagon rings inserted into the tube and inversely proportional to increase in in the Reynolds number and approximately constant to increase nanofluids concentration at the same Reynolds number.

- The highest increase obtained values were 0.23, 0.15 and 0.11. It was recorded at Reynolds number of 5000 when all concentration of (Al<sub>2</sub>O<sub>3</sub>-water) nanofluids flow

with insert of 29, 14, and 9 of the pentagon rings were used respectively, While the highest increment value was 0.04 when all concentrations of ( $\text{Al}_2\text{O}_3$ -water) nanofluids flow was only used.

- The lowest increase obtained values were (0.09, 0.12 and 0.19). It was recorded at Reynolds number of 15000 when all concentration of ( $\text{Al}_2\text{O}_3$ -water) nanofluids flow with insert of 9, 14, and 29 of the pentagon rings were used respectively, while the lowest increment value was 0.03 when all concentration of ( $\text{Al}_2\text{O}_3$ -water) nanofluids flow was only used as shown below in Chart 31.

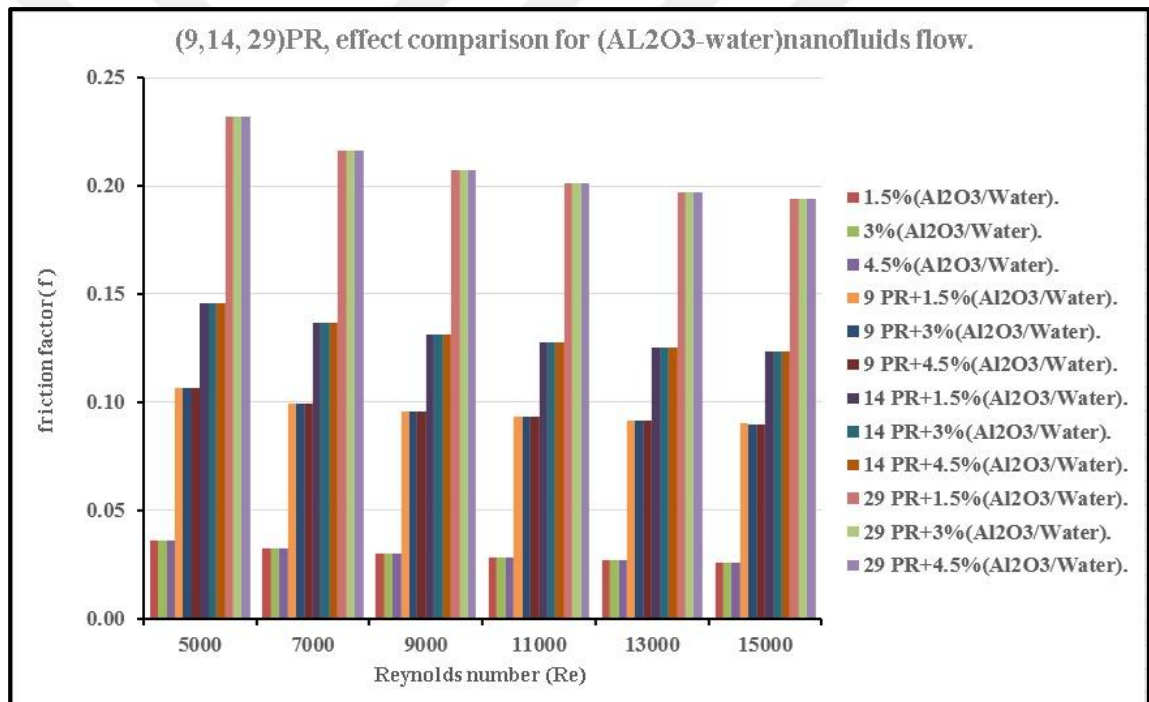


Chart 31. Friction factor vs. Reynolds number.

### 3.6.4. On the ( $T_s$ )

The values of the surface temperature (K) decreased after inserting 9, 14, and 29 of the pentagon rings from the recorded values when using nanofluids only. The decrement was directly proportional to increase in in the Reynolds number, nanofluids concentration, and a number of Pentagon rings inserted into the tube).

- The highest decrease obtained values were 315, 319 and 322 K. It was recorded at Reynolds number of 15000 when 4.5% of (AL<sub>2</sub>O<sub>3</sub>-water)nanofluids flow with insert of 29, 14, and 9 of the pentagon rings were used respectively, while the highest decrease recorded value was 327 K when 4.5% of (AL<sub>2</sub>O<sub>3</sub>-water) nanofluids flow was only used.
- The lowest decrease obtained values were 375, 370 and 360 K. It was recorded at Reynolds number of 5000 when 1.5% of (Al<sub>2</sub>O<sub>3</sub>-water) nanofluids flow with insert 9, 14, and 29 of the pentagon rings were used respectively, while the lowest decrease recorded value was 387 K when 1.5% of (Al<sub>2</sub>O<sub>3</sub>-water) nanofluids flow was only used as shown below in Chart 32.

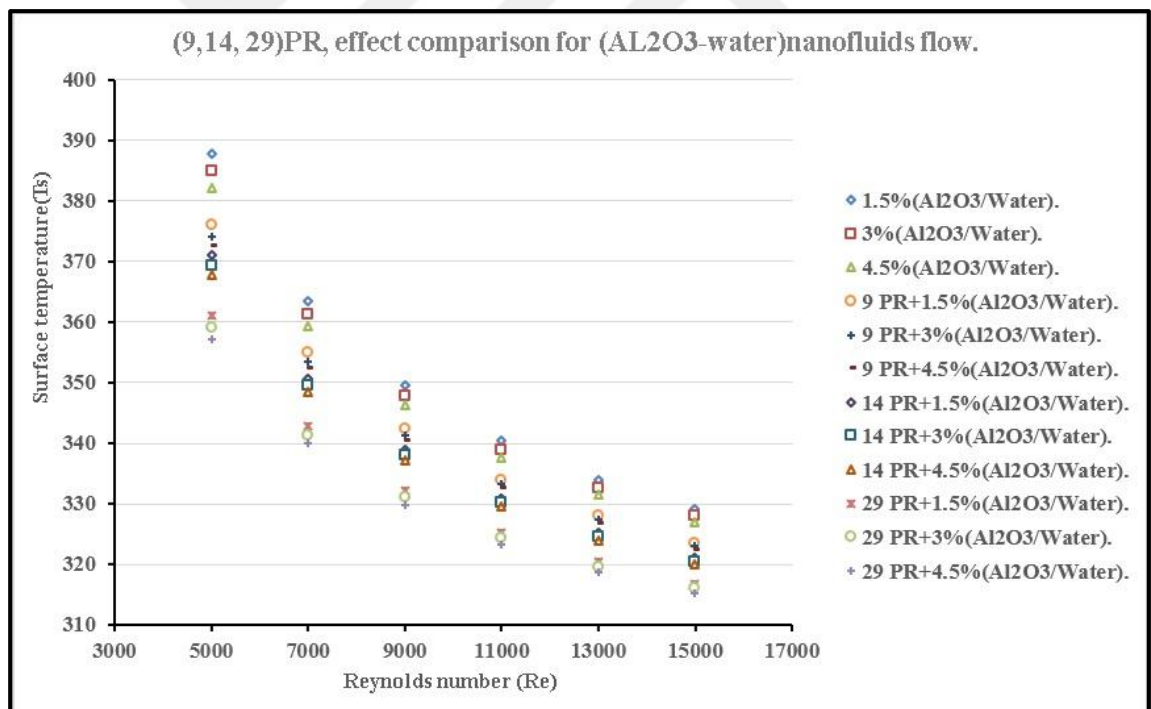


Chart 32. Surface temperature vs. Reynolds number.

### 3.6.5. On the ( $\Delta p$ )

The values of the pressure drop per unit length (Pa/m) increased after inserting 9, 14, and 29 of the pentagon rings from the recorded values when using nanofluids only. The increment was directly proportional to increase in in the Reynolds number, nanofluids concentration, and a number of Pentagon rings inserted into the tube.

- The highest increase obtained values were 193.58, 123.11 and 89.87 Pa/m. It was recorded at Reynolds number of 15000 when 4.5% of ( $Al_2O_3$ -water) nanofluids flow with insert of 29, 14, and 9 of the pentagon rings were used respectively, while the highest increase was 25.71 Pa/m when 4.5% of ( $Al_2O_3$ -water) nanofluids flow was only used.
- The lowest increase obtained values were 11.11, 15.19 and 24.12 Pa/m. It was recorded at Reynolds number of 5000 when 1.5% of ( $Al_2O_3$ -water) nanofluids flow with insert of 9, 14, and 29 of the Pentagon rings were used respectively. While the lowest increment value was 3.73 Pa/m when 1.5% of ( $Al_2O_3$ -water) nanofluids flow was only used as shown below in Chart 33.

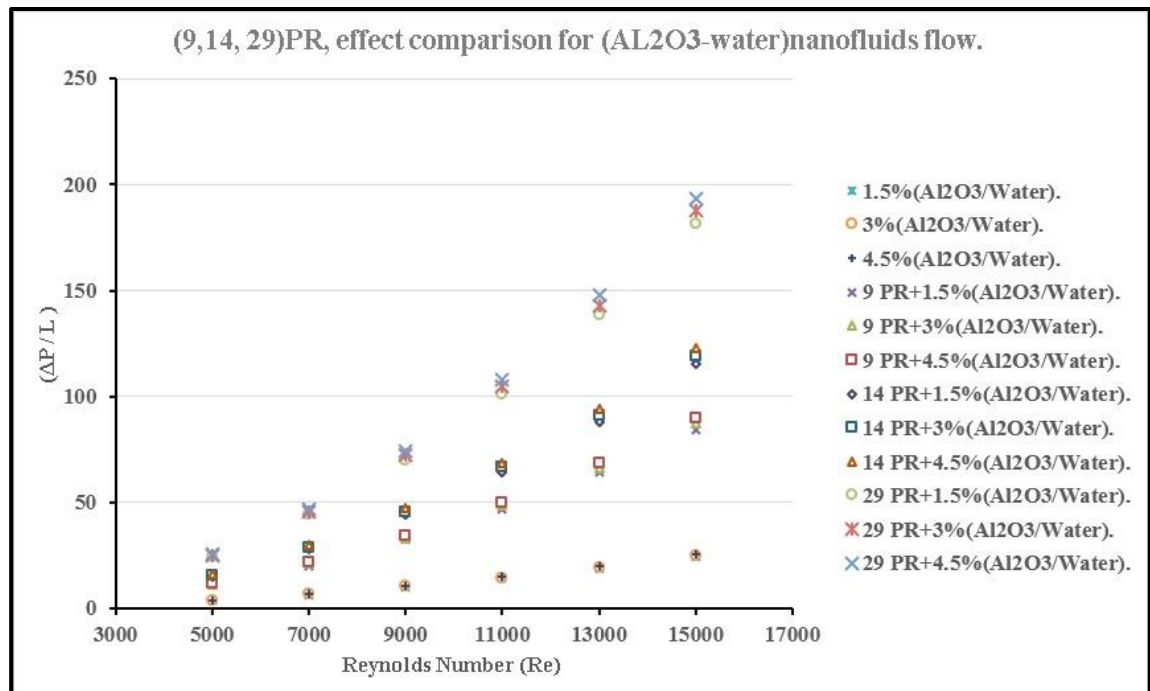


Chart 33. Pressure drop vs. Reynolds number.



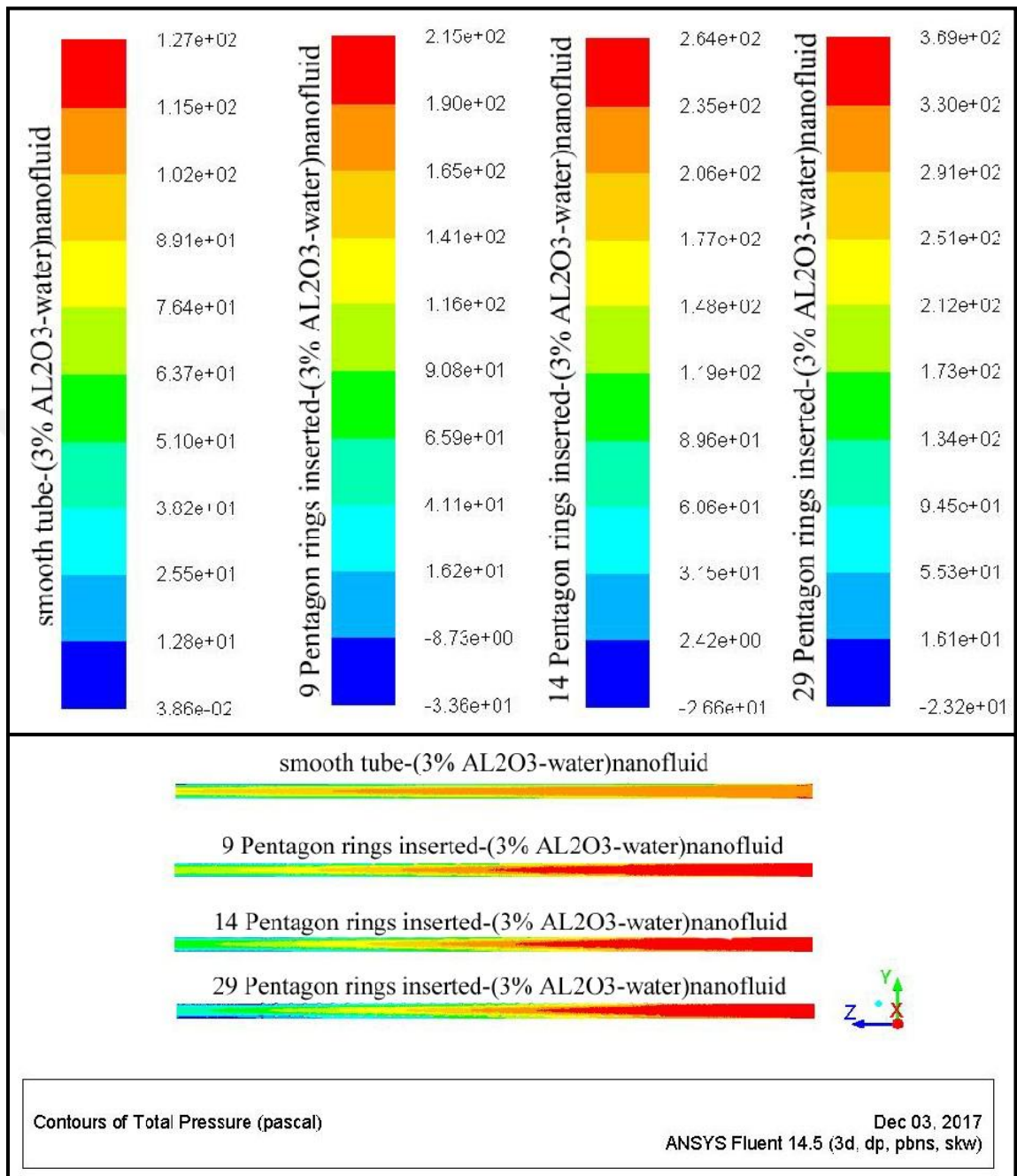


Figure 22. Comparison of total pressure counters for 3% (AL<sub>2</sub>O<sub>3</sub>-water) nanofluid flow between the smooth tube and a tube fitted with 9, 14, and 29 pentagon rings observed at Reynolds number of 15,000.



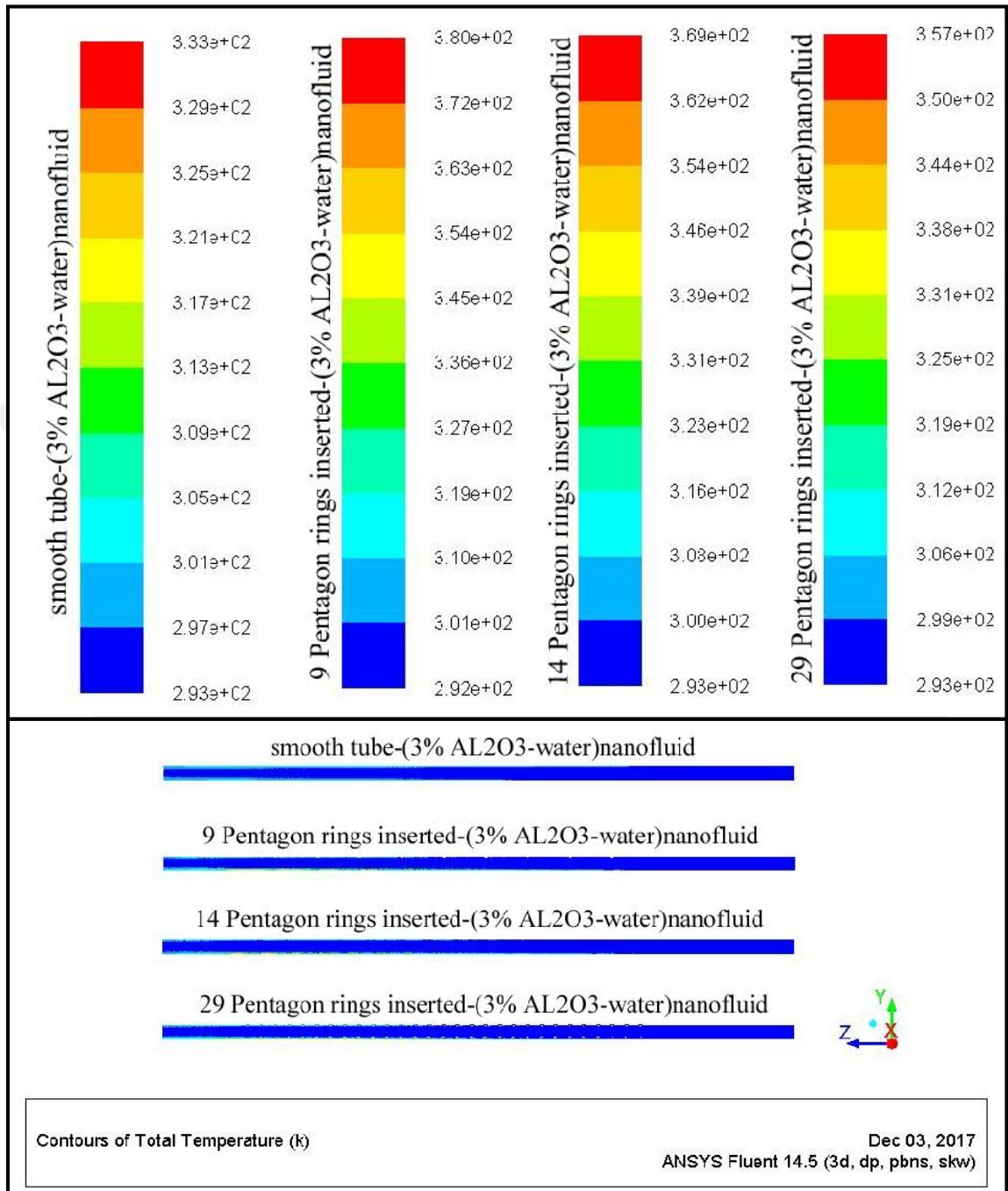


Figure 23. Comparison of total temperature counters for 3% (AL<sub>2</sub>O<sub>3</sub>-water) nanofluid flow between the smooth tube and a tube fitted with 9, 14, and 29 pentagon rings observed at Reynolds number of 15,000.

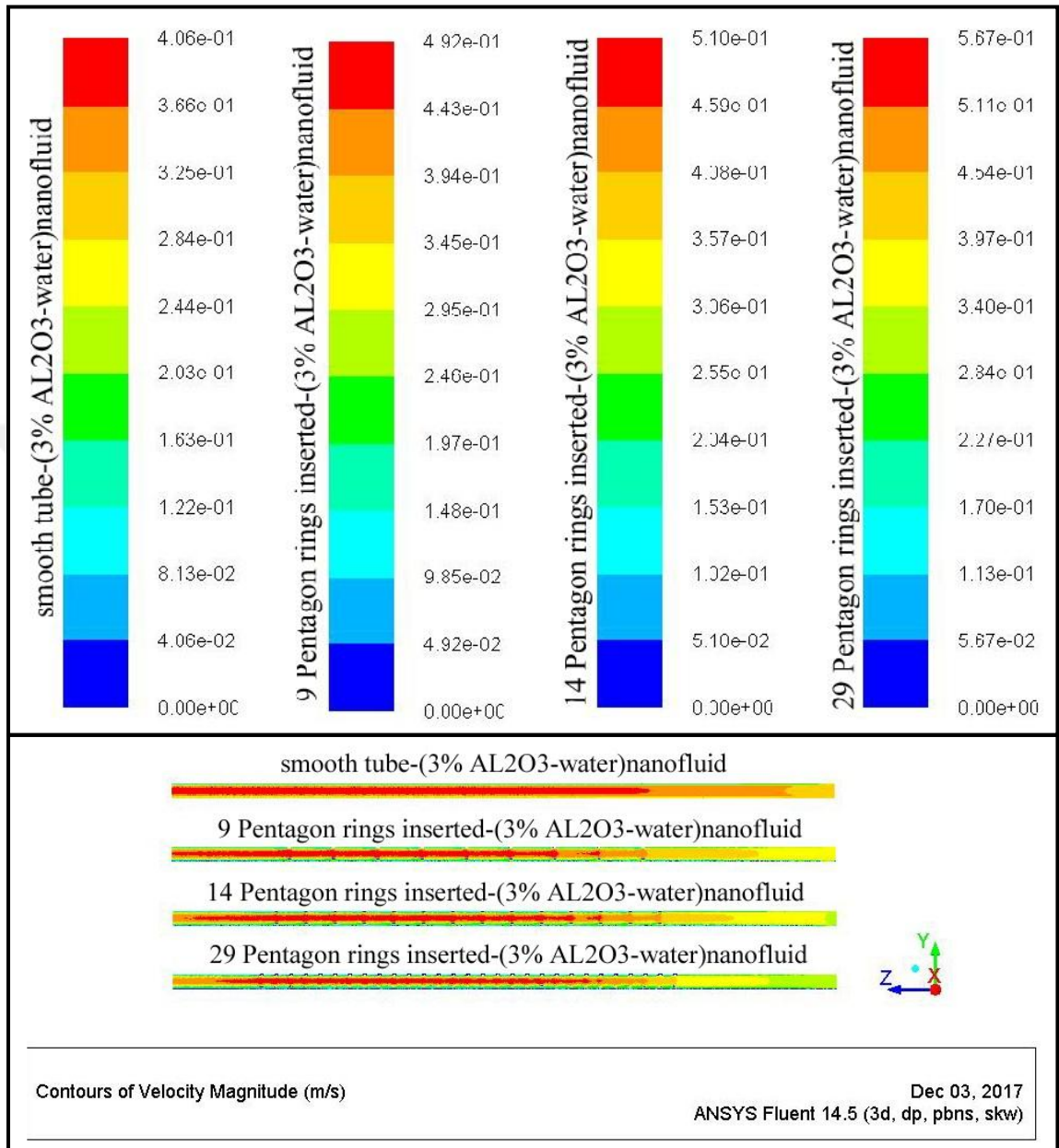


Figure 24. Comparison of velocity magnitude counters for 3 % ( AL<sub>2</sub>O<sub>3</sub>-water) nanofluid flow between the smooth tube and a tube fitted with 9, 14, and 29 pentagon rings observed at Reynolds number of 15,000.

### 3.7. Summary table of results comparison

Table 6: Results comparison.

No	$\phi$	Effect of	Re	T1	T2	Ts	Tb	h	P1	P2	$\Delta P$	Nu	F				
1	0%	Water flow	Water flow	5000	293	314	391	303	572	12	7	5	48	0.04			
				15000	293	299	330	296	1472	89	54	35	123	0.03			
			9 Pentagon rings inserted.	5000	293	331	377	312	765	23	6	16	64	0.11			
				15000	293	306	324	299	2038	177	55	122	170	0.09			
			14 Pentagon rings inserted.	5000	293	331	372	312	829	28	6	22	69	0.15			
				15000	293	305	322	299	2222	223	55	167	186	0.12			
			29 Pentagon rings inserted.	5000	293	332	363	312	986	41	6	35	82	0.23			
				15000	293	305	317	299	2686	319	55	263	225	0.19			
			2	1.5%	(AL <sub>2</sub> O <sub>3</sub> -H <sub>2</sub> O) nanofluid flow	Nanofluid flow	5000	293	314	388	303	593	12	7	6	47	0.04
							15000	293	299	329	296	1522	92	56	36	120	0.03
9 Pentagon rings inserted.	5000	293				330	376	312	779	23	7	17	62	0.11			
	15000	293				305	324	299	2060	183	57	126	163	0.09			
14 Pentagon rings inserted.	5000	293				331	371	312	847	29	7	23	67	0.15			
	15000	293				305	321	299	2276	230	57	173	180	0.12			
29 Pentagon rings inserted.	5000	293				331	361	312	1024	43	6	36	81	0.23			
	15000	293				304	317	299	2786	330	57	272	220	0.19			
3	3.0%	(AL <sub>2</sub> O <sub>3</sub> -H <sub>2</sub> O) nanofluid flow				Nanofluid flow	5000	293	314	385	303	614	13	7	6	46	0.04
							15000	293	299	328	296	1573	95	58	37	117	0.03
			9 Pentagon rings inserted.	5000	293	330	374	312	801	24	7	17	60	0.11			
				15000	293	305	323	299	2104	189	59	131	157	0.09			
			14 Pentagon rings inserted.	5000	293	330	369	312	871	30	7	24	65	0.15			
				15000	293	305	321	299	2330	238	59	179	174	0.12			
			29 Pentagon rings inserted.	5000	293	331	359	312	1064	44	7	37	79	0.23			
				15000	293	304	316	299	2899	340	59	281	216	0.19			
			4	4.5%	(AL <sub>2</sub> O <sub>3</sub> -H <sub>2</sub> O) nanofluid flow	Nanofluid flow	5000	293	314	382	303	635	13	7	6	45	0.04
							15000	293	299	327	296	1623	98	60	39	115	0.03
9 Pentagon rings inserted.	5000	293				330	372	311	818	25	7	18	58	0.11			
	15000	293				305	323	299	2149	195	61	135	152	0.09			
14 Pentagon rings inserted.	5000	293				330	368	312	891	31	7	24	63	0.15			
	15000	293				305	320	299	2386	246	61	185	169	0.12			
29 Pentagon rings inserted.	5000	293				331	357	312	1104	45	7	39	78	0.23			
	15000	293				304	315	299	3018	351	61	290	213	0.19			

### 3.8. The performance evaluation analysis ( $\eta$ )

The definition of performance evaluation analysis was previously mentioned in Chapter II under (2.2.7.). The values of the  $\eta$  increased after inserting 9, 14, and 29 of the pentagon rings from the recorded values when using water or nanofluids only. The increment was directly proportional to increase in the Reynolds number, nanofluids concentration, and a number of Pentagon rings inserted into the tube.

- The highest increase obtained values were 2.05, 1.62 and 1.45. It was recorded at Reynolds number of 15000 when 4.5% of ( $\text{Al}_2\text{O}_3$ -water) nanofluids flow with insert of 29, 14, and 9 of the pentagon rings were used respectively while the highest increment value was 1.10 when 4.5% of ( $\text{Al}_2\text{O}_3$ -water) nanofluids flow was only used.
- The lowest increase obtained values were 1.33, 1.44, and 1.72. It was recorded at Reynolds number of 5000 when water flow with insert of 9, 14, and 29 of the Pentagon rings were used respectively, while the lowest value was 1 when water flow was only used as shown in Chart 34.

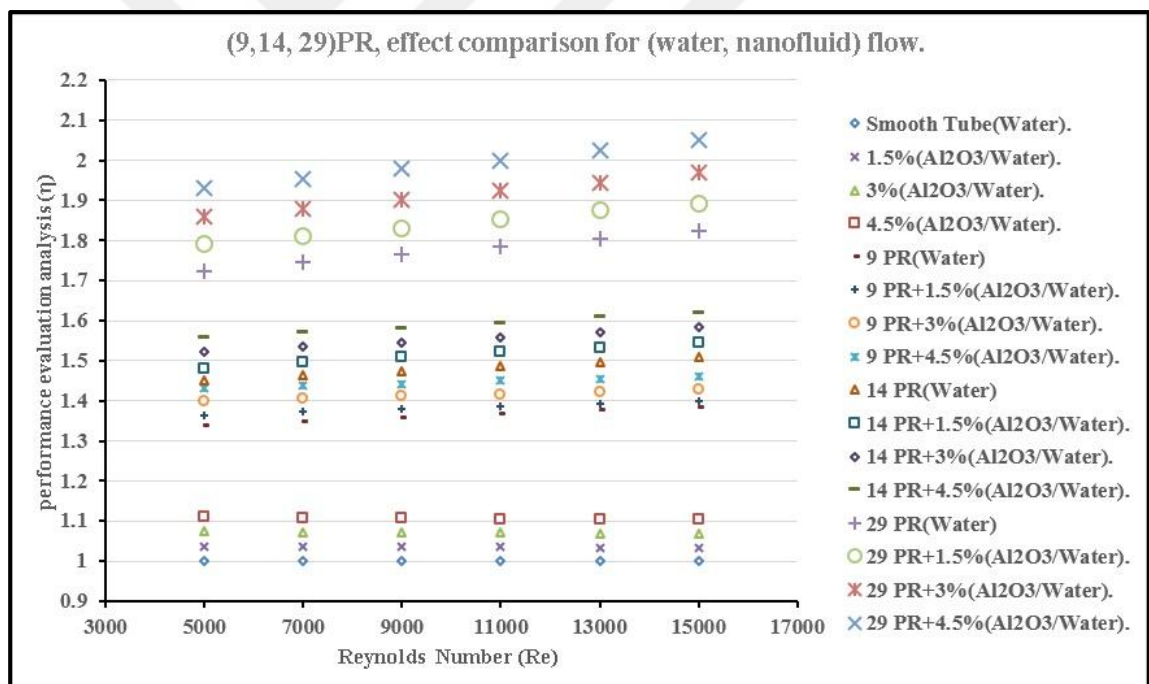


Chart 34.  $\eta$  vs. Reynolds number.

The performance evaluation analysis ( $\eta$ ) for all models was presented at Reynolds number of 15000 as shown in Chart 35.

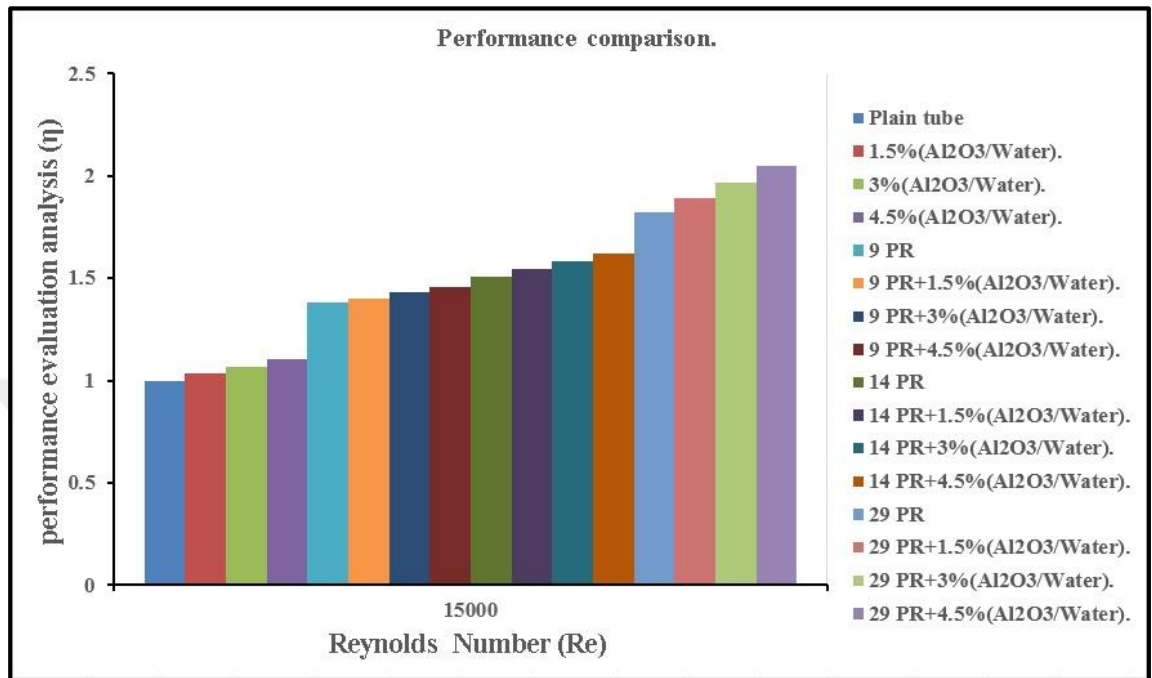


Chart 35.  $\eta$  vs. Re=15000.

## CHAPTER 4

### CONCLUSION AND RECOMMENDATIONS

#### 4.1. Conclusion

In this study, a numerical study of Steady-state turbulent convection was carried out with Reynolds numbers ranging from 5000 to 15000 by using single-phase model of finite volume method within a horizontal circular tube of cases:-

1. Water flows only.
2. (AL<sub>2</sub>O<sub>3</sub>-Water) nanofluids flow only by using three concentrations (1.5, 3, and 4.5 %).
3. Water flow with the addition of the pentagon rings by using three different pitch lengths (d, 2d, 3d).
4. (AL<sub>2</sub>O<sub>3</sub>-Water) nanofluids flow by using three concentrations (1.5, 3, and 4.5 %) with the addition of the pentagon rings by using three different pitch lengths (d, 2d, 3d).

Then, the results obtained were compared to evaluate the thermal performance of each case, and especially the fourth case which represents the main subject of this research.

#### **The prime conclusions of the study are:**

1. The increment of the heat transfer coefficient, pressure drop per unit length was directly proportional to increase in the pentagon rings numbers (decreasing the pitch length), the Reynolds number, and the nanofluids concentration.

2. The increment of the Nusselt number was directly proportional to increase in in pentagon rings numbers (decreasing the pitch length), the Reynolds number, and inversely proportional to increase in the nanofluids concentration.
3. The increment of the friction factor was directly proportional to increase in pentagon rings numbers (decreasing the pitch length) and inversely proportional to increase in in the Reynolds number and approximately constant to increase in the nanofluids concentration at the same Reynolds number.
4. The decrement of the surface temperature was directly proportional to increase in pentagon rings numbers (decreasing the pitch length), the Reynolds number, and the nanofluids concentration.
5. The maximum enhancement ratio obtained was 2.05. It was recorded at Reynolds number of 15000 when 4.5% of ( $\text{Al}_2\text{O}_3$ -water) nanofluids flow with insert of twenty nine of the Pentagon rings inside the tube was used.
6. According to the numerical investigation, the results showed that the configuration of ( $\text{Al}_2\text{O}_3$ -water) nanofluids with the pentagon rings could be used effectively in heat transfer processes.

## 4.2. Recommendations

1. In the case of the inclusion of high numbers of pentagon rings inside the tube, we recommend using Renolds number higher than 15000 in order to achieve higher efficiency with the possibility of reducing the friction factor value.
2. The level of grid refinement was a very important factor for grid sensitivity and we can recommend using a computer with a high-specification when you decide to conduct a numerical investigation and this will be better for results' accuracy purpose.
3. Using other configurations of pentagon rings with different nanoparticle types may improve the performance of heat transfer better.



## REFERENCES

- [1] Wang, X.-Q., & Mujumdar, A. S., 2008. A review on nanofluids-part I: theoretical and numerical investigations. **Brazilian Journal of Chemical Engineering**, **25**(4): 613.
- [2] Urkude, S. S. U., & Farkade, H. S. F., 2016. Heat Transfer Augmentation Techniques in Circular Tube Fitted With Swirl Flow Generator: A Review. (Web page: <http://www.ijtrd.com/papers/IJTRD5438.pdf>), (2016).
- [3] Manglik, R., 2003. Heat Transfer Enhancement.pp. 1029. *In: Heat transfer handbook* ). University of Cincinnati, Ohio.
- [4] Joshis, S., & Kriplani, V. 2011. Review of heat transfer augmentation with tape inserts. **International Journal of Engineering Science and Technology**, **3**(3).
- [5] Choi, S. U., & Eastman, J. A. 1995. Enhancing thermal conductivity of fluids with nanoparticles. Paper presented at the International mechanical engineering congress and exhibition, San Francisco, CA (United States).
- [6] Uddin, M., Al Kalbani, K. S., Rahman, M., Alam, M., Al-Salti, N., & Eltayeb, I., 2016. Fundamentals of nanofluids: evolution, applications and new theory, *International Journal of Biomathematics and Systems Biology*. **International Journal of Biomathematics and Systems Biology**, **2**(1): 1.
- [7] Sarada, S. N., Raju, A., Radha, K. K., Atanasiu, V., Doroftei, I., & Rozmarin, C. 2010. Experimental numerical analysis enhancement of heat transfer in a horizontal circular tube using mesh inserts in turbulent region. **European Journal of Mechanical and Environmental Engineering**, **2010**(53): 2.
- [8] Huang, Z., Nakayama, A., Yang, K., Yang, C., & Liu, W. 2010. Enhancing heat transfer in the core flow by using porous medium insert in a tube. **International Journal of Heat and Mass Transfer**, **53**(5): 1164-1174.
- [9] Fan, A., Deng, J., Nakayama, A., & Liu, W. 2012. Parametric study on turbulent heat transfer and flow characteristics in a circular tube fitted with louvered strip inserts. **International Journal of Heat and Mass Transfer**, **55**(19): 5205-5213.
- [10] Bhuiya, M., Ahamed, J., Chowdhury, M., Sarkar, M., Salam, B., Saidur, R., Masjuki, H., & Kalam, M. 2012. Heat transfer enhancement and development of correlation for turbulent flow through a tube with triple helical tape inserts. **International Communications in Heat and Mass Transfer**, **39**(1): 94-101.
- [11] Vathare, R., & Hebbal, O. 2013. CFD Analysis of Enhancement of Turbulent Flow Heat Transfer in a Horizontal Tube with Different Inserts. **International Journal of Engineering Research & Technology**, **2**(8): 14.
- [12] Tikhe, P., & Andhare, A. 2015. Heat Transfer Enhancement in Circular Tube using Twisted Tape Inserts of Different Width Ratio under Constant Wall Heat flux Condition. **International Journal of Engineering Research & Technology (IJERT)**, **4**(06): 6.
- [13] Dagdevir, T., Keklikcioglu, O., & Ozceyhan, V. 2015. Numerical investigation to enhance heat transfer in a circular tube with nozzles formed sinusoidal geometry, *Int. Journal of Scientific and Technological Research*, **2**(1): 1-15.
- [14] Sheikholeslami, M., Ganji, D., & Gorji-Bandpy, M. 2016. Experimental and numerical analysis for effects of using conical ring on turbulent flow and heat transfer in a double pipe air to water heat exchanger. **Applied Thermal Engineering**, **100**(2016): 805-819.



- [15] Uzagare, N., & Bansod, P. 2016. Enhancement of Heat Transfer Using V-Jagged Twisted Tape In Circular Tube. **IOSR Journal of Mechanical and Civil Engineering**, **13**(2): 14-17.
- [16] Saroj, R., & Mahendra, S. 2016. Experimental Investigation of Heat Transfer and Fluid Flow Characteristics Using S-shape Inserts through Circular Tube in Turbulent Zone. **International Journal for Research in Applied Science & Engineering Technology**, **4**(II): 354-360.
- [17] Nagarajan, P. K., & Sivashanmugam, P. 2011. Heat Transfer Enhancement Studies in a Circular Tube Fitted with Right-Left Helical Inserts with Spacer. **International Journal of Mechanical, Aerospace, Industrial, Mechatronic and Manufacturing Engineering**, **5**(10): 4
- [18] S. D., Kadhum, A. A. H., Takriff, M. S., & Mohamad, A. B. 2013. CFD analysis of heat transfer and friction factor characteristics in a circular tube fitted with horizontal baffles twisted tape inserts. **IOP Conference Series: Materials Science and Engineering**, **50**(2013): 012034.
- [19] Oni, T. O., & Paul, M. C. 2014. Numerical simulation of turbulent heat transfer and fluid flow in different tube designs. **Proceedings of the World Congress on Engineering, II** (2014): 6.
- [20] Patil, S. V., Dongare, G. U., Haval, S. S., & Ambekar, P. L. 2016. Heat Transfer Enhancement through a Circular Tube Fitted with Swirl Flow Generator. **IOSR Journal of Computer Engineering (IOSR-JCE)**: 18-23.
- [21] Arulprakasajothi, M., Elangovan, K., Reddy, K. H. C., & Suresh, S. 2016. Experimental investigation on heat transfer effect of conical strip inserts in a circular tube under laminar flow. **Frontiers in Energy**, **10**(2): 136-142.
- [22] Bhuyan, M. M., Deb, U. K., Shahriar, M., & Acherjee, S. 2017. **Simulation of heat transfer in a tubular U-loop pipe using the rectangular inserts and without insert**. Paper presented at the AIP Conference Proceedings.
- [23] Sundar, L. S., & Sharma, K. 2010. Turbulent heat transfer and friction factor of Al<sub>2</sub>O<sub>3</sub> nanofluid in circular tube with twisted tape inserts. **International Journal of Heat and Mass Transfer**, **53**(7): 1409-1416.
- [24] Eiamsa-ard, S., & Wongcharee, K. 2012. Single-phase heat transfer of CuO/water nanofluids in micro-fin tube equipped with dual twisted-tapes. **International Communications in Heat and Mass Transfer**, **39**(9): 1453-1459.
- [25] Saeedinia, M., Akhavan-Behabadi, M., & Nasr, M. 2012. Experimental study on heat transfer and pressure drop of nanofluid flow in a horizontal coiled wire inserted tube under constant heat flux. **Experimental Thermal and Fluid Science**, **36**: 158-168.
- [26] Kahani, M., Heris, S. Z., & Mousavi, S. M. 2013. Effects of curvature ratio and coil pitch spacing on heat transfer performance of Al<sub>2</sub>O<sub>3</sub>/water nanofluid laminar flow through helical coils. **Journal of Dispersion Science and Technology**, **34**(12): 1704-1712.
- [27] Ramteke, S. N., & Ate, V. P. 2014. Heat Transfer Enhancement of Pure Distilled Water and Al<sub>2</sub>O<sub>3</sub> Nanofluid in Circular Pipe with Twisted Tape Insert. **International Journal of Engineering Research & Technology**, **3**(6): 1757-1760.
- [28] Eiamsa-ard, S., Kiatkittipong, K., & Jedsadaratanachai, W. 2015. Heat transfer enhancement of TiO<sub>2</sub>/water nanofluid in a heat exchanger tube equipped with overlapped dual twisted-tapes. **Engineering Science and Technology, an International Journal**, **18**(3): 336-350.

- [29] Mirzaei, M., & Azimi, A. 2016. Heat transfer and pressure drop characteristics of graphene oxide/water nanofluid in a circular tube fitted with wire coil insert. **Experimental Heat Transfer**, **29**(2): 173-187.
- [30] Sadeghi, O., Mohammed, H., Bakhtiari-Nejad, M., & Wahid, M. 2016. Heat transfer and nanofluid flow characteristics through a circular tube fitted with helical tape inserts. **International Communications in Heat and Mass Transfer**, **71**: 234-244.
- [31] Andreozzi, A., Manca, O., Nardini, S., & Ricci, D. 2016. Forced convection enhancement in channels with transversal ribs and nanofluids. **Applied Thermal Engineering**, **98**: 1044-1053.
- [32] Vazifeshenas, Y., Yousefi, R., & Rahimi, E. 2017. An Investigation of Highly Turbulent Flow Heat Transfer Enhancement through Modified Twisted Tape Inserts and NanoFluids. **Journal of Water and Environmental Nanotechnology**, **2**(3): 195-205.
- [33] Cengel, Y. A., 2003. Heat Transfer A practical Approach (2nd ed.). McGraw-Hill, Mexico, 874 pp.
- [34] Petukhov, B., 1970. Heat transfer and friction in turbulent pipe flow with variable physical properties. **Advances in heat transfer**, **6**: 503-564.
- [35] Dittus, F., & Boelter, L., 1930. Publications on Engineering, vol. 2. **University of California at Berkeley, Berkeley, CA**: 443-461.
- [36] Gnielinski, V., 1976. New equations for heat and mass transfer in turbulent pipe and channel flow. **Int. Chem. Eng.**, **16**(2): 359-368.
- [37] Blasius, H., 1908. Grenzschichten in Flüssigkeiten mit kleiner Reibung (German). **Z. Math. Phys.**, **56**: 1-37.
- [38] Pak, B. C., & Cho, Y. I., 1998. Hydrodynamic and heat transfer study of dispersed fluids with submicron metallic oxide particles. **Experimental Heat Transfer an International Journal**, **11**(2): 151-170.
- [39] El Bécaye Maïga, S., Tam Nguyen, C., Galanis, N., Roy, G., Maré, T., & Coqueux, M., 2006. Heat transfer enhancement in turbulent tube flow using Al<sub>2</sub>O<sub>3</sub> nanoparticle suspension. **International Journal of Numerical Methods for Heat & Fluid Flow**, **16**(3): 275-292.
- [40] Vajjha, R. S., Das, D. K., & Kulkarni, D. P., 2010. Development of new correlations for convective heat transfer and friction factor in turbulent regime for nanofluids. **International Journal of Heat and Mass Transfer**, **53**(21): 4607-4618.
- [41] Kijjarvi, J., 2011. Darcy friction factor formulae in turbulent pipe flow. **Lunowa Fluid Mechanics Paper**, **110727**.
- [42] Maddah, H., Alizadeh, M., Ghasemi, N., & Alwi, S. R. W., 2014. Experimental study of Al<sub>2</sub>O<sub>3</sub>/water nanofluid turbulent heat transfer enhancement in the horizontal double pipes fitted with modified twisted tapes. **International Journal of Heat and Mass Transfer**, **78**: 1042-1054.
- [43] Versteeg, H., & Malalasekera, W., 2007. An Introduction to Computational Fluid Dynamics (Second ed.). Pearson Education Limited, Harlow-England, 517 pp.
- [44] Patel, G., 2010. CFD Simulation of Two-phase and Three-phase Flows in Internal-loop Airlift Reactors. Lappeenranta University of Technology, MSc Thesis, Lappeenranta, 85 pp.
- [45] Stenmark, E., 2013. On Multiphase Flow Models in ANSYS CFD Software. Chalmers university of technology, MSc Thesis. Sweden, 75 pp.

- [46] Fluent, I., 2006. FLUENT 6.3 user's guide. Fluent documentation.
- [47] Saha, G., 2016. Heat Transfer Performance Investigation of Nanofluids Flow in Pipe. University of Glasgow , PhD Thesis. UK , 232 pp.
- [48] Çengel, A., 1998. Property Tables and Charts (SI Unit):(Web page: <https://www.researchgate.net/file.PostFileLoader.html?id=54c8f917cf57d749248b4689&assetKey=AS%3A273740741447683%401442276287686.>).
- [49] Masuda, H., Ebata, A., & Teramae, K., 1993. Alteration of thermal conductivity and viscosity of liquid by dispersing ultra-fine particles. Dispersion of Al<sub>2</sub>O<sub>3</sub>, SiO<sub>2</sub> and TiO<sub>2</sub> ultra-fine particles.
- [50] Yu, W., & Choi, S., 2003. The role of interfacial layers in the enhanced thermal conductivity of nanofluids: a renovated Maxwell model. **Journal of Nanoparticle Research**, **5**(1-2): 167-171.
- [51] Santra, A. K., Sen, S., & Chakraborty, N., 2009. Study of heat transfer due to laminar flow of copper–water nanofluid through two isothermally heated parallel plates. **International Journal of Thermal Sciences**, **48**(2): 391-400.

## CURRICULUM VITAE

### PERSONAL DATA

Name and Surname: : Muqdad AL-JANABI  
 Nationality : Iraq (IQ)  
 Birth Date and Place : April 1, 1983, Baghdad  
 Marital Status : Married  
 Tel: : +90 537 345 69 75  
 Fax :  
 email : [engineer.muqdad@gmail.com](mailto:engineer.muqdad@gmail.com)  
 Address : Mehmet Timucin Cad. Ibrahim Avsar Apt. Blok NO 25  
 Kapı NO 2 Talas , KAYSERİ

### EDUCATION

Degree	Institute	Date of Graduation
MSc	FEN Bilimler Enstitüsü	-----
Bachelor's	University of technology, Baghdad	2005
High School	Al Murooj Preparatory School for Boys.	2001

### PROFESSIONAL EXPERIENCE

Year	Institute	Mission
2006- Currently	Baghdad Municipality	Mechanical Engineer

### Languages

Arabic and English.

### PUBLICATIONS

- Özceyhan V., Al-Janabi M., Keklikcioğlu O., Dağdevir T., "Numerical investigation of heat transfer augmentation of Al<sub>2</sub>O<sub>3</sub>-water nanofluids with pentagonal ring in turbulent flow conditions", I.International Scientific and Vocational Studies Congress , NEVŞEHİR, TÜRKİYE, 5-8 Ekim 2017, pp.---